MECHANICAL DEGRADATION OF A POLYURETHANE ELASTOMER

by

JOEY LOU MEAD

S.B., Massachusetts Institute of Technology (1981)
S.M., Massachusetts Institute of Technology (1984)

SUBMITTED TO THE DEPARTMENT OF MATERIALS SCIENCE AND ENGINEERING IN PARTIAL FULFILLMENT OF THE REQUIREMENTS OF THE DEGREE OF

DOCTOR OF PHILOSOPHY

at the

MASSACHUSETTS INSTITUTE OF TECHNOLOGY

FEBRUARY, 1986

Signature of Author _____
Department of Materials Science and Engineering
January 10, 1986

Certified By _____
David K. Roylance
Thesis Supervisor

Accepted By _____
Bernhardt J. Wuensch
Chairman, Department Graduate Committee

MECHANICAL DEGRADATION OF
A POLYURETHANE ELASTOMER

by

JOEY LOU MEAD

Submitted to the Department of
Materials Science and Engineering
on January 10, 1986 in partial fulfillment of the
requirements for the degree of Doctor of Philosophy in
Polymers

ABSTRACT

The effect of cyclic compression loading and heat build-up on a polyurethane elastomer was studied to determine the failure mechanisms. At three different loading conditions it was possible to fail specimens by internal cracking.

All the failures occurred at temperatures below those at which thermogravimetric analysis showed volatilization. From DSC studies the hard segment transition temperature was found to increase after fatigue loading. The transition temperature increase was caused by thermal annealing at the high temperatures encountered during fatigue. Swelling analysis of fatigued specimens indicated no significant chain scission was required for failure. Comparison of infrared spectra from unfatigued and fatigued material indicated no permanent chemical reactions were involved in the failure process.

Measurement of the elastic modulus showed a progressive decrease in modulus values with increasing number of fatigue cycles. This modulus reduction was attributed to a type of stress softening, requiring a combination of high temperatures and compression loading.

Specimen failure occurred through the formation of cracks generated at the center of the specimen, which exhibits the highest temperatures. As the hard segment transition temperature is approached a reduction in the material properties leads to rupture under extensional strain.

Thesis Supervisor: Dr. David K. Roylance

Title: Associate Professor of Materials Engineering

TABLE OF CONTENTS

LIST OF ILLUSTRATIONS

LIST OF TABLES

ACKNOWLEDGEMENTS

I wish to express my thanks to my thesis advisor, Professor David Roylance, for his guidance and enthusiasm. His support and encouragement made this experience an enjoyable one. Also, I would like to acknowledge Mr. Jacob Patt of the U.S. Army Tank-Automotive Command for his support of this work.

The Army Mechanics and Materials Research Center, of Watertown, Massachusetts, deserves recognition for their assistance in the preparation of samples and material characterization. In particular, I would like to thank Margaret Roylance, William Houghton, Gary Foley, Rebecca Jurta, Emily McHugh, James Sloan, and Judy Yeaton for their help. My thanks also go to the Polaroid Corporation for supplying technical assistance and materials for this research.

I would like to thank the graduate students in the polymers group for their many helpful discussions, especially Adra Acton, Sachchida Singh, Anoop Agrawal, and Leonard Buckley. I gratefully acknowledge the work of Preston Kemp, Brian Latt, and Linda VanDuyne, who served as undergraduate assistants on this project. To Lisa Kaminski I give my sincere appreciation for her assistance in document preparation, and to both Lisa and Adra my appreciation for their moral support.

Finally, I would like to thank my parents, my brother, and Alex Edsall for their understanding and encouragement.

1. Introduction

Military tracked vehicles, such as tanks and personnel carriers, use rubber pads on their tracks to reduce road damage, damp vibrations, reduce noise, and give traction. With the high loads and speeds encountered by modern tracked vehicles, the rubber pads often fail in an undesirably short time. Replacement of these pads currently contributes to a substantial portion of the cost of vehicle maintenance. Improving the lifetime of the pad material would help reduce these costs, and this research is aimed at this goal.

This study was undertaken to investigate the types of damage which occur under repeated cyclic loadings similar to those found in normal service. Under these conditions substantial heat build-up occurs, leading to permanent thermomechanical degradation. This research has been directed at determining the failure mechanisms that occur under cyclic compression loading.

The material chosen for this study is a polyether polyurethane urea. This material has shown good wear resistance in rough-terrain track testing, and is a possible replacement for more traditional rubber compounds. Further, the urethane is not so highly compounded as the traditional elastomers, and this simplifies many of the analytical techniques needed for its analysis.

Specifically, this work involved thermogravimetric analysis (TGA) to characterize the purely thermal degradation process, and compression-compression fatigue to investigate thermomechanical degradation. Physical and chemical changes occurring during fatigue were monitored by differential scanning calorimetry, swelling in dimethyl formamide, dynamic mechanical spectroscopy, and infrared spectroscopy.

Under three different loading conditions it was possible to fail specimens through cracks generated at the center of the test specimen. DSC analysis showed an increased hard segment transition temperature due to thermal annealing effects. All samples had a decreased elastic modulus (E') after fatigue, which may be due to stress-softening (Mullin's effect). Only one block tested showed any significant changes by swelling analysis, but this may be due a processing anomaly (for example, an exotherm during cure might lead to degradation of the material). The main failure mechanism appears to be softening of the hard segment followed by rupture. The cracks appear at the center of the block, which is the hottest area, supporting this mechanism.

This thesis will include background information to acquaint the reader with prior literature pertaining to the thermal degradation and structure - property relationships of polyurethanes, and a description of the materials and experimental work. A short summary of the conclusions drawn from each experiment will be given at the end of each experimental

section, as well as a discussion of the major findings and suggestions for future research areas, at the end of this work.

2. Background Information

2.1. Urethane Elastomers.

Cast urethane elastomer systems, such as the one used in this study, are generally prepared by the reaction of an isocyanate terminated prepolymer with a low molecular weight curative such as a diol or diamine. The prepolymer is usually prepared by end-capping a polyether or a polyester with a diisocyanate, forming a urethane bond with two free isocyanates, which can be further reacted[1]. This reaction can be written as:

$$\text{HO-polyether-OH} + \text{OCN-R-NCO} \rightarrow \text{OCN-R-NHCO}_2\text{-polyether-CO}_2\text{NH-R-NCO}$$

Next, the prepolymer is reacted with a "curative". If a diol is used, a polyurethane is formed. If a diamine is reacted, a polyurethane urea is formed. The amine curing reaction is shown below.

$$\text{H}_2\text{N-R-NH}_2 + \text{OCN-polyetherurethane-NCO} \rightarrow \text{-(R-NHCONH-polyetherurethane-NHCONH)}_n\text{-}$$

If an excess of isocyanate is used crosslinking may occur through the formation of allophanates or biurets, with the biuret reaction occurring more rapidly than the allophanate reaction[1].

Biuret

Allophanate

Urethanes formed in this manner are usually two-phase systems, in which the polyether or polyester forms a domain of aggregated "soft segments," and the isocyanate and curative form hard segment domains. These hard segments act as physical crosslinks, often enhancing the physical properties of the polymer.

2.2. Structure and Properties of Urethane Elastomers.

The properties of urethane elastomers can be varied by many factors such as: different isocyanate groups, curatives, soft segment polymers, and reaction conditions. The degree of phase separation also plays an important role in the mechanical properties of polyurethanes. It is important to understand the mechanical properties of polyurethanes, as the hysteresis and modulus determine the heat build-up characteristics of the material. A brief overview of the relation between component structure and material properties is given below.

Pigott et al.[2] studied a series of polyester polyurethanes with varying components. They compared the influence of diisocyanate on a polyurethane, prepared with polyethylene adipate and extended with 1,4 butanediol, and found isocyanates with increased molecular bulkiness and rigidity to have higher modulus (300% modulus) and hardness. Reduced

symmetry and methyl substituents decreased the modulus, tensile and tear strength, and hardness values. For different polyesters the presence of side chains reduced the modulus and tensile strength. Aromatic glycol extenders were found to give higher modulus, tear strength, and hardness than aliphatic glycols. The introduction of urea groups through the addition of water leads to an increase in the tear strength and modulus[1]. The tensile strength, modulus, tear strength, and hardness depend on the concentration of urea groups, as does the T_g. Because the elastomer used in this study is a polyurethane urea we would expect the material to exhibit high modulus and tear strength values.

The cure temperature can also affect the properties of the elastomer. For example, in our system an exotherm during cure may cause the properties of the center of the specimen to vary from the outside portions. The relationship between cure temperature and properties is described below. It was found that the hardness, tensile strength, and elongation decreased as the cure temperature was raised above 100°C, for a polyurethane prepared from toluene diisocyanate (TDI), polyoxypropylene glycol (PPG), and 3,3'-dichloro-4,4'-diaminodiphenylmethane (MOCA)[1]. This was attributed to the increased formation of biuret groups above 100°C. The extent of biuret formation can also be controlled by varying the ratio of isocyanate to amine. For a polymer prepared from 2,4-TDI and MOCA, cured at 100°C, the maximum hardness and modulus were obtained at a 0.8 ratio of amine to isocyanate[1]. The tear strength increased as the ratio increased up to 1.0. The biuret groups were felt to disrupt

the interchain forces leading to a reduction in modulus, even though an increase in crosslink density, for a conventional rubber, would be expected to increase the modulus.

In fact, crosslink formation has been reported to cause an anomalous decrease in the modulus[2]. In the studies of Pigott et al.[2], where the crosslink density in the hard segment was changed by adding different amounts of trimethylol propane during chain extension to a polyester polyurethane, the modulus was found to decrease, then increase, as the crosslink density was changed.

Cooper and Tobolsky[3] found similar results for a polyester polyurethane. In one case the material was crosslinked with triol and in another specimen benzoyl peroxide was used as a crosslinking agent. The benzoyl peroxide was believed to form crosslinks in the hard segment by the production of a free radical on the methylene linkage of diphenylmethane-4,4'-diisocyanate (MDI), although due to the complexity of the radical reaction it is difficult to ascertain if all the crosslinking actually did occur in the hard segment. The increased crosslinking was felt to disrupt the ordering and packing efficiency of the hard segment polymer chains, reducing interchain attractions, and leading to a weakening of the polymer. These findings indicate the importance of intermolecular attractions for polyurethane properties.

The increase in crosslink density did have an effect on the high temperature properties. The retention of properties at high temperatures is critical in applications where the elastomer system is subjected to heat build-up, as in tank track pads. Increasing the amount of triol moved the high temperature modulus reduction (hard segment transition) to progressively higher temperatures[2]. Thus, increased crosslink density leads to better high temperature properties, but with a loss in modulus at room temperature.

Schollenberger and Dinbergs[4] discussed the changes in high temperature properties by the addition of covalent crosslinks to the virtual network of a polyurethane. This virtual network is formed by the aggregation of hard segments, or urethane linkages, into domains. These domains are held together by hydrogen bonding, Van der Waal's forces, and the association of π electrons in the aromatic rings. The polyurethanes can be crosslinked by the addition of organic peroxides, which are believed to form carbon-carbon covalent bonds between methylene groups. Sulfur curing can also be used when an unsaturated group exists on the urethane chain.

Schollenberger and Dinbergs[4] studied a polyurethane prepared with diphenylmethane-p,p'-diisocyanate (MDI), poly(tetramethylene adipate) glycol, and 1,4 butanediol. An organic peroxide was added to make the covalently crosslinked material. They found the covalently crosslinked material to retain its integrity at high temperatures (100°C), while the

virtually crosslinked material melted. The covalently crosslinked material showed a higher modulus, but lower extensibility, when compared to the virtually crosslinked material at 25°C. At higher temperatures (100°C), the covalently crosslinked material showed lower extensibility and tensile strength than at 25°C. The virtually crosslinked material melted at the higher temperature and could not be tested. In tear tests the virtually crosslinked material showed only slightly better strength at 25°C, than the covalently crosslinked material. At 100°C the covalently crosslinked material showed reduced tear strength, and the virtually crosslinked material had melted. The virtually crosslinked material was found to have better flex life than the covalently crosslinked material.

In a polyurethane system the aggregation of urea and urethane groups gives a polyurethane elastomer a seemingly higher crosslink density than would be expected by primary crosslinks alone. Weisfeld et al.[5] studied the temperature dependent effects of primary and secondary bonds on the modulus. For primary crosslinks they assumed a modulus-temperature dependence following the statistical theory of rubber elasticity, and for secondary bonds they assumed an Arrhenius temperature dependence. They were able to separate the modulus into two contributions; one from the primary crosslink density and the other from secondary bonds. For an MDI, poly(ethylene/propylene adipate), MOCA-cured polyurethane, they found a correlation between the urea content and the modulus contribution from secondary crosslinks. They found the contribution from secondary

bonding to increase as the primary crosslink density (biuret bonds) decreased. The secondary crosslinking contribution was more than sufficient to compensate for the loss in primary crosslinks, and in fact the total modulus increased even though the primary crosslink density decreased. For a material without any primary crosslinks the modulus data fitted the Arrhenius Law directly.

Weisfeld et al.[5] also studied a polyester polyurethane cured with dicumyl peroxide. For this system the primary crosslink density interfered very little with the secondary bonding. The authors felt the primary bonding occurred mainly in the polyester regions, and did not interfere with the secondary bonding of the urethane segments.

Rutkowska and Balas[6] applied the method of Weisfeld et al. to the study of primary and secondary bonding in a series of polyurethanes prepared from oligo(ethylene adipate), MDI, MOCA, and 1,4 butylene glycol. They found that increases in the NCO:OH ratio from 2.75 to 5.0, during the prepolymer preparation, caused an increase in the total crosslink density, and increases in both the primary and secondary crosslinks. This was attributed to the formation of more rigid chains, which produces a more favorable environment for hydrogen bonding and Van der Waal's interactions. Polymers prepared from MOCA had a higher number of secondary crosslinks as compared to glycol-cured polymers. They determined, on the basis of IR measurements of hydrogen bonding, that the primary crosslink density, measured by the Weisfeld method, contained

some hydrogen bonding contributions. From these studies it appears that hydrogen bonding plays an important role in the mechanical properties of polyurethanes.

Cain et al.[7] found a correlation between hydrogen bonding and physical property changes for a polyurethane prepared from TDI, PTMEG, and MOCA. Above 150°C a loss of modulus was observed in the Rheovibron data. A break in the H-bonded NH stretch frequency was seen at nearly the same temperature. They also found a decrease in room temperature properties as a result of heat treatment above 150°C. Thus, hydrogen bonding will influence the temperature dependence of polyurethane properties.

Phase separation also influences the mechanical and thermal properties of polyurethanes. Ng et al.[8] studied the effect of molecular weight distribution (MWD) on the properties of a polyurethane prepared from PTMEG, piperazine, and 1,4 butanediol bischloroformate. This polymer could not participate in intermolecular hydrogen bonding. The glass transition of the soft segment was found to depend on the hard segment content, but not the MWD or molecular weight of the hard segment. This was attributed to the increased number of hard segments acting as filler particles, raising the T_g of the matrix. As the MWD of the hard segment was narrowed, the glass transition temperature of the hard segment increased. The authors suggested that a narrow MWD would lead to improved phase separation and crystallization, and therefore a higher T_g. The narrow hard segment MWD material had a higher plateau modulus value,

assumably because of the more perfect hard segments. More diffuse, less perfect domains were expected to give a lower modulus.

From the work done in this thesis we have found the temperature at which the hard segment transition occurs will determine the failure of the specimen. Above the hard segment transition, the material properties are drastically reduced. Therefore, it is helpful to understand what influences the transition temperature of the hard segment. Schneider et al.[9] studied the thermal transition behavior of 2,4 and 2,6 TDI polyurethanes. The 2,4 TDI polymers varied in properties as the urethane concentration was changed. The T_g and a higher temperature transition, T_2, were both found to increase with increasing urethane content. The increase in T_g with urethane content was believed due to increased phase mixing as the urethane content increased. T_2 was thought to be from a weak domain structure. For the 2,6 TDI polymers T_g was found to be independent of the urethane content. No T_2 transition was found, but a transition above 100°C, T_3, was found to be dependent on the urethane content. The lack of urethane concentration dependence for T_g in the 2,6 TDI polymers indicated a highly ordered hard segment domain with little phase mixing.

Sung[10] compared the properties for 2,4 TDI polyurethanes cured with either butane diol or ethylene diamine. The soft segment was polytetramethylene oxide (PTMO) of molecular weight (MW) 1,000 or 2,000. For the butane diol system the soft segment and hard segment T_gs

increased with urethane content only for PTMO of MW 1,000. Changes in the urethane content also brought about mechanical property changes for this system. As the urethane content increased the material changed from rubbery to almost plastic behavior. This would be expected if there were considerable phase mixing.

When the MW of the soft segment was increased to 2,000 very little dependence on urethane content was seen for the thermal transitions. Similarly, very little dependence on urea content was seen for the ethylene diamine cured system at either molecular weight PTMO. Where thermal transition behavior is independent of the urethane or urea content a well phase-separated system can be expected.

The PTMO 1,000 series, cured with ethylene diamine, showed a higher modulus, higher tensile strength, and lower elongation at break compared to the PTMO 2,000 material. For the PTMO 1,000 series an increase in urea content produced higher tensile strength and modulus, but lower elongation at break. At the same urea content, the PTMO 2,000 material showed lower hysteresis than the PTMO 1,000 material, probably because of better phase separation in the 2,000 MW material.

The influence of fatigue on mechanical properties of polyurethanes is of direct interest to this study. It has been reported that under repeated flexing softening and loss of modulus occurs[1]. In the case of a TDI, poly(tetrahydrofuran), MOCA-cured polyurethane most of the softening

occurred in the first cycle. It was not reported if this loss of modulus was a reversible process. Increasing the crosslinking through biurets or branched prepolymers reduced these losses. The higher crosslink density reduced heat build-up on flexing, but also lowered the resistance to flexing.

We can relate some of the results found in other systems to the polyurethane used in this work. The system we have studied would be expected to show similar behavior to TDI, PTMO or PTMEG, MOCA-cured systems.

2.3. Thermal Degradation of Polyurethanes.

The thermal degradation of polyurethanes is a complex process. The thermal degradation reactions may be important for determining the failure processes of urethanes where high temperatures are present, such as occurs during the testing done for this work. The decomposition of the urethane group can occur through several mechanisms[11].

$$RNCOOR' \rightarrow RN=C=O + R'OH$$

$$RNHCOOCH_2CHR' \rightarrow RNH_2 + CO_2 + R'CH=CH_2$$

$$RNHCOOR' \rightarrow RNHR' + CO_2$$

The urea group may decompose to form an isocyanate and an amine[11]. The above reactions produce chain rupture. The isocyanates which have been

formed may then react to form other products such as carbodiimides and isocyanurates[11].

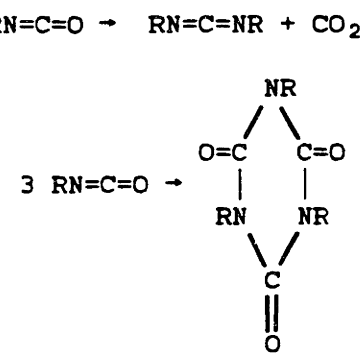

The formation of carbodiimides and isocyanurates does not lead to permanent chain rupture.

By direct pyrolysis of N-monosubstituted polyurethanes into a mass spectrometer, Ballisteri et al. found the primary decomposition process is the dissociation of the urethane to isocyanate and diol[12].

Foti, Maravigna, and Montaudo investigated the effect of N-methyl substitution on a series of polyurethanes and polyureas. They found the N-methyl substituted polymers to have a higher thermal stability in nitrogen than the unsubstituted polymers[13]. This was explained by a change in the decomposition pathway. Unsubstituted polymers can degrade by a low-energy hydrogen transfer to form the corresponding isocyanate and alcohol or amine. In N-methyl substituted polymers, this pathway no longer exists.

The products of pyrolysis when placed in a mass spectrometer support the decomposition pathway for unsubstituted polymers as a depolycondensation process[14]. For N-disubstituted polyurethanes with an aliphatic chain attached to the oxygen, the degradation occurs through a transition state involving a six-member ring[14].

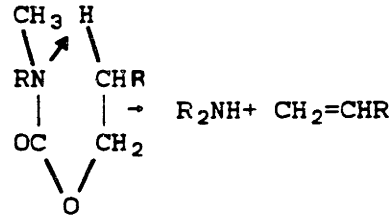

In N-disubstituted polyurethanes that contain aromatic groups attached to the oxygen, a cyclic compound was isolated[14].

Grassie and Zulfiqar studied the formation of products such as amines, ureas, olefins, and carbon monoxide[15]. A polyurethane prepared from 1,4 butanediol and diphenylmethane-4,4'-diisocyanate (MDI) was used for this study. By thermal volatilization analysis and infrared spectroscopy on collected fractions, they concluded that the primary process was depolycondensation. This was determined in part because thermogravimetric analysis in nitrogen had a lower weight loss than under vacuum, and they felt the nitrogen reduced the diffusion rate of products out of the film, allowing them more time to undergo secondary reactions. Further support came by measuring the production of carbon dioxide with varying film thickness. If carbon dioxide is produced from a secondary

reaction, more should be produced with a thicker film, because the primary products will have less chance to diffuse out and are more likely to undergo secondary reactions with the surrounding material.

Butanediol undergoes secondary reactions giving tetrahydrofuran and water. The isocyanate can undergo reactions to produce carbodiimide and CO_2, which were found as degradation products. When the carbodiimide was degraded with butanediol at 350°C dihydrofuran, carbon monoxide, tetrahydofuran, water, butadiene, and hydrogen cyanide were obtained.

The addition of a polyester soft segment to the MDI-butanediol system changes the thermal decomposition[16]. Grassie, Zulfiqar, and Guy synthesized the polyester from adipic acid, ethylene glycol, and propylene glycol. There was an increase in stability and a decrease in the amount of residue at 500°C with increasing soft segment content. The residue decreases because the polyester decomposes to volatile products, while the urethane decomposition products can undergo secondary reactions to produce nonvolatile material. In the degradation of these urethanes neither carbodiimide nor any of the degradation products of carbodiimide and butanediol, (dihydrofuran, CO, HCN, and butadiene), could be detected. It was suggested that carbodiimide was not formed due to increased amine formation by the acid groups formed from ester group decomposition. The amine groups then react with isocyanates to give urea structures. The decomposition products of butanediol, tetrahydrofuran and water, were obtained. The other volatile products were ethylene,

propylene, carbon dioxide, ethylene and propylene oxide, acetaldehyde, cyclopentanone, adipic anhydride, aniline, ethylene glycol, and propylene glycol.

Grassie and Mendoza[18] studied the thermal degradation of polyethylene glycols, often used as a soft segment material, by the use of infrared, mass spectroscopy, gas-liquid chromatography, and gas chromatograpy - mass spectroscopy (GC-MS). The presence of the observed products, such as formaldehyde, ethylene oxide, propane, butane, methoxyacetaldehyde, and ethoxyacetaldehyde, could be explained by a random scission mechanism at either the C-O or C-C bonds. Two products, water and ethylene glycol, were explained on the basis of reactions occurring at the chain ends. These reactions may be helpful in studying any fatigue degradation products from the polyether soft segment of our material.

Davis and Golden[17] studied the thermal degradation of polytetramethylene oxide, the soft segment material used in our study. When heated in air at 111°C the polymer was completely degraded, but under vacuum the degradation was significantly less. After the initial degradation in vacuum the polymer was stable to temperatures in excess of 150°C. Above this temperature the polymer completely degraded. The lower temperature degradation was attributed to peroxide groups formed in the presence of air, while scission directly on the polymer chain was believed to occur at higher temperatures. Analysis of the volatile products formed from pyrolysis showed a large number of components, none

of which were a major fraction. There was no monomer found. Infrared analysis showed the presence of an OH and an aldehydic C=O band.

Thermogravimetric analysis(TGA) of several polyurethanes in nitrogen, prepared from TDI and MDI, indicated that the polymers were stable up to their melting points (melting points 203-320°C) [19].

Engel, Reegan, and Weiss investigated the stability of crosslinked polyester urethanes. A series of polymers were prepared from branched polyesters and MDI [20]. The branched polyesters were prepared by reacting adipic acid with trimethylol propane, and a mixture of ethylene glycol and trimethylol propane, with adipic acid. Heat aging tests showed that decomposition increased with increasing urethane/ester ratio. If the urethane/ester ratio is held constant, the crosslinking density does not appear to have any effect. Samples lost weight at a higher rate in nitrogen than in air indicating that decomposition proceeds through a nonoxidative reaction of the urethane group.

The TGA showed that the decomposition temperature increased with decreasing urethane/ester ratio. Again crosslinking density showed no effect. The TGA traces were almost identical for both air and nitrogen.

Polyether glycol-TDI polymers decompose at 200°C in both vacuum and helium, mainly through urethane group dissociation [11]. Random decomposition of the polyether begins at 250-320°C.

Ferguson and Petrovic studied a series of amine-cured polyurethanes, prepared from TDI and polytetrahydrofuran, which would be similar to our system, by TGA and DTA in air[21]. The temperature at 10% weight loss was lower for pure soft and pure hard segment than expected from the data of intermediate compositions. This suggests that there may be mutual stabilization. There are two stages of degradation in the TGA; the stability (temperature at 10% weight loss) in the initial stage, increases as the concentration of soft segment increases. In the later stage of degradation, the stability (temperature at 50% weight loss) decreases with increasing soft segment concentration. For two different soft segment molecular weights, the stability seemed unaffected. The polyurethanes were also degraded in nitrogen, which showed a result similar to air degradation. The initial stability increased with increasing soft segment concentration.

The DTA showed an exothermic peak (labeled β) where the rate began to rise sharply. This was followed by an endothermic peak (γ) at the maximum rate of weight loss. At higher temperatures another exothermic peak (δ) was noted. Neither of the exothermic peaks were found when the polymer was degraded under nitrogen. It was determined that the β peak was due to oxidation of the soft segment and the δ peak to oxidation of the hard segment.

Ferguson and Petrovic summarized the degradation as follows: initial weight loss was due to cleavage of the urea and urethane bonds. The soft

segment degradation begins near 300°C, with the initial oxidation of polytetrahydrofuran (PTHF) believed due to oxygen attack on the carbon α to the ether oxygen. The γ peak is probably caused by oxidation products evaporating. The δ peak is most likely associated with the oxidation of aromatic residues.

Flynn, Pummer, and Smith obtained kinetic parameters from TGA with a heating rate of 2°C/min[22]. These kinetic parameters can be compared to the kinetic parameters obtained by thermogravimetric analysis for our system. Two polyurethanes were prepared, one from MDI and a 1,000 molecular weight diol synthesized from tetrahydrofuran and butanediol, and the other from a slightly crosslinked TDI polymer with the same polyether and butanediol. Activation energies of about 38 kcal/mole were obtained for both polymers. Above 5% weight loss the activation energies decreased slowly.

Gaboriaud and Vantelon studied the thermal degradation of a polyurethane prepared from MDI and propoxylated trimethylol propane by pyrolysis and TGA under helium[23]. Activation energies of 34.8 and 35.8 kcal/mole for dynamic and isothermal methods, respectively, were obtained. The isothermal analysis indicated random scission.

Colodny and Tobolsky made stress relaxation measurements on a series of polyurethanes prepared from 2,4 TDI and a polyester made from 80-20 mole% ethylene-propylene adipate[24]. Some of the polymers were

crosslinked to give either a urethane crosslinked product or a product with biuret and urea groups. Stress relaxation was performed over a range from 100 to 140° at 20% elongation. They found activation energies for the linear polymers, calculated from the temperature dependence of the characteristic relaxation time, to be approximately zero. The activation energies for the crosslinked polymers were about 30 kcal/mole. The cleavage reactions were believed due to the urethane, urea, and biuret groups. The relaxation times, which are inversely proportional to the rate constants for chain scission, for the samples with urethane linkages were five times larger than for the samples with urethane, urea, and biuret linkages. It can be seen that the urethane-only polymers have a much lower rate constant for chain scission than for a urethane, urea, and biuret containing polymer. Stress relaxation on polyester and polyether urethanes gave similar rates of decay, indicating that neither the polyester nor the polyether were the sites for the cleavage reaction[25].

Further work on the stress relaxation of polyurethane networks showed two stress decay processes[26]. The slower process was directly related to the amount of urethane groups in a network chain. Singh and Weissbein suggested that the faster process was due to weak links such as substituted urea, mixed anhydride, biuret, or allophanate groups. The rate of the slower process was independent of the concentration of urethane groups per unit network volume and appeared linear, suggesting that the urethane bond breakage followed an apparent first order rate

equation. The activation energy for this reaction was calculated to be 29.6 kcal/mole.

Singh, Weissbein, and Mollica compared polyether and polyester urethanes to determine the relative stabilities of these polyurethanes[27]. The polyester was polyethylene adipate glycol and the polyether was polytetramethylene ether glycol. The isocyanate was TDI and they were cured with a triol. Both continuous and intermittent stress relaxation were carried out. The intermittent relaxation should give an indication of the reversibility of the reaction. The continuous relaxation curves showed that the rate of chain scission was greater for the polyether than for the polyester. The intermittent curves showed that the polyester chain scission was reversible whereas the polyether was not. Comparison of continuous relaxation curves for the polyester based urethane in air and nitrogen showed the chain scission was not oxidative in nature for the polyester. The polyether showed differences in air and nitrogen. The curve was similar to the polyester when under nitrogen, but not when run under air, indicating some oxidative process was occurring in the polyether. The intermittent stress relaxation data supported this and showed that the polyether chain cleavage in air was oxidative and irreversible. In contrast, the polyester chain scission was reversible in both air and nitrogen.

In conclusion, most of the literature indicates that in thermal degradation the initial reaction is the dissociation of the urethane,

urea, allophanate, or biuret bond. The products from this reaction can undergo subsequent reactions. The polyether or polyester will degrade at slightly higher temperatures (50° or more higher) to form a variety of products. These reactions can produce chain scission, so if they occur during fatigue, we would expect the changes in properties to reflect this. One change due to chain scission might be a decrease in the crosslink density, which can be determined by swelling or modulus measurements. Fatigue effects on the two-phase nature of the polyurethane will have to be investigated and taken into account in making these measurements.

Infrared spectroscopy can be used to determine what types of chemical reactions are occurring, and these can be compared to reactions reported in the literature.

3. Experiments and Results

3.1. Materials and Specimen Preparation.

The material chosen for this study was a commercial polyether polyurethane-urea system, prepared from a toluene diisocyanate (TDI) prepolymer and a diamine curative, trimethylene glycol-di-p-amino benzoate. The urethane is not so highly compounded as the traditional elastomers, and this simplifies many of the analytical techniques needed for its analysis. Also, this material has shown good wear resistance in rough-terrain track testing, and is a possible replacement for more traditional rubber compounds.

Molded blocks, 2.5 in. x 2.5 in. x 3 in., were prepared by the following method. The diamine curative, an off-white granular powder, was weighed into a beaker covered with aluminum foil. The beaker was then filled with argon gas, which served to reduce the exposure of the contents to atmospheric moisture. The prepolymer, a light amber to colorless solid, was weighed in a similar manner. For a 350g test block, the weight of prepolymer was 293.1g and the weight of the curative was 57.9g. An extra gram of curative was included to compensate for the loss that occurred during pouring.

The prepolymer was heated in a 100°C oven and the curative

(m.p. 140°C) was melted in a 150°C oven. Dissolved gases were removed from the melted curative by a vacuum desiccator attached to two mechanical vacuum pumps. When degassing was complete the curative was returned to the oven. The molten prepolymer was then degassed and allowed to cool to 90°C. The curative was removed from the oven, poured into the beaker containing the prepolymer, and mixed quickly with a wooden dowel. Complete mixing required about 20 seconds. The polyurethane mixture was then degassed for approximately two minutes to remove any gas entrapped during the mixing procedure. The removal of gas was indicated when a head of foam formed on the mixture and then broke. The beaker was then taken out of the desiccator and the polymer was quickly poured down the stirring rod into a preheated mold (100°C), which had been sprayed with a silicone mold release. After filling the mold, the top plate was put back on and the mold was placed in the 100°C oven. After 45 minutes the block had set up and could be removed from the mold. The block was returned to the oven and allowed to cure at 100°C for four to five hours.

Several problems occurred during polymer preparation because of the short working pot life of four minutes and the low prepolymer preheat temperature relative to the melting point of the curative. When the prepolymer is not heated to a sufficiently high temperature, the curative will solidify, producing small curative flakes throughout the specimen. In the initial attempts at specimen preparation this problem produced blocks with incorrect stoichiometry, as well as reduced properties

because of the crack initiation sites in the curative flakes. With the prepolymer and/or curative at too high a temperature, the pot life of the polyurethane is reduced due to the increased reaction rate of the components at higher temperatures. This resulted in premature gelation, which occurred twice before degassing was complete.

Using better temperature control and the method described above, it was possible to prepare blocks which were essentially free from gas bubbles and were well mixed. The use of two vacuum pumps allowed the polymer mixture to be degassed with sufficient time for pouring before gelation. Six test specimens were prepared in this manner. The blocks were aged for two weeks at room temperature before testing. Four blocks molded by the manufacturer were also tested.

The blocks were trimmed with a band saw and sanded to final dimensions of 2.5 in. x 2.5 in. x 2.5 in. before fatigue testing. The blocks were kept cool during machining, because heating might affect the polymer's properties.

Preparing specimens for later analysis presented some problems, since most cutting equipment causes extreme heating. Because heating would interfere with the results, the following method was devised. Specimens for swelling and Rheovibron tests were first cut using a water cooled saw, then sliced into thin strips with a microtome. The initial cut was approximately 1/2 inch from the center of the block, 1/2-inch wide, and

cut parallel to the loading direction. The microtome slices were made as close to the center of the saw cut piece as was possible. The very center of the piece usually had large cracks, making it impossible to use for these tests. The microtome slices were made perpendicular to the loading direction.

3.2. Fatigue Testing.

Compression-compression fatigue testing was done on all blocks with a servohydraulic Instron model 1331. Different maximum loads were used to determine what effects loading conditions made. Compression-compression fatigue data were obtained at a frequency of 6.5 Hz and a 0.1 ratio of minimum-to-maximum stress. The specimens were tested between two parallel flat plates, with a sinusoidally varying load. The testing was done in load control mode on the Instron, because it was felt this would more accurately simulate tank track pad conditions. To prevent the blocks from slipping out of the test machine, double stick tape was placed between the specimen and the plate. The temperature of the blocks was monitored during testing by a digital thermometer connected to two thermocouples, which were inserted into holes drilled at the center and halfway between the center and top of the block as shown in Figure 1[66]. For specimens 1-3 only the center temperatures were recorded.

The loading conditions for all the blocks are shown in Table 1. The maximum temperature measured is shown next to the cycle count at which

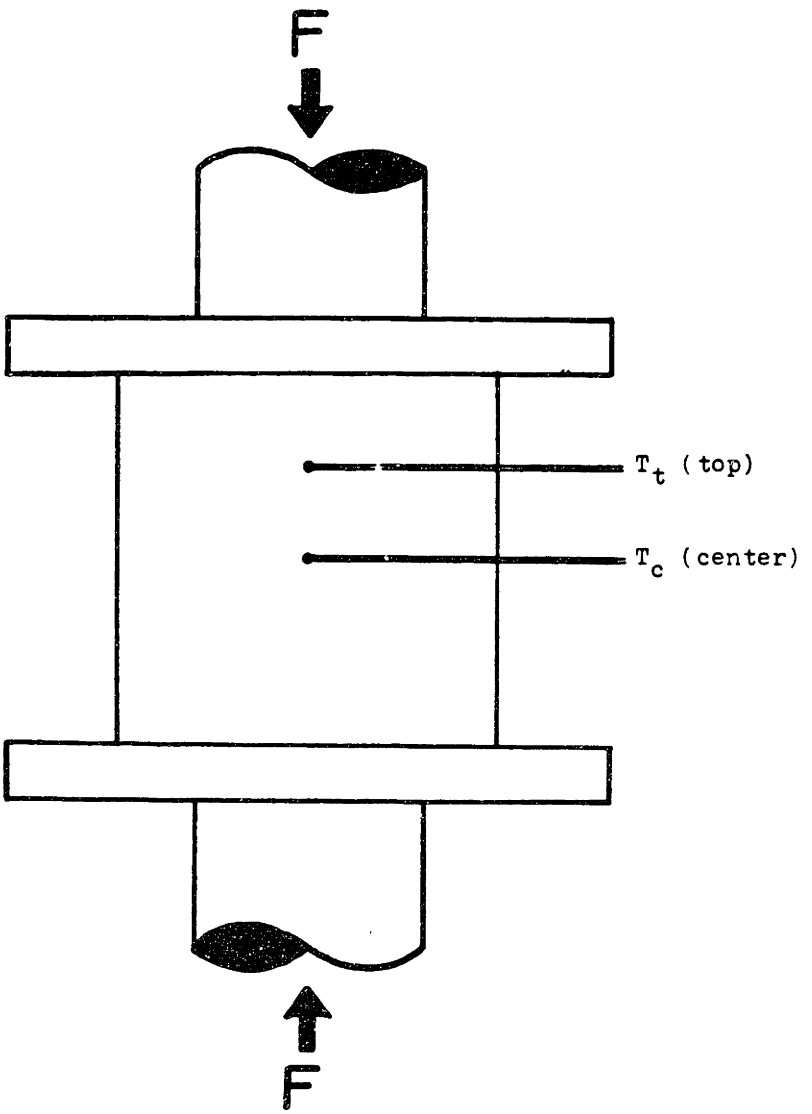

Figure 1. Test Geometry[66]

the maximum temperature was measured. Often the final test temperature could not be measured because of thermocouple failure.

Table 1. Fatigue Test Data

Specimen#	Max Load(lb)	Max Temp(C)-Cyles	Failure-Cycles
1	variable	177	failure
2	6,000	170-8,240	failure-9,270
3	6,000	140-7,416	stopped-7,416
4	8,000	?	failure-3,714
5	6,000	156-3,710	failure-5,355
6	5,000	170-8,285	failure-8,367
7	5,000	155-7,975	stopped-8,000
8	6,000	173-2,725	stopped-4,284
9	6,000	120-2,110	stopped-3,214
10	4,500	91-54,000	stopped-2,182,610

All blocks were 2.5 in. high with the exception of blocks number 2 and 3, which were 3 in. high. Blocks numbered 1-3 and 10 were obtained commercially. The corresponding maximum stresses for the maximum loads of 8,000 lbs, 6,000 lbs, 5,000 lbs, and 4,500 lbs were 1,280 psi, 960 psi, 800 psi, and 720 psi, respectively. The testing we have done is not fatigue testing in the usual sense due to the small number of blocks tested. The extensive analysis required for each block, in order to determine the failure mechanism, limited the total number of blocks that could be tested.

During compression fatigue testing of the polyurethane blocks temperature data were collected and are shown in graphs of temperature versus number of compression cycles. The temperature rise at a similar

thermocouple position for all blocks tested at a given load is shown the graphs, with the exception of block number 10. Figures 2 and 3 show the top and center temperatures of the two blocks tested at 5,000 lbs maximum load (blocks 6 and 7)[66]. The top and center temperatures of the three blocks tested at 6,000 lbs maximum load (blocks 5,8,and 9) are shown in Figures 4 and 5[66]. Figure 6 contains the center and top thermocouple temperature data for block number 10, which was tested at 4,500 lbs maximum load.

To measure block temperatures during compression fatigue thermocouples inserted into drilled holes appear to be an acceptable method. As may be seen in the temperature plots, the data are relatively free from scatter. However, in some of the graphs a break in the curve is found near the end of the test. The temperature is seen to drop, then continue to rise with a similar slope as before, although at slightly lower temperatures. This scatter may be explained by thermocouple slippage. As the blocks crack during testing the thermocouple may be displaced toward cooler portions of the specimen; the temperature continues to rise as the testing proceeds, only at a lower temperature. The fact that this anomaly in the data occurs only for the center thermocouple, where the displacements are the highest, tends to support this theory.

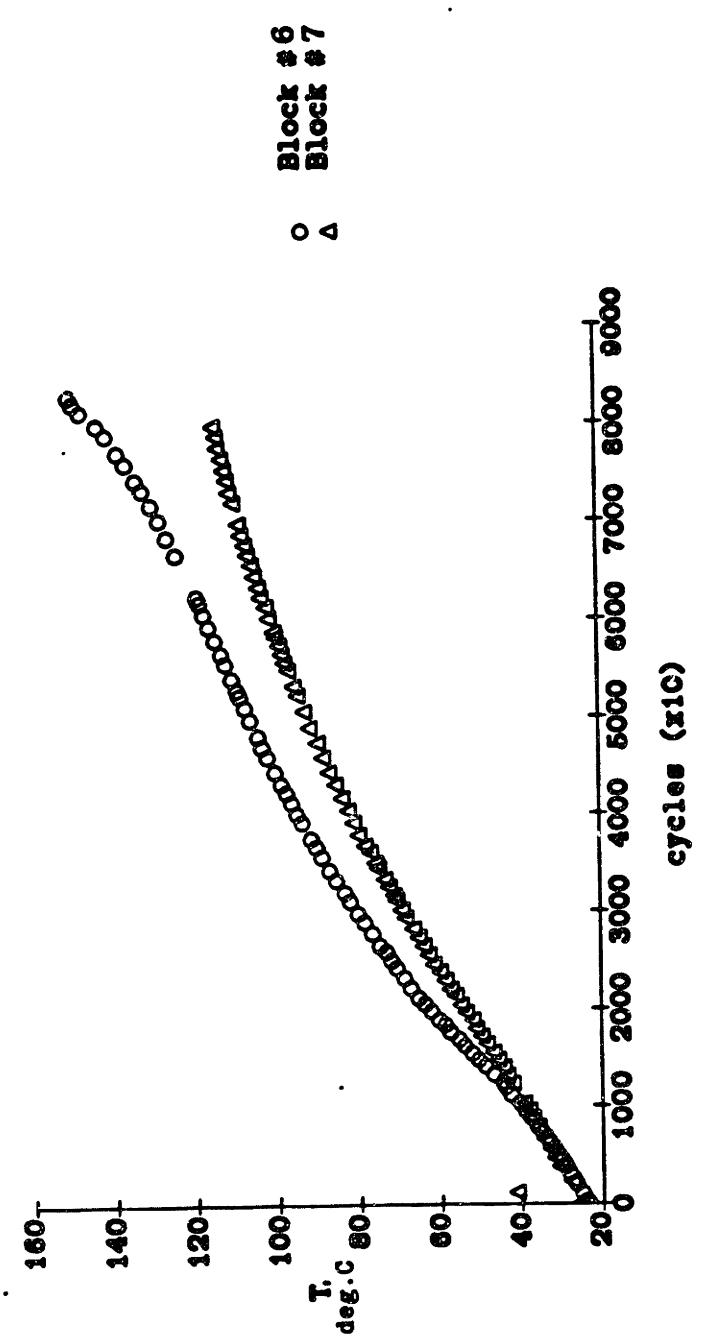

Figure 2. Top Thermocouple Temperatures (5,000 lbs)[66]

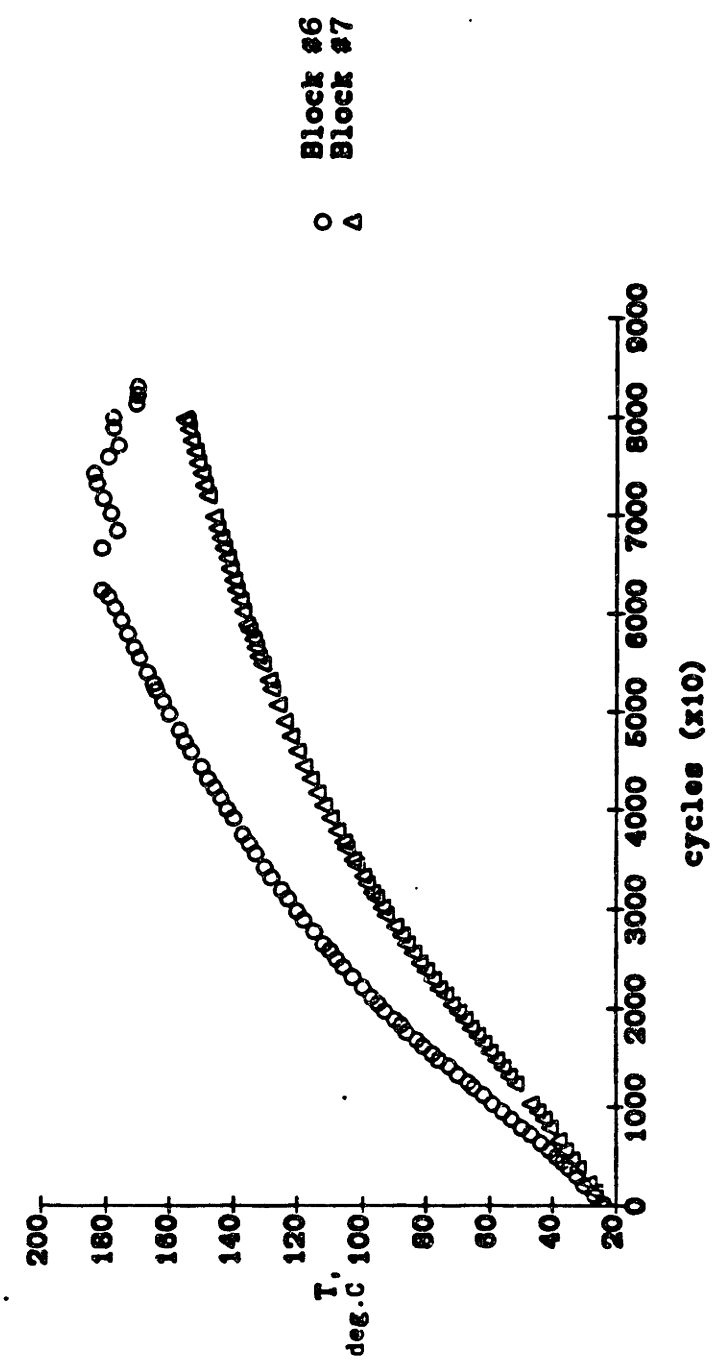

Figure 3. Center Thermocouple Temperatures (5,000 lbs)[66]

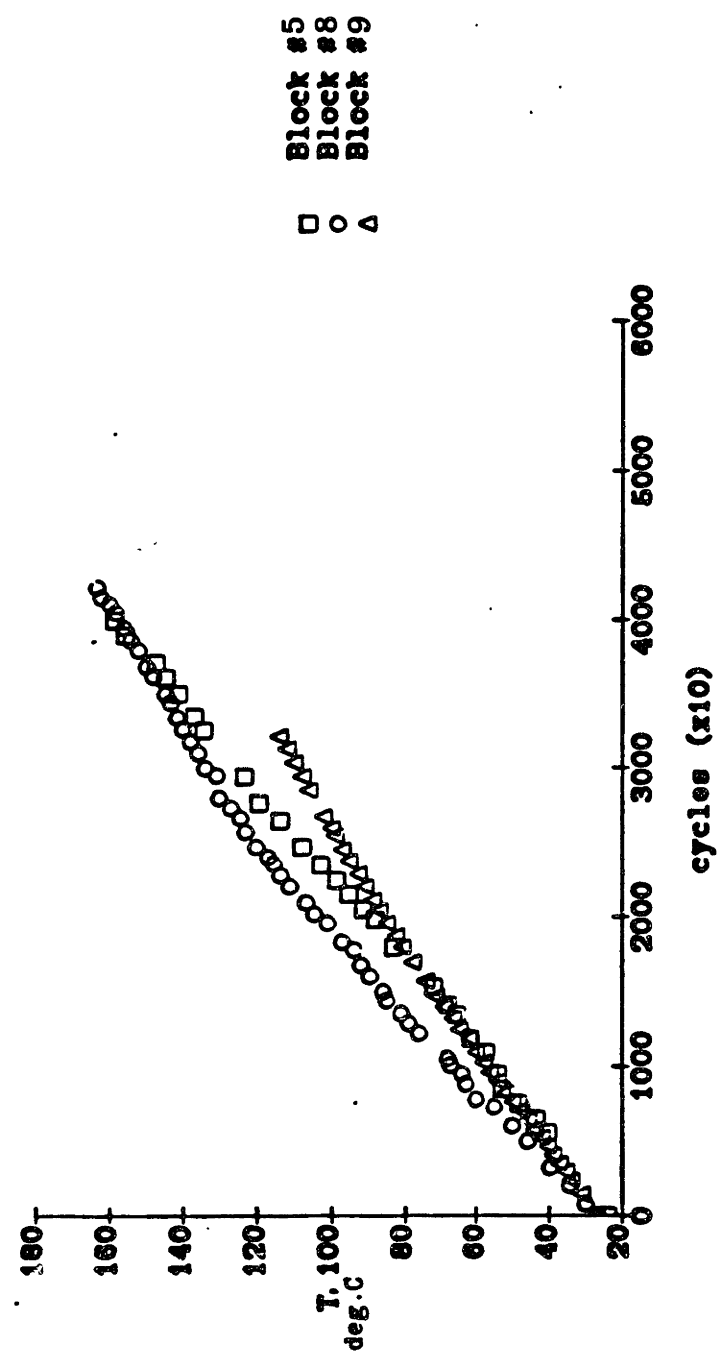

Figure 4. Top Thermocouple Temperatures (6,000 lbs)[66]

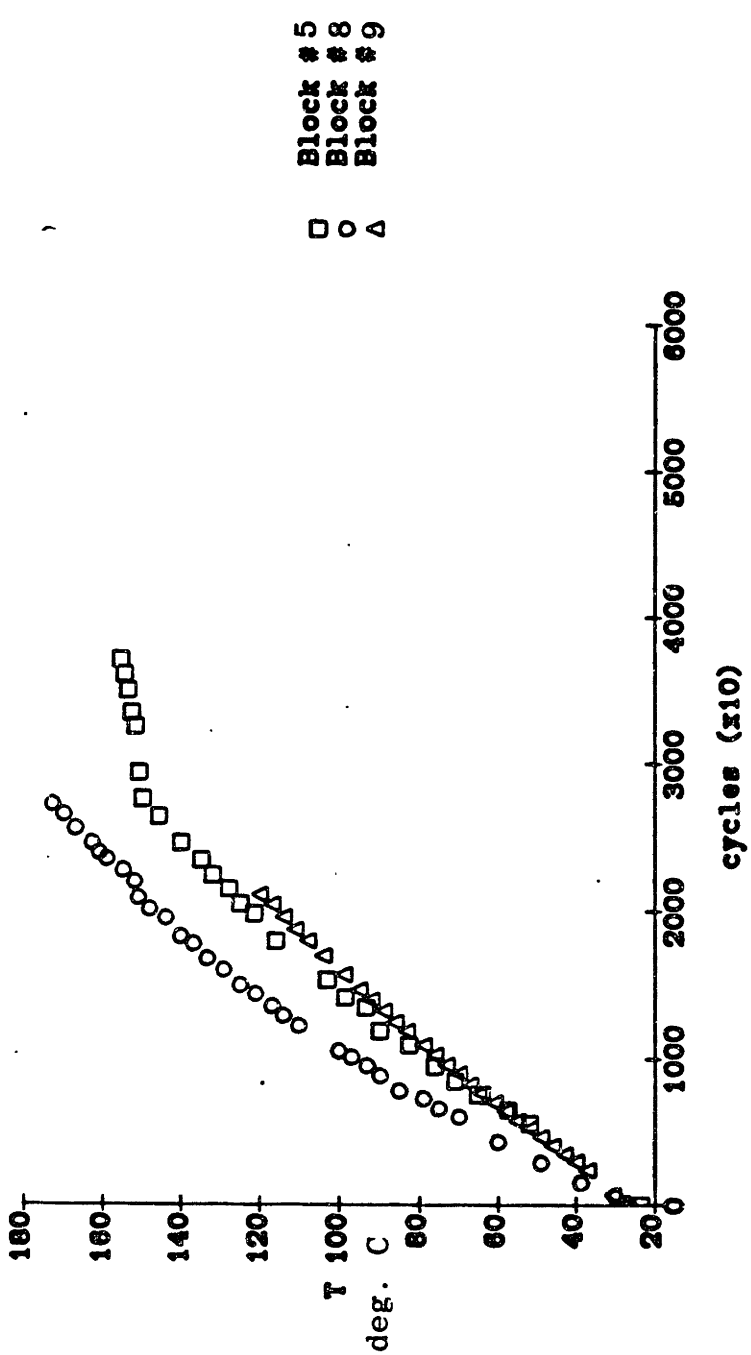

Figure 5. Center Thermocouple Temperatures (6,000 lbs)[66]

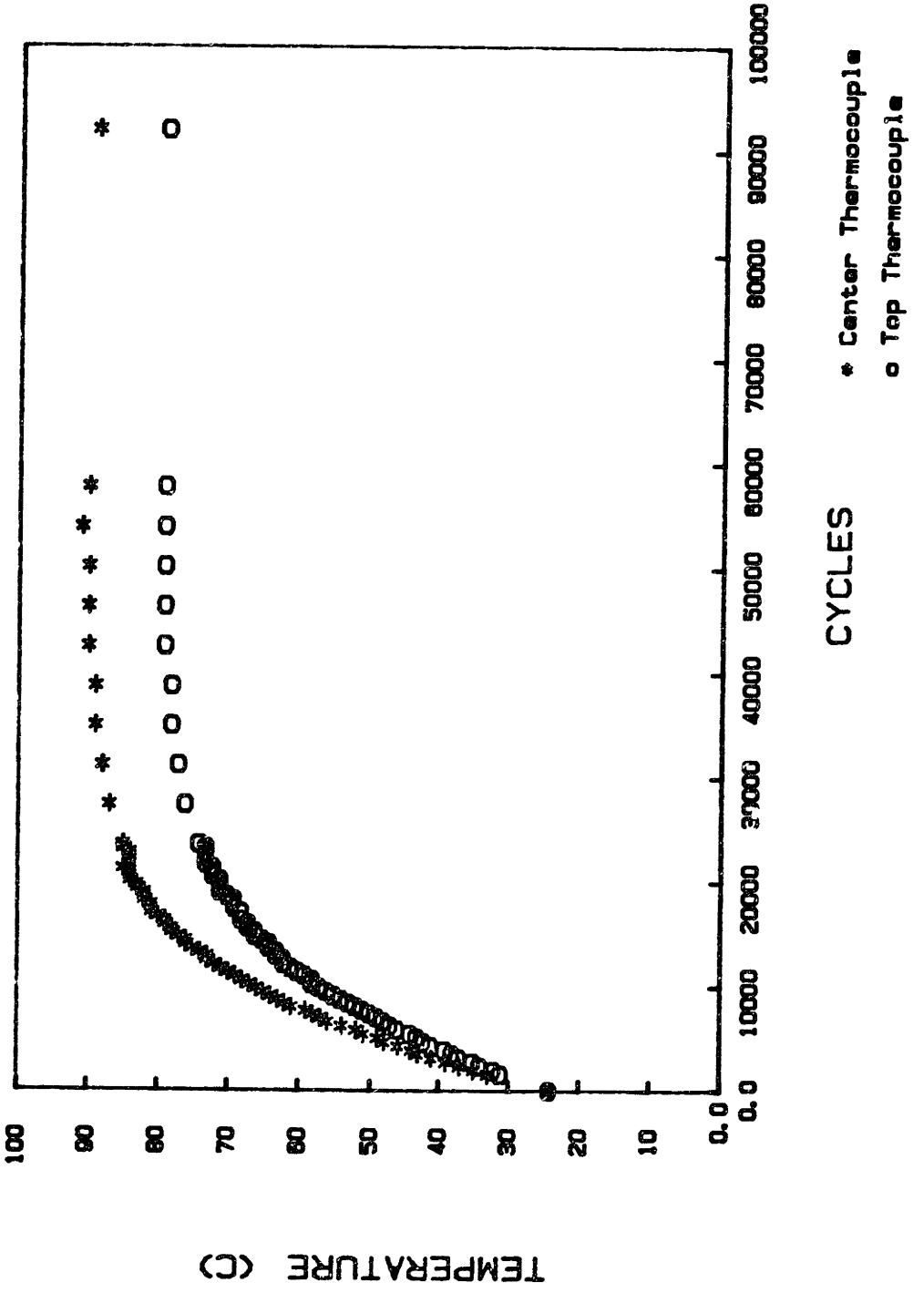

Figure 6. Thermocouple Temperature Data (4,500 lbs)

3.3. Approximate Thermal Analysis.

To obtain a rough estimate of the heat build-up in the urethane blocks, the temperature rise can be calculated using the following equation for the transient state heat flow by conduction[28].

$$T_r = Q/WS$$

where T_r is the temperature rise rate in degrees/min, Q is the heat input in cal/min, W is the part weight, and S is the specific heat in cal/g-°C. The equilibrium temperature rise above ambient (ΔT) can be calculated from

$$\Delta T = RQ/60KA$$

where A is the surface area, R is the distance from the center to the surface, and K is the coefficient of thermal conductivity in cal-cm/s-cm^2 - °C. The above relation considers only the flow of heat by conduction[29]. Q can be calculated from the following equation[28]

$$Q = 0.143\ E_H$$

where E_H is the heat energy input in N-cm/s. We can determine E_H for a given cyclic loading by[28]

$$E_H = (\sigma_1^2 - \sigma_2^2)\ \omega f_d / E_c$$

where σ_1 and σ_2 are the maximum and minimum stresses, ω is the test frequency, f_d is the damping factor, and E_c is the compression modulus.

E_c is a function of the shape factor (S_F) of the test piece, where S_F is defined as the ratio of the loaded area to the force free area. The compression modulus can be calculated by[30]

$$E_c = E_o(1+2kS_F^2)$$

where E_o is the Young's modulus of the material, S_F is the shape factor, and k is a numerical factor.

From Rheovibron data a value for E_o was determined to be 1.89×10^9 dynes/cm^2. The values for E_o will vary with the temperature and the amount of deformation, but for a first approximation E_o was assumed independent of these variables. The value of S was taken to be 0.45 cal/g-°C[28], k was assumed to be 0.5, K was taken to be 0.002, and f_d was assumed to be 0.15. For a fatigue test on a 2.5 in. cube with 4,500 lbs maximum load, 450 lbs minimum load, and a frequency of 6.5 Hz, the rate of temperature rise was calculated to be 1.6°C/min. This value is close to that which was observed experimentally. Assuming that heat loss occurs only through the side surfaces an equilibrium temperature rise of 35°C was calculated. From the actual test (block #10) the temperature

rise was 65°C. This method is good for a first approximation of the heat build-up, but for a more detailed analysis, finite element modeling should be used.

3.4. Internal Stress in Compression.

In addition to understanding the heat build-up under compression, we need to be aware of the mechanical stresses that the compressed block experiences. For blocks that are bonded to end plates, the force applied can be viewed as being composed of two portions: one part is responsible for the surface displacement and a second shear displacement is added to restore points on the rubber surface to their original positions on the compression surface[33]. For a linearly elastic, incompressible, and isotropic material this stress state produces a hydrostatic pressure component within the block. This hydrostatic pressure has a maximum at the center and a parabolic decrease towards the outside. As the height of the block increases the maximum internal pressure decreases[34]. When the thickness of the block increases the effect of the constrained surfaces (shear forces) will contribute less to the stress distribution in the block[34].

Reed and Thorpe[35] determined the shear stresses in a compressed block by finite element analysis. The shear stresses were found concentrated in the top outside corners and negligible at the center. Therefore, although there may well be some small amount of shear stresses at the

center of the block, their contribution to the failure mechanism is likely to be small.

For a compressed sample with frictionless surfaces, Treloar[31] states the equilibrium strain in a compressed block is the same as the equilibrium strain for a specimen biaxially strained perpendicular to the loading direction. For Treloar's case no bulging effects occur as in our test.

Under fatigue all blocks taken to failure exhibit cracks formed at the center of the specimen. These cracks run perpendicular to the loading direction. Figure 7 shows the internal cracks, generated during fatigue testing, on a cut section of one of our specimens. Figure 8 shows the internal cracks for a clear polyurethane of a different composition than our specimens.

Buckley[32] ran compression tests on cylindrical specimens of styrene-butadiene rubber in a Goodrich Flexometer. He found a similar type of failure, with internal and/or external cracks running perpendicular to the loading direction. Although Buckley felt the stress state in his test would be much more complex than Treloar described for uniaxial compression, Buckley suggested the observed failures could be due to biaxial extension. The strains in the center of the specimen would be similar to a flat sample extended in two directions. The model

Figure 7. Specimen Cut Open To Reveal Internal Center Cracks After Failure

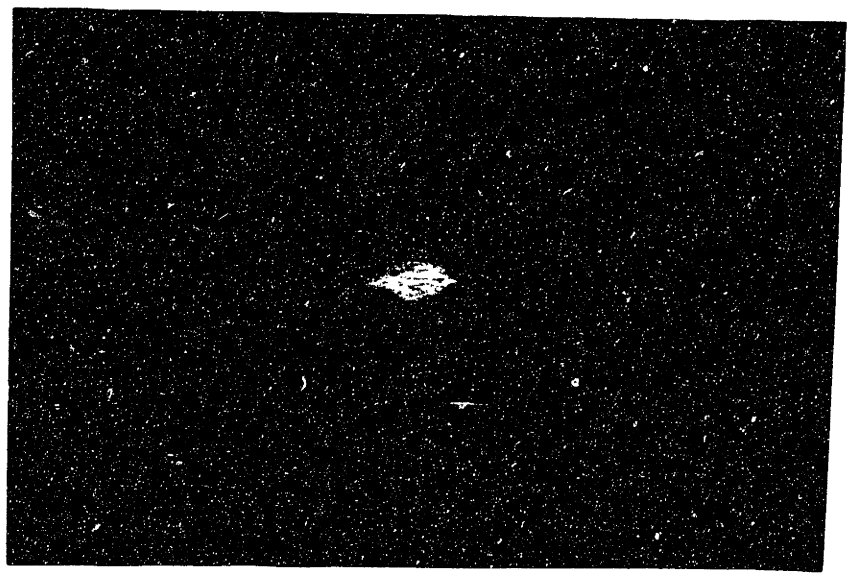

Figure 8. Uncut Specimen Showing Internal Cracks

which Buckley used to describe his failures is shown, with changes to represent a square cross-sectional surface as in our specimens, in Figure 9.

In this model the compressed specimen exhibits bulging. A slice taken from the center of the specimen, perpendicular to the loading direction, shows extensions similar to those of a biaxially stretched sample. These extensions are believed to cause biaxial tensile failure of the specimen[32].

Finite element analysis for a block loaded under 4,500 lbs maximum load gives us a better understanding of the stresses involved in the fatigue testing[36]. The finite element code used for this calculation has been described elsewhere[63] and assumes a material which behaves linearly and a linear strain displacement equation. Figure 10 shows the distorted mesh of a block loaded under uniform pressure[36]. Only a quarter of the loaded specimen is shown because of symmetry considerations. From this figure we can see that an element taken from the middle of the top edge (upper left in Figure 10) shows only downward movement under hydrostatic pressure. A center element (lower left corner in Figure 10) exhibits a compressive strain vertically and a horizontal extensional strain. Essentially no shear displacement is evident. Considerable shear displacement is seen in the upper right hand corner of Figure 10, which corresponds to the top outer edge of the loaded specimen. Upward displacement of the outer edge occurs because the finite element analysis

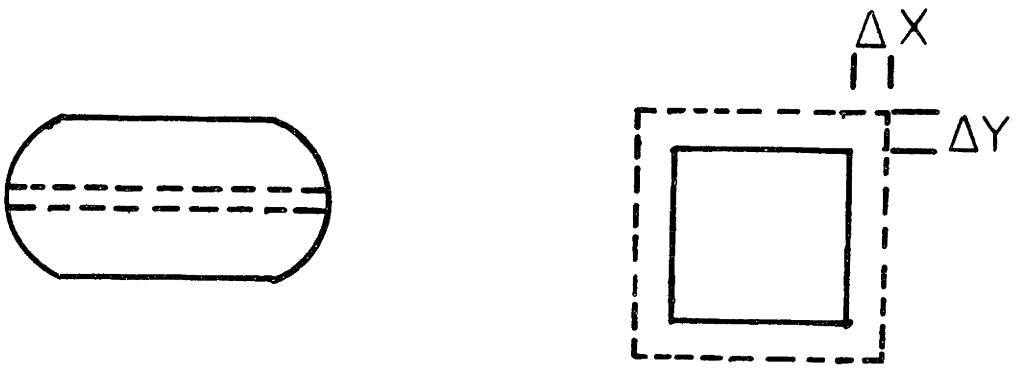

a. Compressed Block

b. Center Section

Figure 9. Biaxial Extension Model of a Compressed Block

was run under uniform pressure rather than uniform displacement. In an actual test the downward displacement is uniform, and the analysis shows the load must increase toward the outer edge to achieve this.

Figure 11 shows the distortional strain energy, which has been normalized to the maximum strain energy calculated[36]. The heat generation rate is dependent on the distortional strain energy as can be seen in Figure 12, which shows the normalized temperature contour plots. From Figures 11 and 12 we can see that the shape of the areas of highest temperatures and distortional strain energy correspond to the shape of the failure as seen in Figure 8.

The results of our testing correlate well with the experiments of Buckley and the finite element analysis. Under compression cycling heat build-up occurs; the hottest portion of the specimen being the center of the block. The center portion of the block is subjected to extensional strain, and as the temperature at the center of the block approaches the hard segment transition temperature, the material properties at the center of the specimen will degrade (high temperature properties will be addressed in a later section). This weakening of the center portion of the specimen, in conjunction with the extensional strain, causes failure at the center of the specimen.

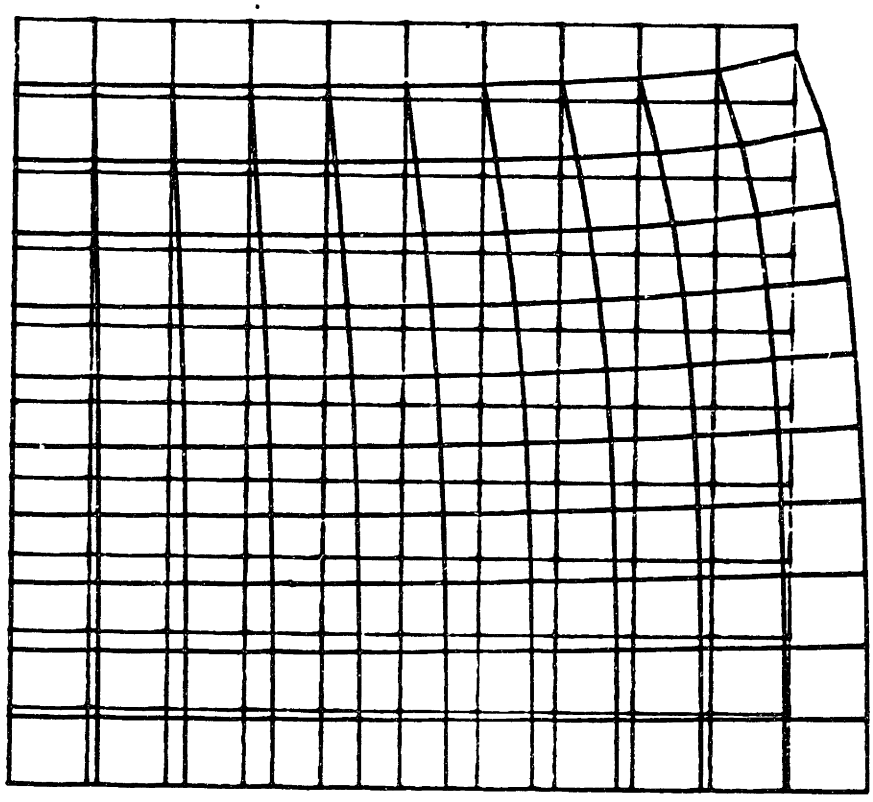

Figure 10. Distorted Mesh Under Uniform Pressure[36]

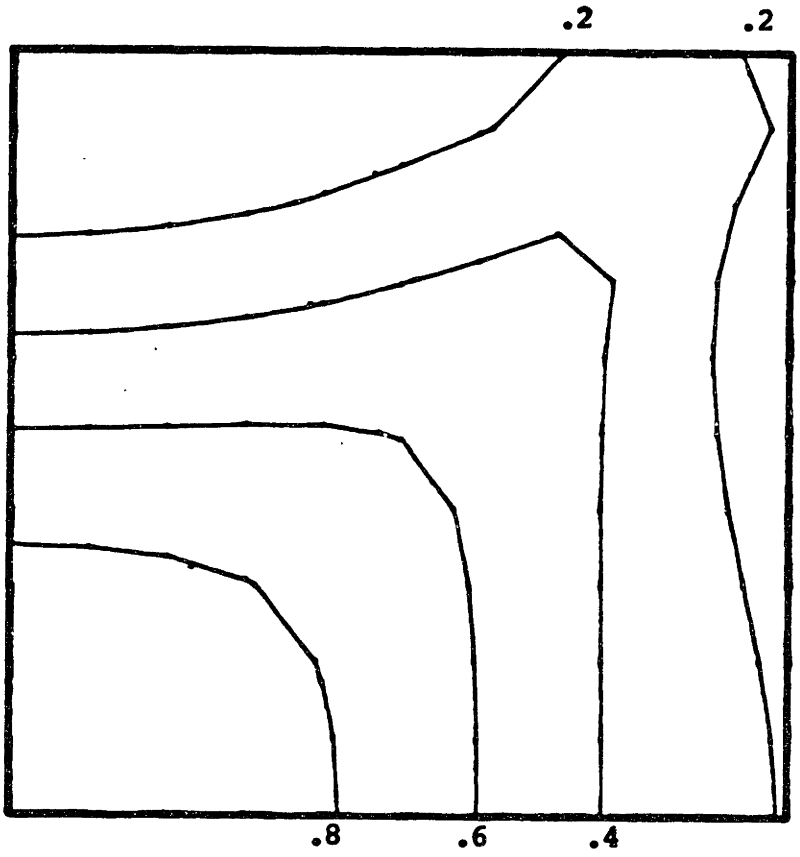

Figure 11. Normalized Distortional Strain Energy[36]

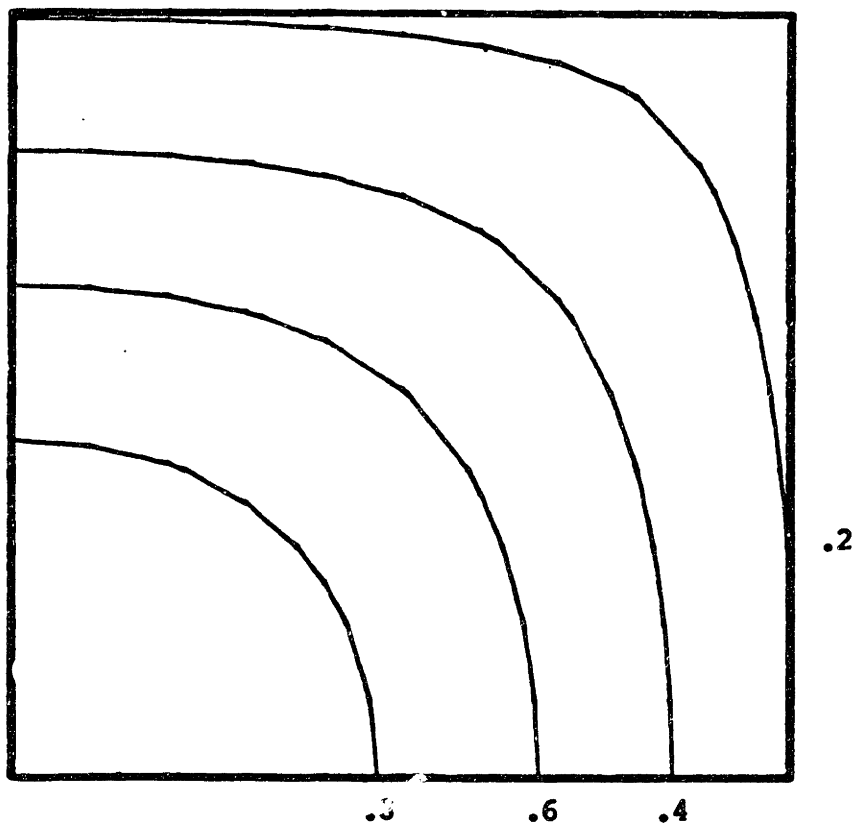

Figure 12. Normalized Temperature Contour Plots[36]

3.5. Thermogravimetric Analysis.

Thermogravimetric Analysis (TGA) can be used as a means of quantifying the purely thermal aspect of thermomechanical damage in track pad elastomers. The thermogravimetric weight-loss versus temperature curves can be analyzed to obtain a kinetic model of the process. From among several possibilities, the method of Freeman and Carroll[37] was adopted as a reasonably reliable and efficient technique. They take thermal degradation to be an n-th order rate process obeying a kinetic equation of the sort:

$$-dW/dt = kW^{n}$$

where W is the weight of material reacting and n is the order of the reaction. The rate constant k may be written as the Arrhenius relation.

$$k = Ze^{-E/RT}$$

Here Z is a frequency factor and E the activation energy for the reaction. Combining these equations and using $(dW/dt) = (dW/dT)(dT/dt)$:

$$-\frac{dW}{dT} = \rho_T = \frac{Z}{(RH)} e^{-E/RT} W^{n}$$

where RH = dT/dt is the heating rate. For a single run the difference form is[38]

$$\Delta \log \rho_T = n\Delta \log W - (E/2.3R)\ \Delta(1/T)$$

A plot of $\Delta \log W$ versus $\Delta \log \rho_T$ at equal 1/T increments should produce a line whose slope is n and whose intercept will yield E.

TGA traces were obtained using a DuPont 1090 at a heating rate of 10°C/min. A computer program has been written which will digitize the information from the TGA trace at equal 1/T increments. $\Delta \log W$ and $\Delta \log \rho_T$ are calculated and can be replotted. The TGA trace for unfatigued material (specimen 1) in nitrogen is shown in Figure 13.

There are two distinct peaks in the derivative plot, indicating more than one reaction is occurring. Each peak was analyzed separately to determine the kinetic constants for each reaction. (A similar method has been used for Laminac 4116, a styrenated polyester[39].) Data were analyzed for one process occurring from 513K - 573K, and another from 663K - 713K; these are plotted in Figures 14 and 15. There is a third peak in between the two analyzed. This peak is not well separated making it difficult to obtain data. Since no consistent results could be obtained, no data will be reported for this peak.

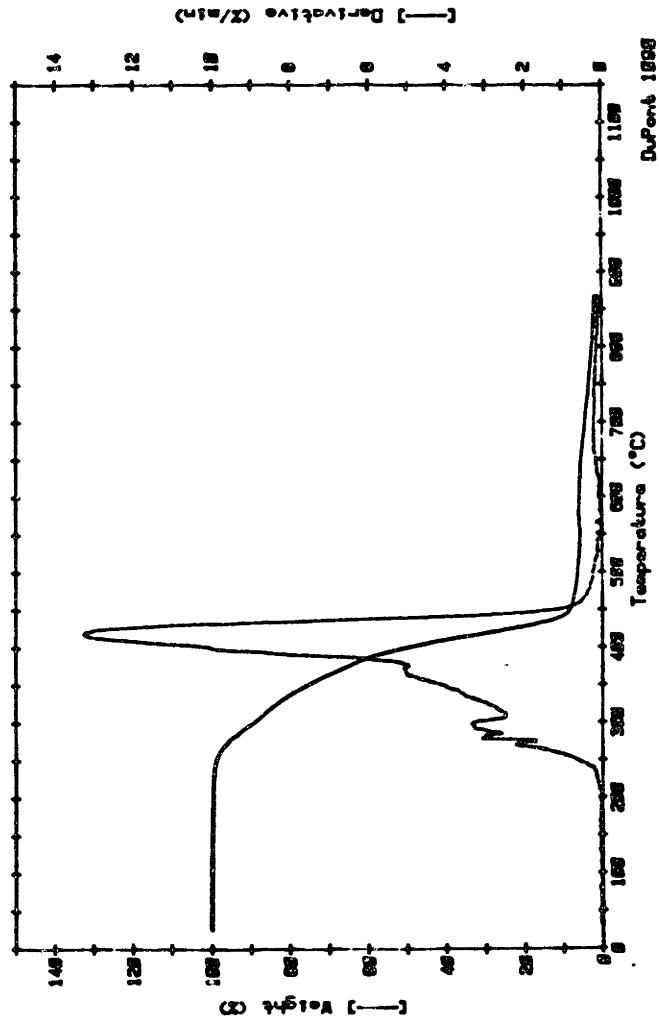

Figure 13. TGA in Nitrogen

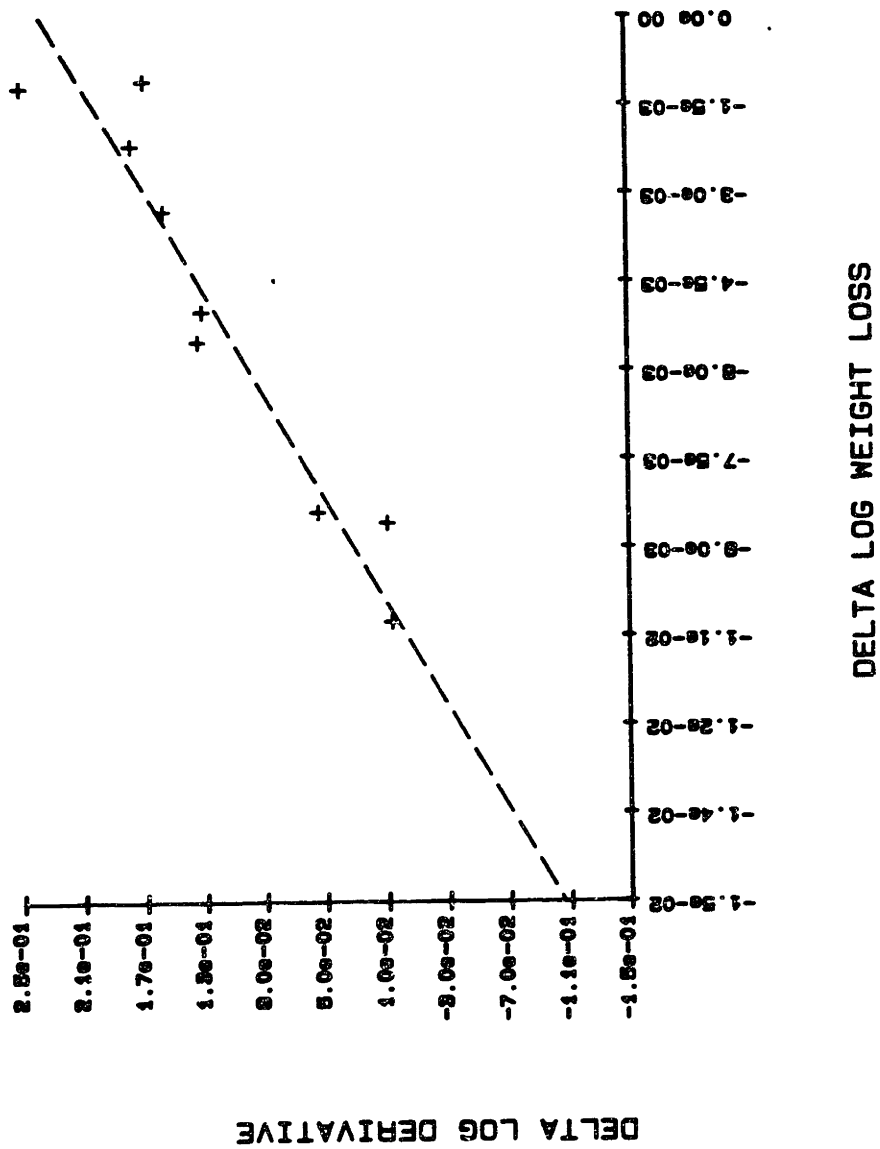

Figure 14. Freeman-Carroll Plot 513-573K

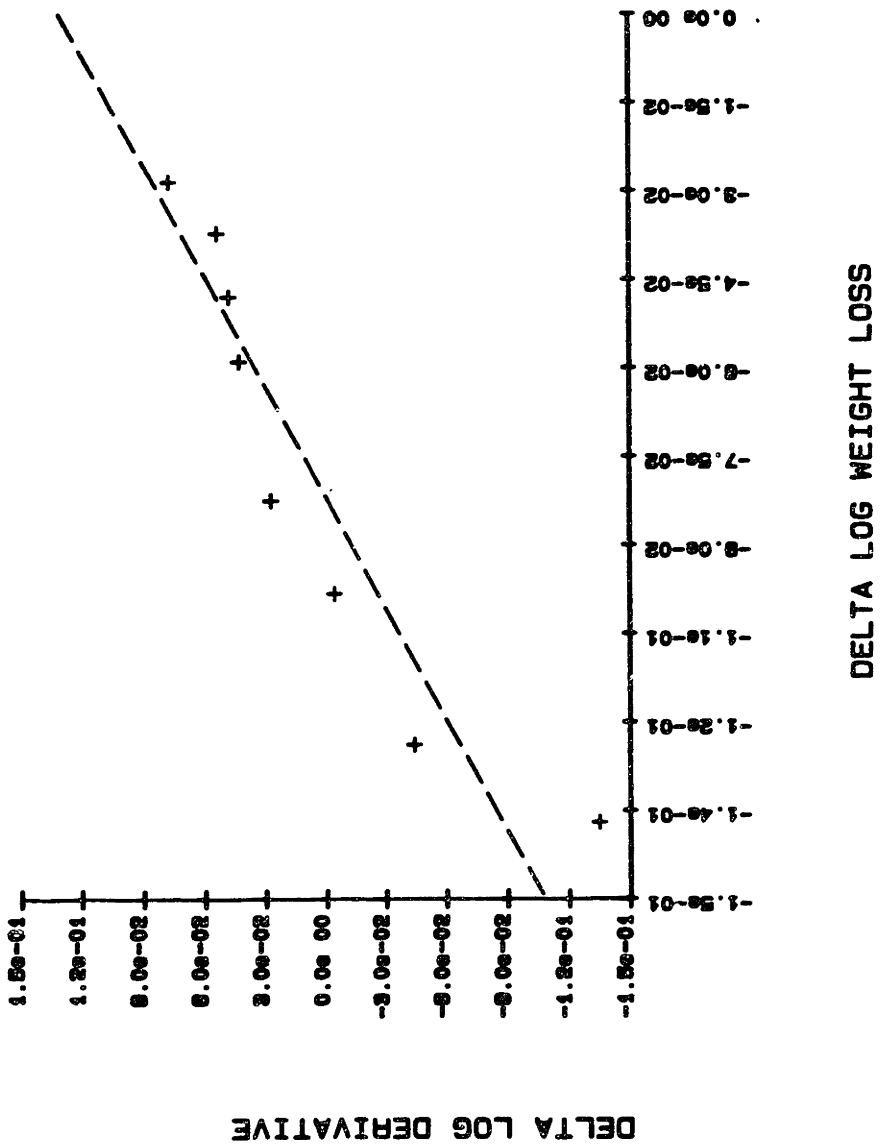

Figure 15. Freeman-Carroll Plot 663-713K

As can be seen there is some scatter, which is an inherent problem with the Freeman and Carroll method; it arises when discrete numerical data are used to construct differences of logarithmic quantities[38].

A linear regression applied directly to the difference plots seems to produce acceptable results, with correlation coefficients of at least 0.9. The regression lines are shown in the plots of Figures 14 and 15, and the numerical values extracted from the slopes and intercepts of these lines are shown in the table below:

Table 2. TGA Kinetic Data

	663-713K	513-573K
Activation energy, kJ/mole	212	198
Reaction order	1.59	2.28

Gaboriaud and Vantelon found activation energies of 145.8 and 150.0 kJ/mole for a MDI - propoxylated trimethylol propane polyurethane[23], and Flynn, Pummer, and Smith obtained an activation energy of 159.2 kJ/mole[22].

From stress-relaxation experiments Colodny and Tobolsky[24] found an activation energy of 125.7 kJ/mole, and 124.0 kJ/mole was found by Singh and Weissbein[26]. The activation energies for our system are slightly higher, but since this is a different system it is not unexpected.

From Figure 13 it is evident that no weight loss occurs before 250°C. Since the specimens fail well before this temperature is reached we can assume that no thermal degradation reactions, which give off volatile products, are involved in the failure mechanism. This does not exclude the possibility that thermal degradation reactions, which do not produce volatile products, are involved in the failure process.

3.6. Differential Scanning Calorimetry.

To investigate what changes in hard and soft segment transitions had occurred from fatigue, differential scanning calorimetry (DSC) analysis was run on specimens of unfatigued and fatigued material. Because of instrument availability some of the DSC analyses were run on a Perkin-Elmer DSC II, and a second group was run on a Perkin-Elmer DSC IV. The initial analysis was on the Perkin-Elmer DSC II, with a heating rate of 40°C/min. The specimen size was approximately 10-20 mg. For the soft segment transition an average of three runs was taken because of the broad transition range. For the unfatigued material (specimen 1) the average soft segment transition temperature was -57°C. The fatigued material (specimen 1) had an average transition temperature of -59°C for the soft segment. Typical runs for unfatigued and fatigued material are shown in Figures 16 and 17, respectively. Compression fatigue did not bring about significant changes in the soft segment transition behavior.

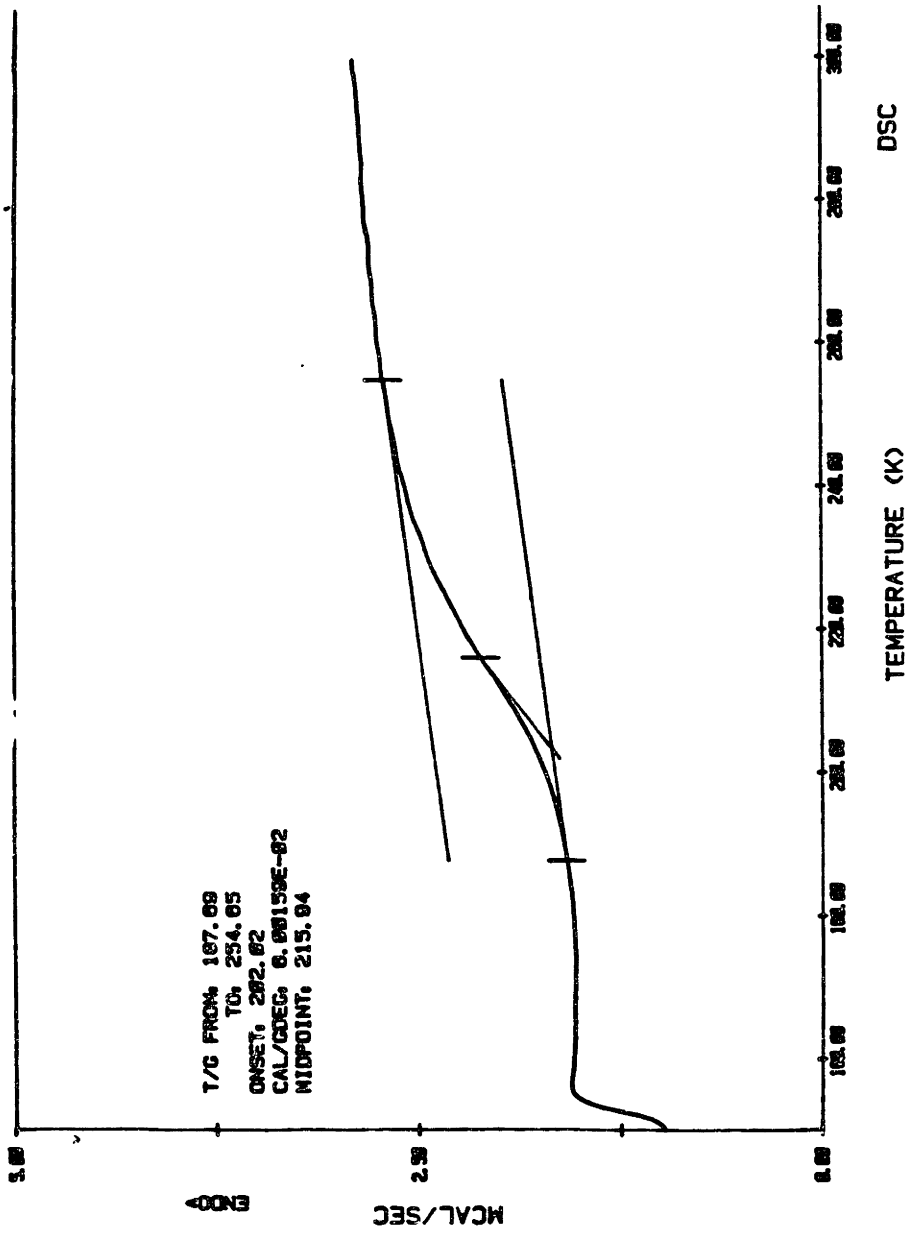

Figure 16. Soft Segment Transition Unfatigued Specimen 1

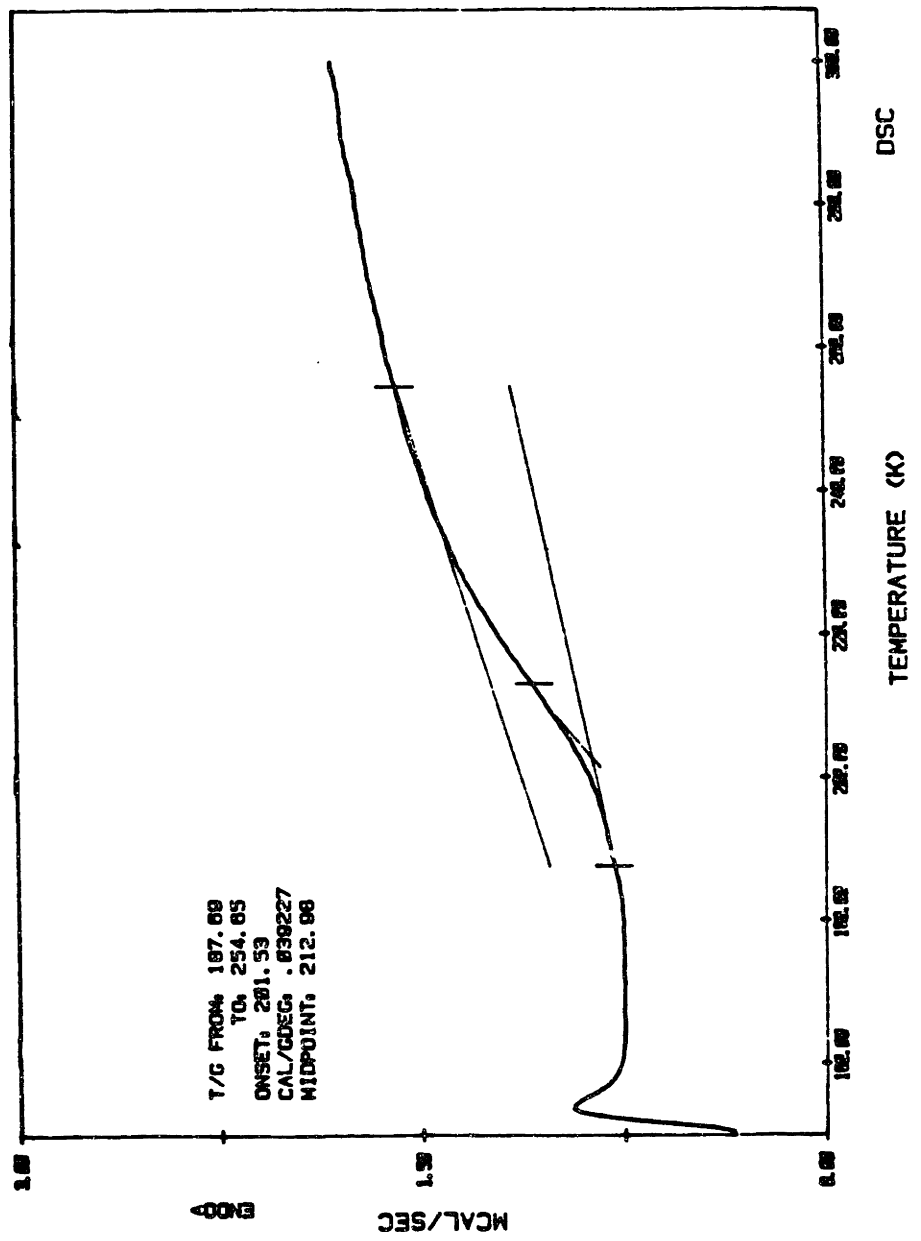

Figure 17. Soft Segment Transition Fatigued Specimen 1

The DSC runs for the hard segment transition were heated at 10°C/min in a Perkin-Elmer DSC IV. For the hard segment transition noticeable changes were brought about by fatigue. The hard segment transition temperature occurs around 180°C for unfatigued material, with what appears to be another transition 20-30° higher. When specimens are taken to failure there is only one transition, which is at nearly the same temperature as the higher temperature transition for the unfatigued material. A typical set of DSC scans is shown in Figures 18-20 for specimen #6. The transition temperatures were 179 and 205°C for the unfatigued material (Figure 18), and 213°C for the fatigued material (Figure 19). A comparison plot is shown in Figure 20.

The data for all the fatigue tests is shown below in Table 3. By comparison of values shown for specimen #9, it is evident that no changes occur in transition temperatures with blocks fatigued to this level.

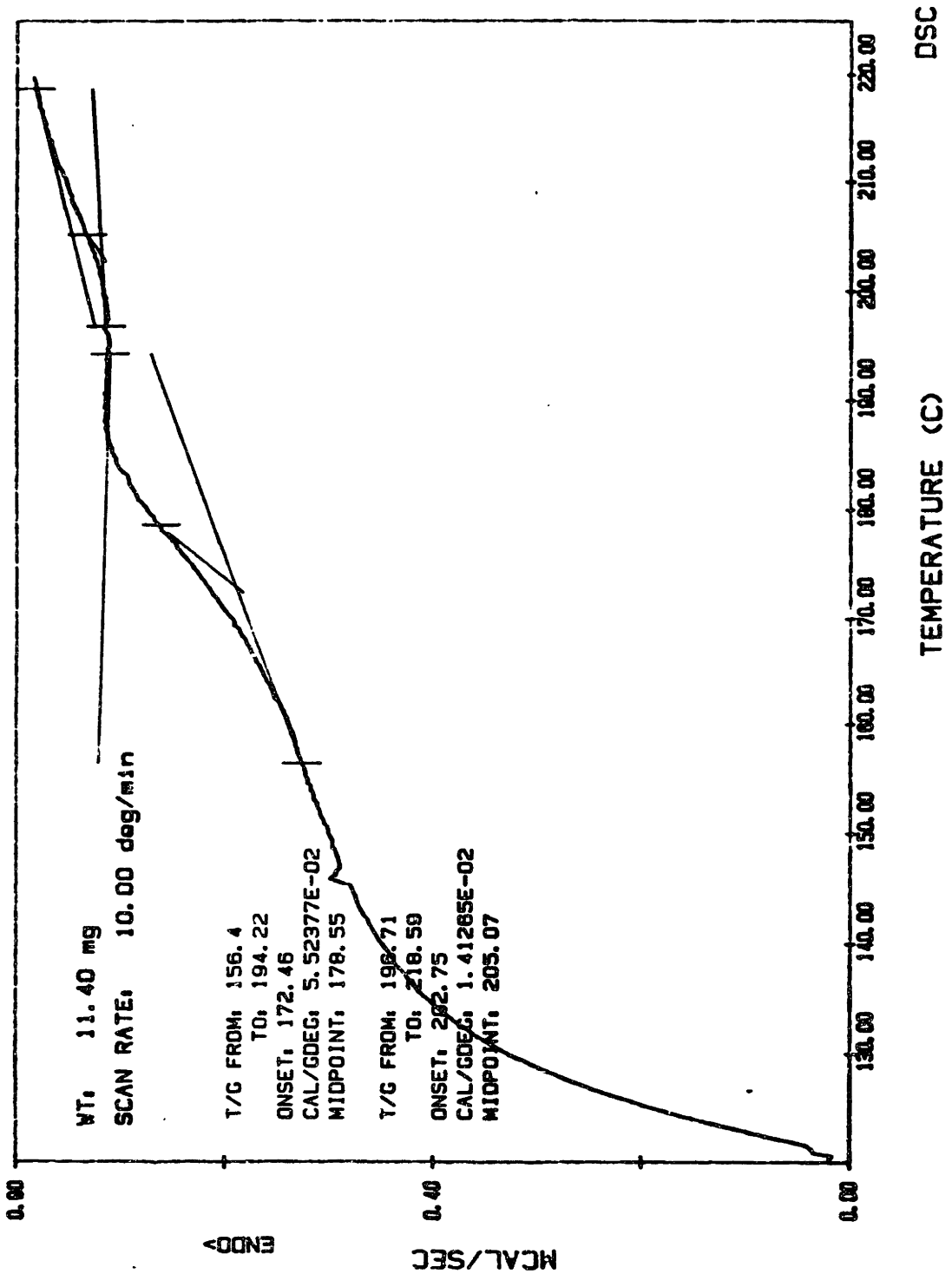

Figure 18. Hard Segment Transition Unfatigued Specimen 6

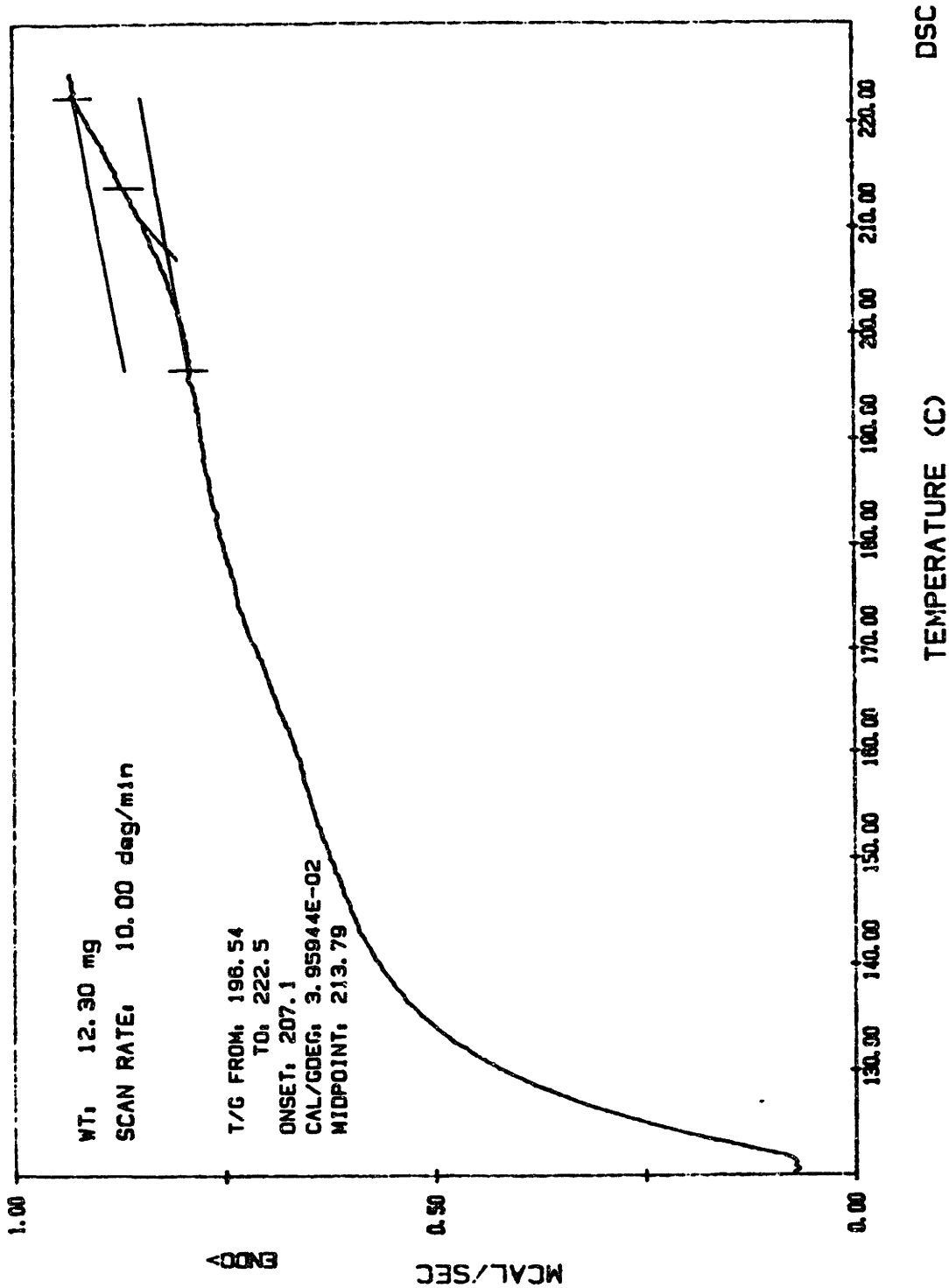

Figure 19. Hard Segment Transition Fatigued Specimen 6

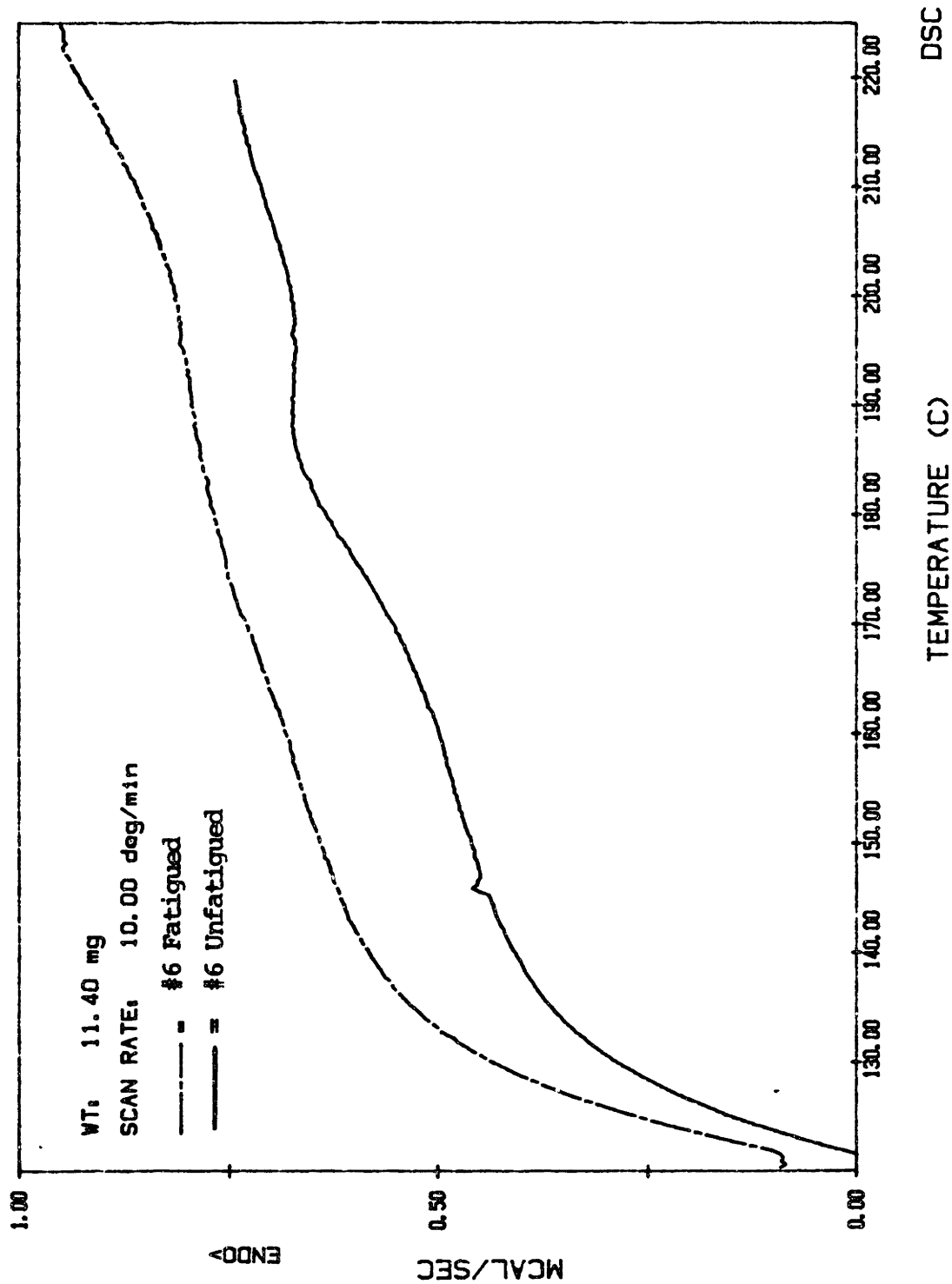

Figure 20. Hard Segment Transition Comparison

Table 3. DSC Analysis

Specimen #	Transition Temp.(C)	Transition Temp.(C)
1 unfatigued	176	204
1 fatigued	187	
2 fatigued	213	
3 fatigued	178	204
4 unfatigued	178	204
4 fatigued		202
5 unfatigued	179	
5 fatigued		207
6 unfatigued	179	205
6 fatigued		213
7 unfatigued	180	206
7 fatigued	182	213
8 unfatigued	179	208
8 fatigued		192
9 unfatigued	178	209
9 fatigued	178	209

One possible explanation for the changes in the hard segment transition after fatigue might be decreased crosslinking through the dissociation of biuret bonds at the high temperatures encountered during testing. To check this possibility, DSC scans of different stoichiometries were run. Three different stoichiometries were analyzed in a Perkin-Elmer DSC IV at a heating rate of 10°C/min. The results are shown in Figure 21. From this figure it can be seen that there is no effect of stoichiometry on the transition temperature. Thus, the degree of crosslinking in the hard segment does not explain why the hard segment transition temperature increases after fatigue.

Thermally annealing specimens in the DSC moves the transition temperature to higher temperatures, showing the changes seen in fatigued specimens can be brought about by high temperatures without the

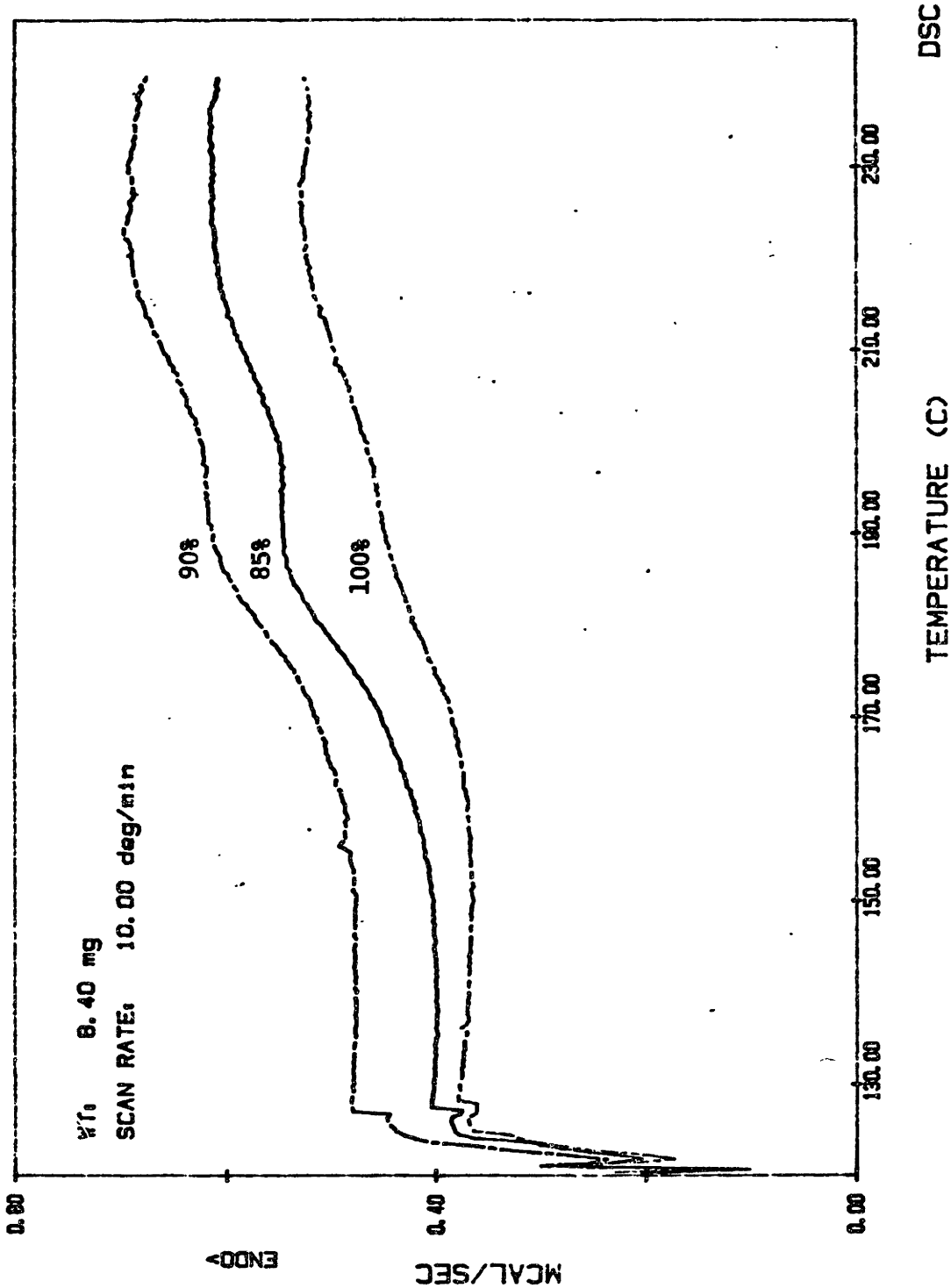

Figure 21. Effect of Stoichiometry on Transition Temperatures

application of stress. This is shown in Figure 22 where annealing unfatigued material from block #4 at 190°C shifts the transition temperature to 205°C.

This annealing effect might be a result of the two phase nature of polyurethanes. Since polyurethane block copolymers are generally two-phase systems, the degree of phase mixing will affect the transition temperatures of both hard and soft segments. Mixing of hard and soft segments has been used to explain the increase in soft segment T_g with increasing hard segment content[40]. Sung and Schneider found the "copolymer equation",

$$1/T_g = W_1/T_{g1} + W_2/T_{g2}$$

(where W_1 and W_2 are the weight fractions, and T_{g1} and T_{g2} are the T_g values for the soft and hard segments), did not predict the T_g value of the material unless hydrogen bond "crosslinking" effects between hard and soft segments were considered[40].

Phase mixing is also expected to have an effect on the hard segment transition as well[41]. Sung, Hu, and Wu found the T_g of the hard segment increased on increasing the urethane content and to be lower in polyurethanes with polyester and polyether soft segments, than in the pure hard segment material[41]. Their explanation for this was some solubilized soft segment in the hard segment material and as the urethane

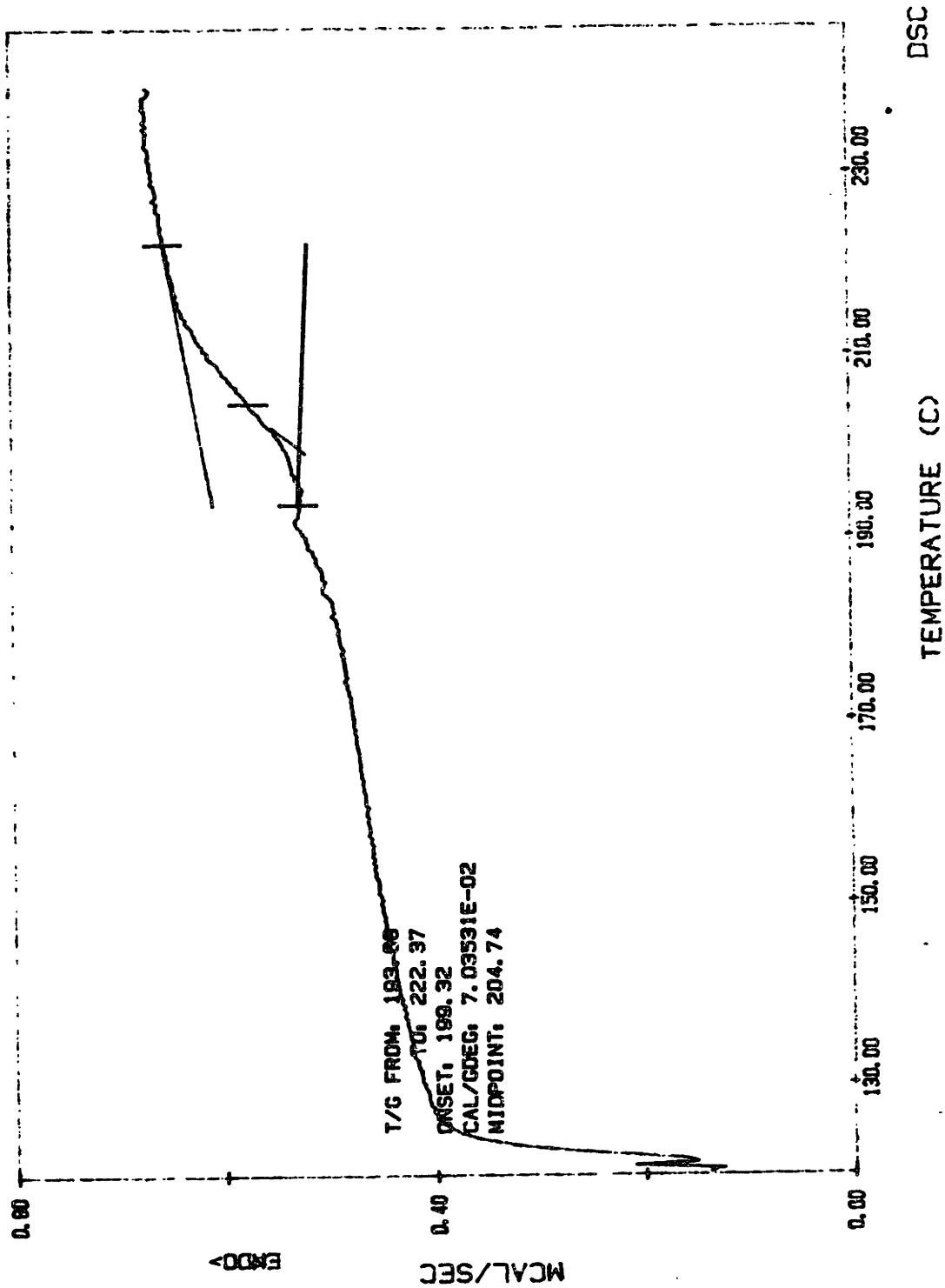

Figure 22. Annealing Effects Unfatigued Block #4

content is increased, the concentration of solubilized soft segment will decrease, because interurethane hydrogen bonding will tend to exclude the soft segment. Polyurethane ureas based on TDI and polyethers were found to have better phase separation than TDI-polyether polyurethanes[10]. In our system there must be some phase mixing because the T_g for the unfatigued specimens is approximately 25° higher than the T_g of the pure polyether (polyether T_g is -85°C[10]).

Thermal annealing studies have been done by numerous researchers. Seymour and Cooper studied MDI-based polyurethanes by DSC and found several high temperature transitions[42]. Annealing moved the lower temperature transitions to progressively higher temperatures until they merged with the highest temperature transition. This was attributed to improved ordering in the hard segment domains[42]. Studies on TDI based polymers indicated that annealing would not improve the hard segment order in polymers prepared from 2,4 TDI[9].

The T_g of the hard segment is higher after both fatigue and heating in the DSC. High temperatures may produce some kind of annealing effects, which could increase the amount of phase separation or improve the ordering of the hard segment. Both these phenomena would increase the hard segment T_g. The increased phase separation might be a viable explanation, since no improved order after annealing was reported in similar systems[9]; however, the T_g of the soft segment does not show any

significant changes after fatigue, and we would expect the soft segment to show changes as well.

Cain[43] studied a polyurethane system very similar to ours, prepared from PTMEG, TDI, and MOCA. He also found the presence of two high temperature transitions. Annealing either moved the lower transition upwards or caused it to disappear. Cain, with the aid of IR measurements at high temperatures, was able to correlate the transitions to hydrogen bonding in the urethane carbonyls (lower temperatures) and urea carbonyls (higher temperatures). It is quite reasonable that our system shows similar behavior. Although we cannot be exactly sure what changes occur to the hard segment structure after annealing, we can conclude that the changes occurring in the DSC scans after fatigue are merely the result of thermal treatment at the high temperatures observed during testing.

3.7. Swelling Studies.

One method of measuring the mechanochemical degradation is to measure the changes in crosslink density (ν_e/V). The use of swelling to study tank pad degradation has already been applied qualitatively by Lawrence [44]. He found that cross country and gravel service caused an increase in crosslink density in both the bulk and the surface of the pad. For paved road service, the pad shows an initial increase, followed by a decrease in the crosslink density. The crosslink density measured

is the effective crosslink density, which includes only those crosslinks that contribute to elastic recovery. In addition to chemical crosslinks, entanglements may also be included. This value should still be useful as a measure of damage.

The crosslink density can be measured by the application of the Flory-Rehner equation on solvent swollen samples[45].

$$\frac{\nu_e}{V} = -\frac{1}{V_s} \times \frac{\ln (1-v_r) + v_r + \chi v_r^2}{v_r^{1/3} - 2v_r/f}$$

ν_e/V is the crosslinking density (mole/cm^3), V_s is the molar volume of the solvent, χ is the polymer solvent interaction parameter, v_r is the volume fraction of rubber in the swollen sample, and f is the functionality of the crosslink.

v_r can be calculated by the weight of the specimen while swollen and after removal of the solvent, if the density of the polymer and solvent are known. This can be calculated by using the following equation[46]

$$v_r = \frac{(D - FT)/\rho}{(D - FT)/\rho + A_o/\rho_s}$$

where D is the deswollen weight of the specimen, F is the weight fraction of non-polymer insoluble components, T is the original weight of the

specimen, ρ and ρ_s are the densities of the polymer and solvent, respectively, and A_o is the equilibrium weight of the solvent absorbed.

For the polyurethaneurea under investigation the swelling solvent chosen was dimethylformamide (DMF). It is believed that this solvent may break up the hard segment hydrogen bonding to allow measurement of the primary crosslink density as degradation proceeds.

To verify that DMF does break up the hard segment domains, and that biuret crosslinkages were present in the polyurethane, two swelling experiments were devised. In one experiment samples of stoichiometry (curative/polymer weight ratio) 85% (both commercial and prepared by us) and 100% (commercial) were placed in hexafluoroisopropanol (known to be a good solvent for polyurethanes) and allowed to stand for approximately 40 hours. In the second experiment similar conditions were used for 100% material, but the solvent was dimethylformamide. For both cases the 100% stoichiometry material dissolved. The 85% stoichiometry material was swollen in hexafluoroisopropanol and DMF, but did not dissolve.

From these experiments we concluded the 85% material was chemically crosslinked, and dimethylformamide does disrupt the hard segment domain structure.

The time required for the swelling of the specimen is limited by diffusion of the liquid into the polymer. To determine the time required

for the specimens to reach equilibrium, specimens were weighed after various periods of time, and the results were plotted using the method presented by Ellis and Welding[46]. The weight ratio is plotted against $t^{1/2}$, where the weight ratio, w', is calculated by

$$w' = (S_t - T)/T$$

where S_t is the swollen weight at time t, and T is the original weight of the specimen.

After equilibrium is reached the specimen should maintain a constant weight. However, this is not always the case. There may be a gradual increase in weight after diffusion is complete, which may be due to oxidative degradation of the specimen[46]. By using this method convenient time limits for swelling measurements can be obtained.

To determine the time required to reach equilibrium four pieces of unfatigued material, each weighing about 0.2 grams, were placed in 40 ml. of DMF at 25°C. At various times they were removed, blotted on filter paper, and weighed in tared, stoppered bottles. A plot of w' versus $t^{1/2}$ is shown in Figure 23. The swelling appears to reach equilibrium after approximately 25 hours, so this time was chosen as the swelling time for future measurements.

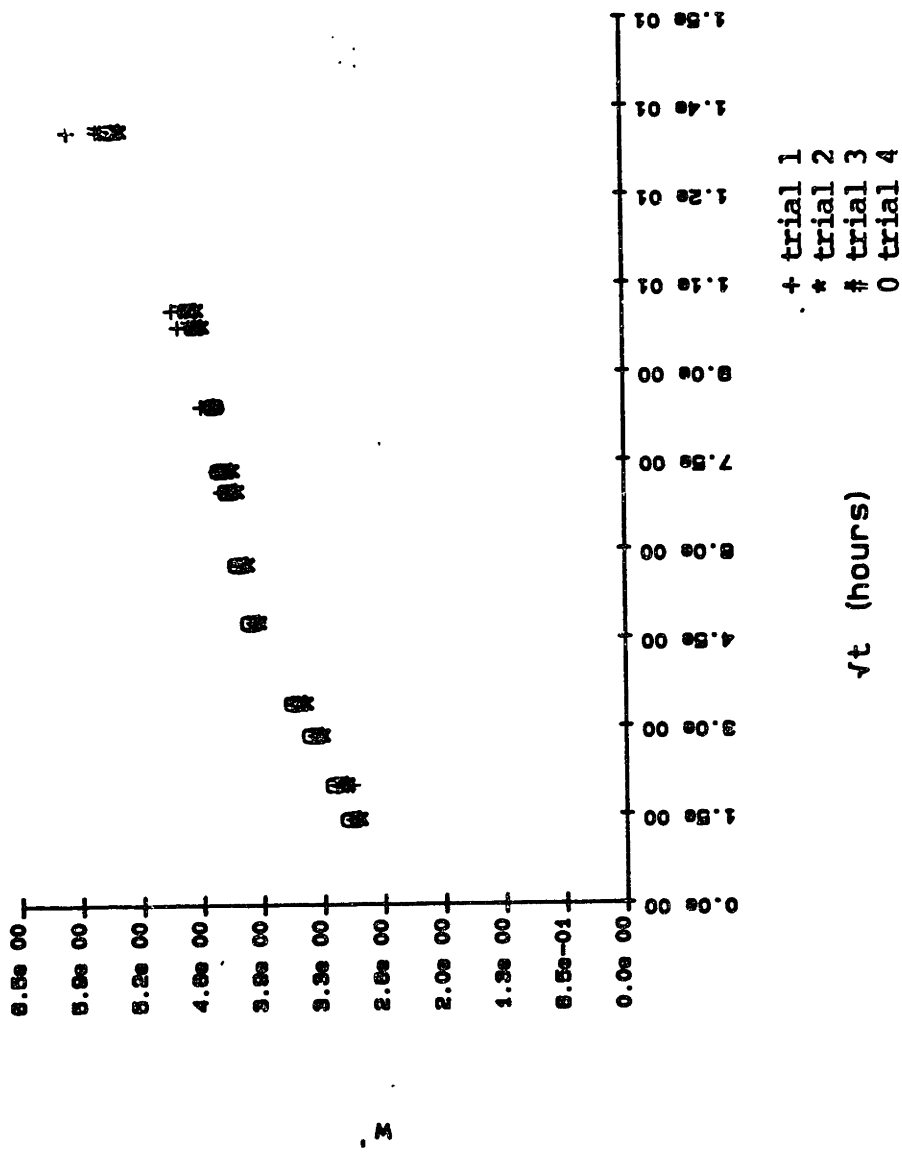

Figure 23. Swelling - w' vs. $t^{\frac{1}{2}}$

In order to calculate v_r from swelling measurements the density of the polymer must be known. The density of both fatigued and unfatigued material (from specimen #1) was measured by suspending a preweighed specimen on a fine wire from the top of a balance. The specimen was immersed in methanol, and the weight was measured. The measured weight was then corrected for changes in the weight of the wire when immersed.

Knowing the density of methanol at the test temperature the density of the specimen can be calculated as:

$$\rho_s = (w_o/(w_o - w_m)) \times \rho_m$$

where ρ_s is the specimen density, w_o is the weight in air, w_m in the weight in methanol, and ρ_m is the density of methanol. The densities calculated by this method are 1.119 g/ml for the unfatigued and 1.120 g/ml for the fatigued specimen. Since there seem to be no density differences between unfatigued and fatigued material, an average value of 1.119 g/ml was used for all calculations. The density of DMF at 25°C is 0.9438 g/ml[47]. For all further calculations it was assumed that F, the fraction of insoluble material, was zero.

To obtain absolute values from swelling measurements, the value of χ must be known. To find a value for χ one can determine the crosslink density by measuring the elastic modulus of swollen specimens (no hard segment stiffening) using the following equation[48].

$$\nu_e/V = F\, v_r^{1/3} / \{ART(\alpha - \alpha^{-2})\}$$

where ν_e/V is the moles of effective network chains per unit volume of polymer, F is the force to obtain an extension α, v_r is the volume fraction of elastomer in the swollen specimen, A is the unswollen cross-sectional area, R is the gas constant, and T is the temperature. This value of the crosslink density can then be used in the Flory-Rehner equation to calculate χ.

For stress-strain analysis specimens were sanded with water cooling to a width of .77 cm. They were sliced with a microtome to a thickness of .09 cm, and the length was 6 cm. Prior to swelling, horizontal lines were drawn on the specimen with liquid paper correction fluid in order to measure strains. The specimen was swollen in DMF for 25 hours, then weighed in a tared bottle. The specimens were unfatigued and taken from specimen 1.

Stress-strain measurements were made using an Instron model 1122. The strain was measured with a cathetometer, then converted to elongation. During this test the specimen was kept in solvent by placing the tensile strip in a clear plastic bag filled with DMF.

For swelling measurements specimens weighing approximately 0.4 grams were placed in 80 ml. of DMF and allowed to swell for 25 hours in a water bath at 25°C. The specimens were weighed as described above. The

deswollen weight was obtained by drying the specimens in a 60°C vacuum oven overnight. By inserting the crosslink density obtained from stress-strain measurements on swollen samples into the Flory-Rehner equation a value for χ of 0.468 was obtained. The crosslink densities calculated by the Flory-Rehner equation with $\chi = 0.468$ are shown below in Table 4 for all the tested specimens. The values reported are the average of at least two runs.

Table 4. Crosslink Density From Swelling

Specimen	% Soluble	v_r	ν_e/V (moles/cm^3)
1 unfatigued	2.3	.183	1.00×10^{-4}
1 fatigued	36.6	.046	3.95×10^{-6}
2 fatigued	2.6	.253	2.47×10^{-4}
3 fatigued	3.7	.207	1.38×10^{-4}
4 unfatigued	2.8	.247	2.27×10^{-4}
4 fatigued	1.5	.293	3.73×10^{-4}
5 unfatigued	6.9	.122	3.89×10^{-5}
5 fatigued	2.1	.240	2.10×10^{-4}
6 unfatigued	11.6	.210	1.52×10^{-4}
6 fatigued	1.5	.275	3.11×10^{-4}
7 unfatigued	4.5	.173	9.10×10^{-5}
7 fatigued	2.6	.257	2.54×10^{-4}
8 unfatigued	2.6	.244	2.21×10^{-4}
8 fatigued	16.2	.292	3.73×10^{-4}
9 unfatigued	3.4	.198	1.39×10^{-4}
9 fatigued	2.0	.250	2.40×10^{-4}
10 unfatigued	3.5	.220	1.64×10^{-4}
10 fatigued	3.2	.234	1.98×10^{-4}

Significant changes after fatigue can be seen only in specimen #1. Specimens 6 unfatigued and 8 fatigued showed large percentages of soluble material, but this may be nothing more than variability from sample to sample, perhaps due to slight variations in the cure temperature. For

the most part no significant changes can be seen in the swelling behavior of any of the other blocks after fatigue. Specimen 5 does show an increase in crosslink density after fatigue. Unfatigued specimens were taken from the outer surface of the blocks before testing, and perhaps the outer surface was improperly cured in the case of specimen 5. The values for the fatigued material represent average values for the specimens, since the test specimen was exposed to a variation in temperature, with the middle portions experiencing higher temperatures than the outer portions. For the most part there is no significant breakdown in the crosslink density, even though the blocks taken to failure cracked during testing. The results for block #10 show that fatigue at low loads for long periods of time does not explain the increased swelling found for block #1. It may be that this block was different from the others, perhaps the starting materials had been degraded in some way, or the processing conditions were different.

From the swelling experiments it can be concluded that no significant permanent chain scission is required for failure of polyurethane elastomers under compression loading. If chain scission did occur, the bonds must have reformed before the samples were analyzed, and this seems unlikely.

3.8. Rheovibron Analysis.

3.8.1. Analysis of Fatigued Specimens.

Polymeric materials are viscoelastic in nature, behaving in a partly viscous and partly elastic manner. When a stress is applied some of the energy is stored by elastic mechanisms, while the viscous response dissipates this energy.

Dynamic mechanical spectroscopy is one method of gaining information about the viscoelastic behavior of a material. In this type of a test a sinusoidally varying stress or strain is applied. The response of the material can be separated into two components: one part in phase with the applied strain and another 90° out of phase[49]. The sinusoidal stress response of the material lags behind the applied strain by a phase angle δ. If the stress is expressed as a complex quantity, then the modulus can also be expressed as a complex quantity[49]

$$E^* = E' + iE''$$

where E^* is the complex modulus. E' is the in phase component or the storage modulus and is related to the elastic properties of the material. E'' is the out-of-phase component or loss modulus and is a measure of the viscous properties. They are given by the following equations[49]:

$$E' = |E^*| \cos\delta$$

$$E'' = |E^*| \sin\delta$$

The phase angle δ is defined as[49]:

$$\tan \delta = E''/E'$$

E" is a measure of the energy dissipated. When the E" curve of a dynamic mechanical spectrum goes through a maximum, some type of molecular motion is occurring on the time scale of the deformation[49].

One instrument that can be used for dynamic mechanical testing is the Rheovibron, which is a forced vibration instrument. The frequency is maintained at a constant value while the data are obtained throughout a range of temperatures. A sinusoidally varying tensile strain is applied to one end of the sample, and the resulting stress response is measured. The amplitude of this strain is kept small (1.0×10^{-3} cm) so that linear viscoelastic response is obtained.

The system used for this research is an Autovibron. It uses the basic Rheovibron DDV-II (Toyo Baldwin Co.), but includes an automation package (Imass, Inc.). The automation package controls sample tensioning, temperature, phase angle measurements, data collection, and data reduction. The frequency used for studying fatigue changes was 110 Hz,

and a temperature range of -130° to 150°C was scanned. The temperature chamber was cooled to -130°C by placing liquid nitrogen in the holder, but the specimen was isolated from direct contact with the liquid nitrogen. Nitrogen gas was blown slowly through the sample chamber to reduce ice formation on the sample and grips. Once the chamber was cooled to -130°C it was allowed to warm up without further addition of liquid nitrogen. This gave a heating rate of about 2° per minute. When the temperature reaches approximately -45°C the heaters assume control and at this stage the heating rate is closer to 1°C per minute.

Specimens were cut from thin microtomed slices with two razor blades attached to a metal plate to produce samples of constant width. The specimen size was .06 x .40 x 4.45 cm. All specimens were taken as close to the center as possible with the exception of block #8, where the specimens were taken from an outer section, because the center portion was too badly damaged to obtain a suitable test piece.

Figures 24 and 25 are typical traces for the unfatigued and fatigued material (taken from specimen #8). Comparison plots for the elastic modulus (E') are shown in Figures 26 - 30. There is some scatter in the data at low temperatures, which is from resonance of the sample and grips. This resonance seems related to poor sample alignment in the grips.

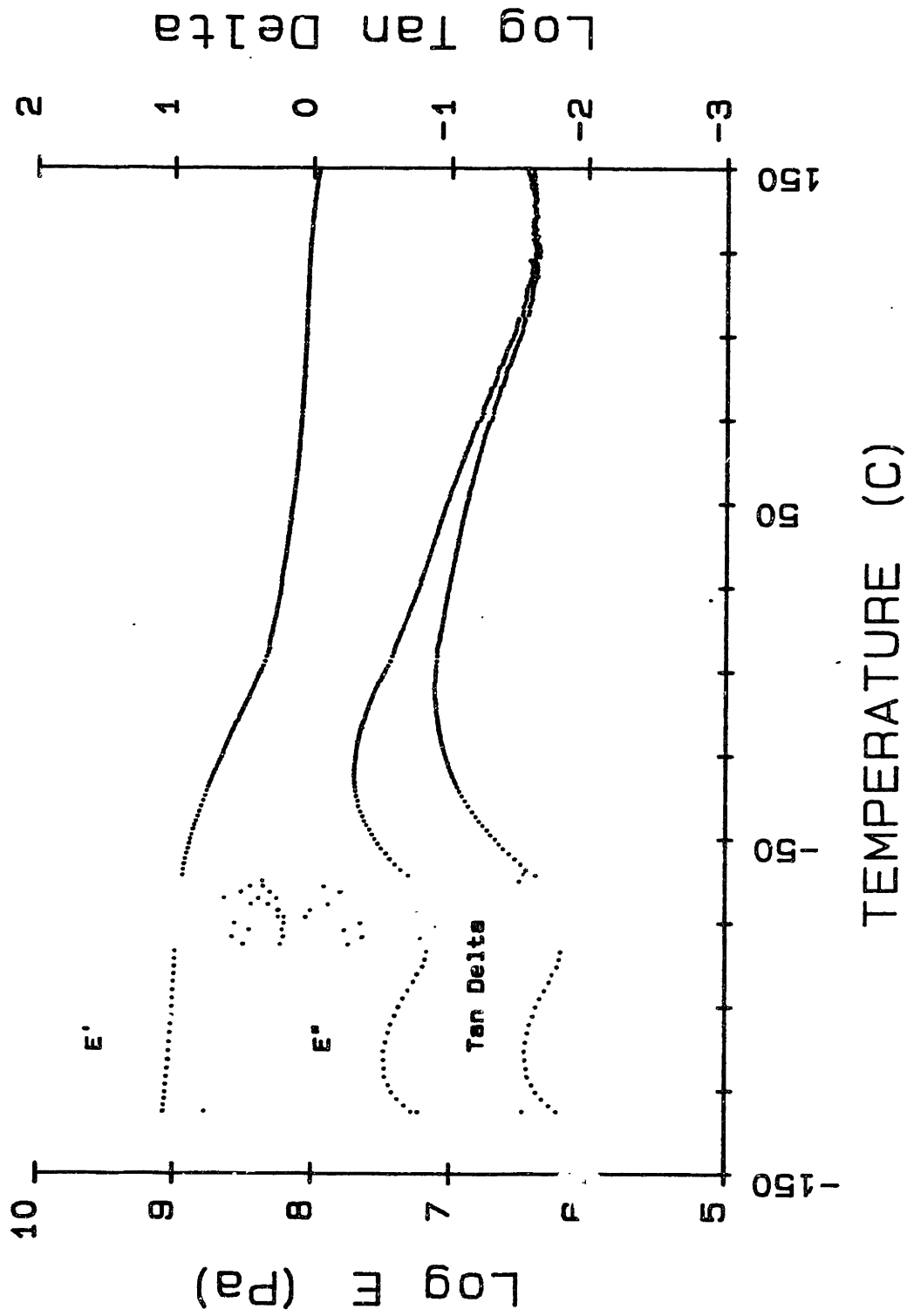

Figure 24. Rheovibron Data Unfatigued Specimen 8

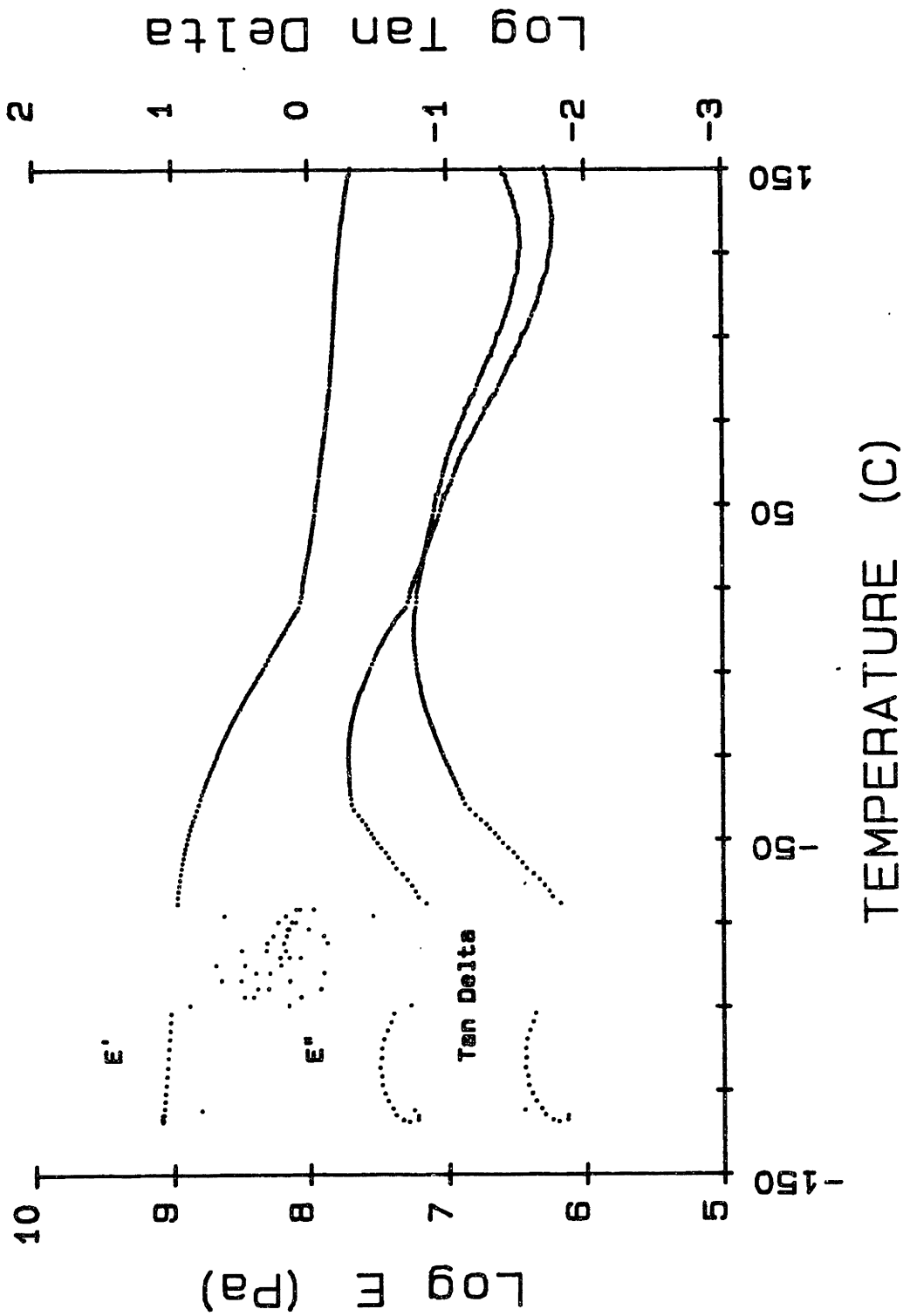

Figure 25. Rheovibron Data Fatigued Specimen 8

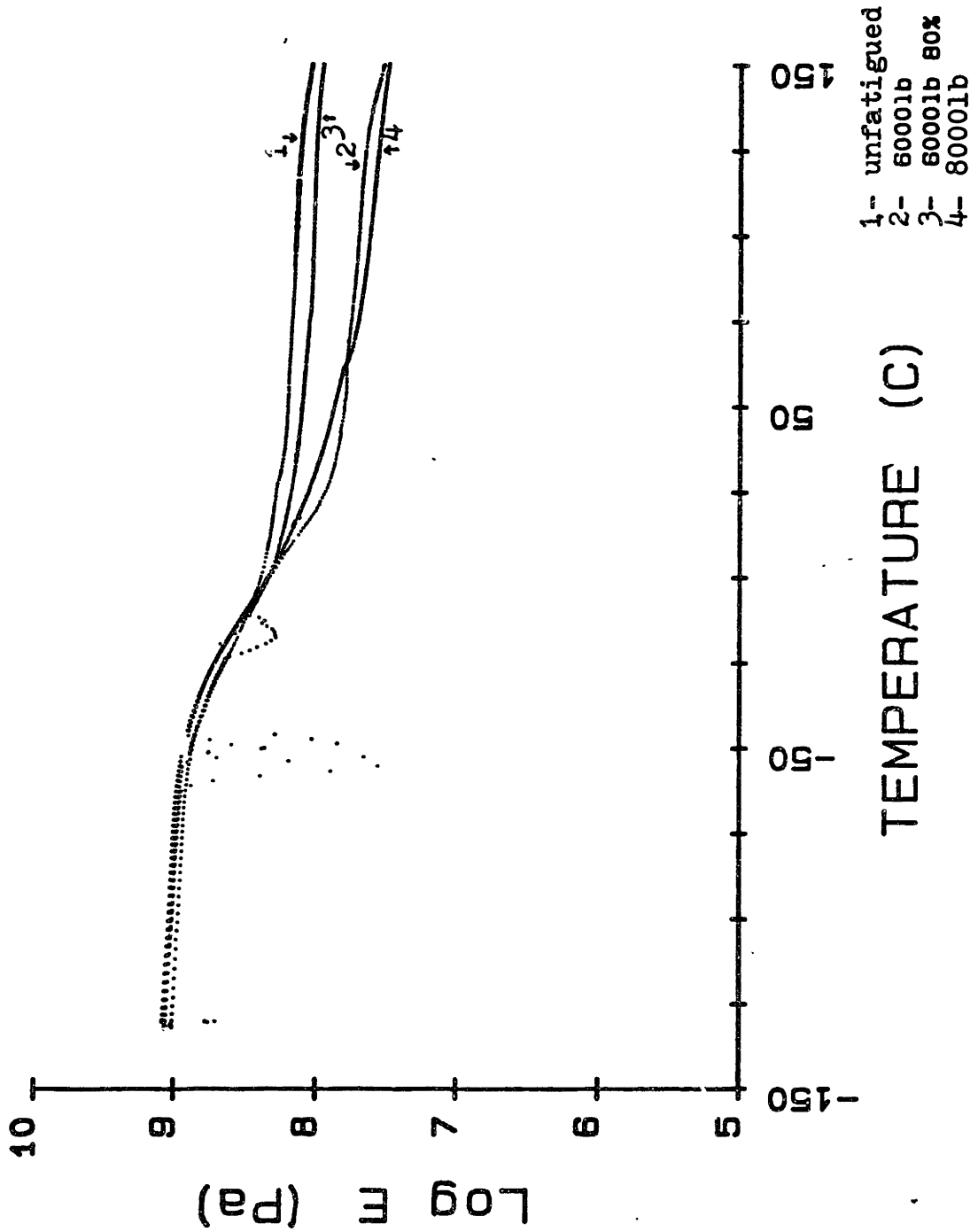

Figure 26. Comparison Plot of Storage Modulus (E') - Specimens 1-3

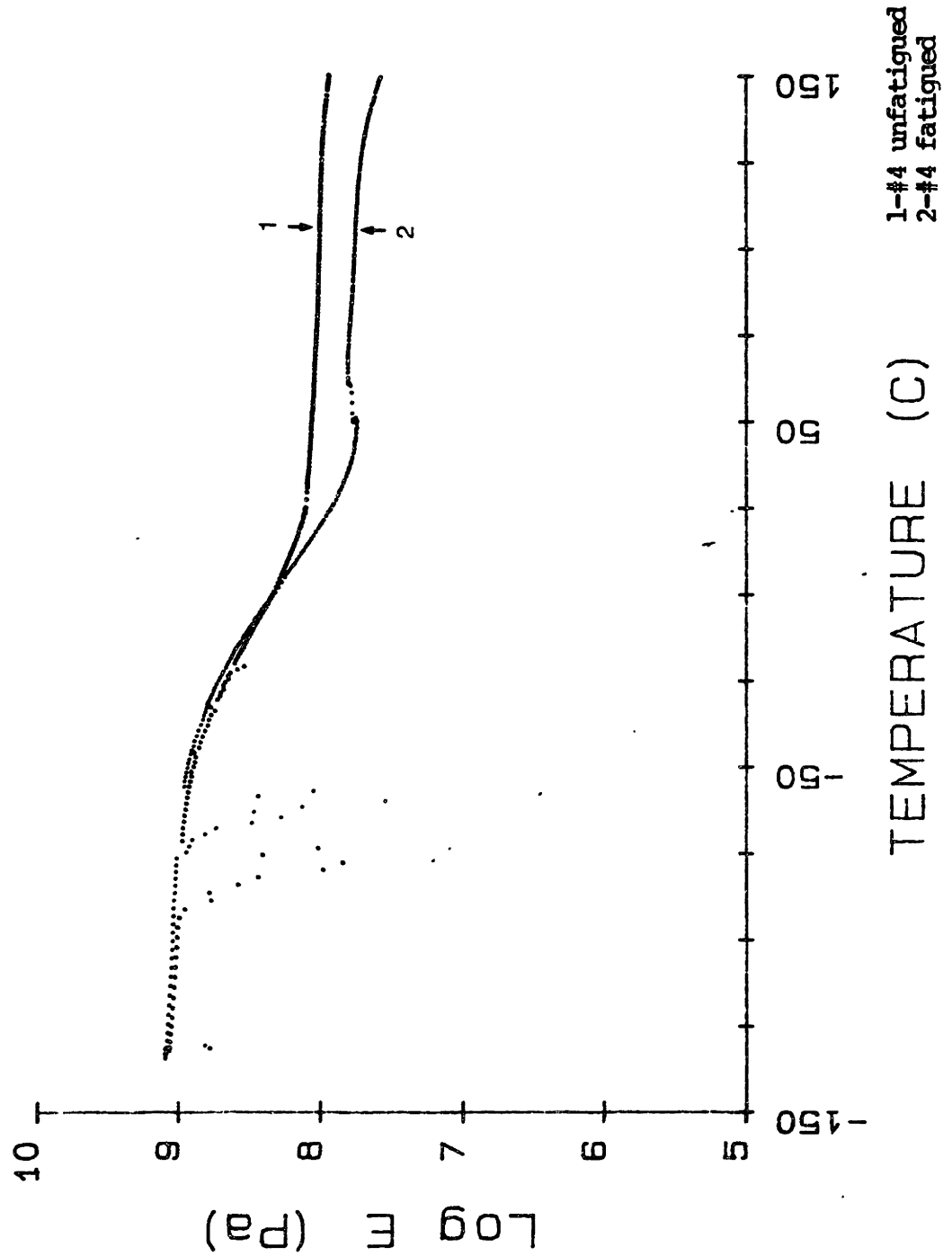

Figure 27. Comparison Plot of Storage Modulus (E') - Specimen 4

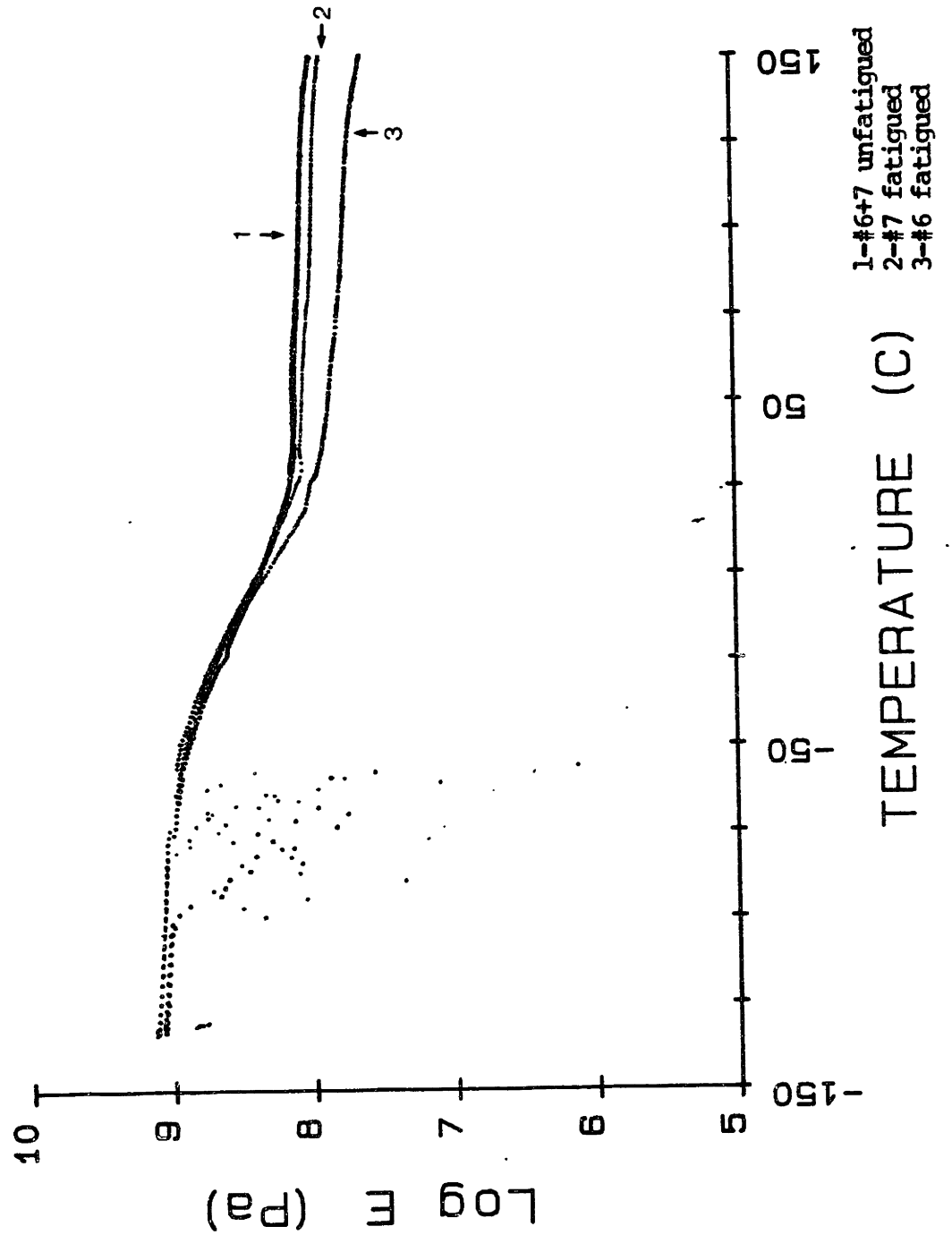

Figure 28. Comparison Plot of Storage Modulus (E')-Specimens 6 & 7

There are two maxima in the E" curves for both fatigued and unfatigued material. One occurs around -110° and the other at -24°C. The peak occurring at -110° has been associated with motion occurring in a series of 4 methylene groups[50,51]. This motion occurs in the amorphous soft segments. There does not appear to be any change in this peak by fatigue.

In some of the traces a shoulder appears on the -25°C peak, occurring around -40°C. Huh and Cooper reported a peak due to absorption of water centered around -50°C[51]. It is possible that water is responsible for this peak since it is not present in all the runs, even for the same specimen type.

The transition at -25°C is the T_g of the soft segment[50,51]. The T_g is associated with micro-brownian motion of the polyether chains. Huh and Cooper have found the T_g of the soft segment to be dependent on domain structure[51]. The T_g of the hard segments occurs at a temperature above 150°C and is not seen in the Rheovibron runs.

Above T_g amorphous polymers exhibit a slight plateau modulus from entanglements. With crosslinking this plateau region is extended. In phase separated systems, such as polyurethanes, the hard segments tend to reinforce the structure, producing an extended plateau region, until the hard segment T_g is reached[52].

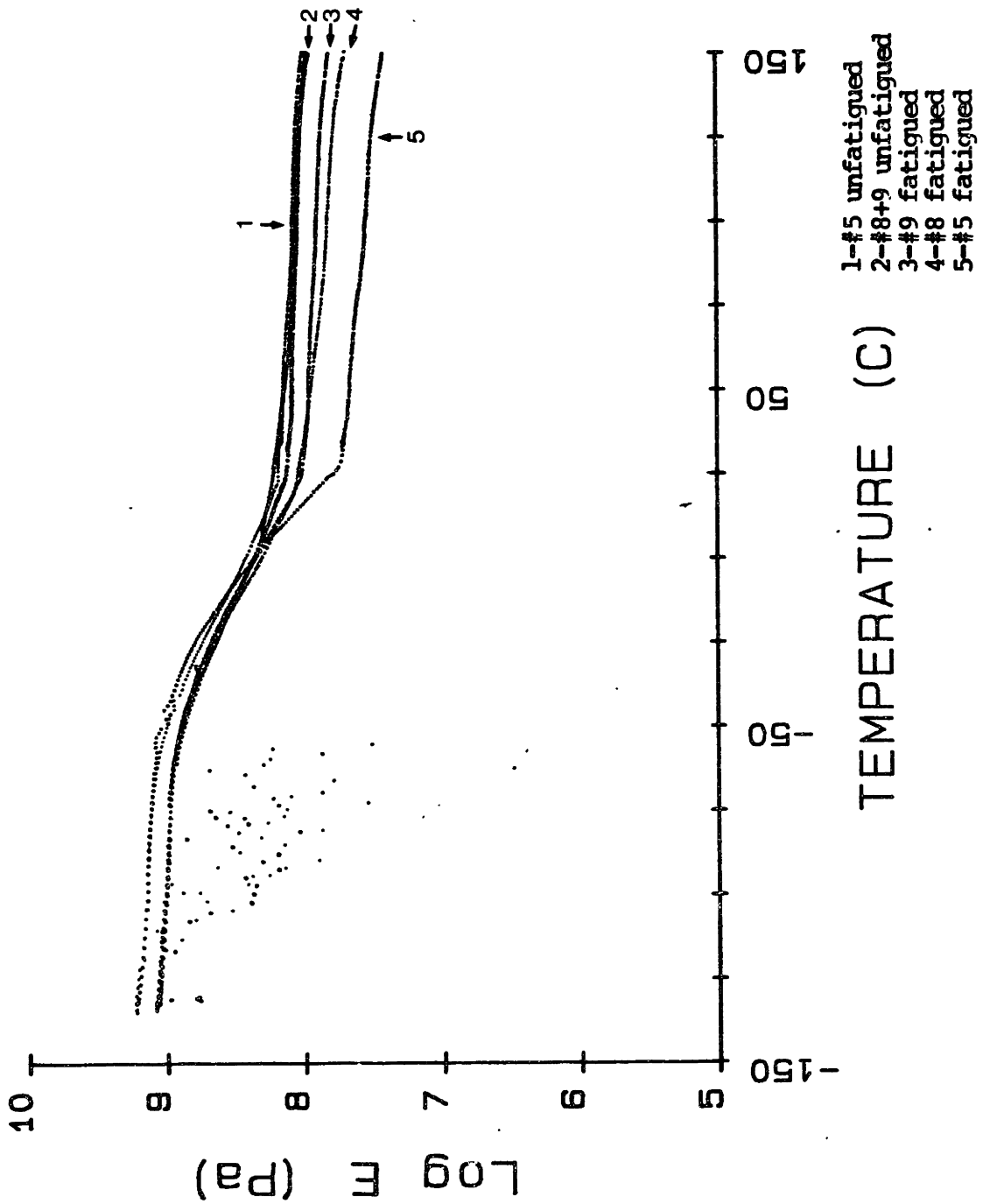

Figure 29. Comparison Plot of Storage Modulus - Specimens 5,8 & 9

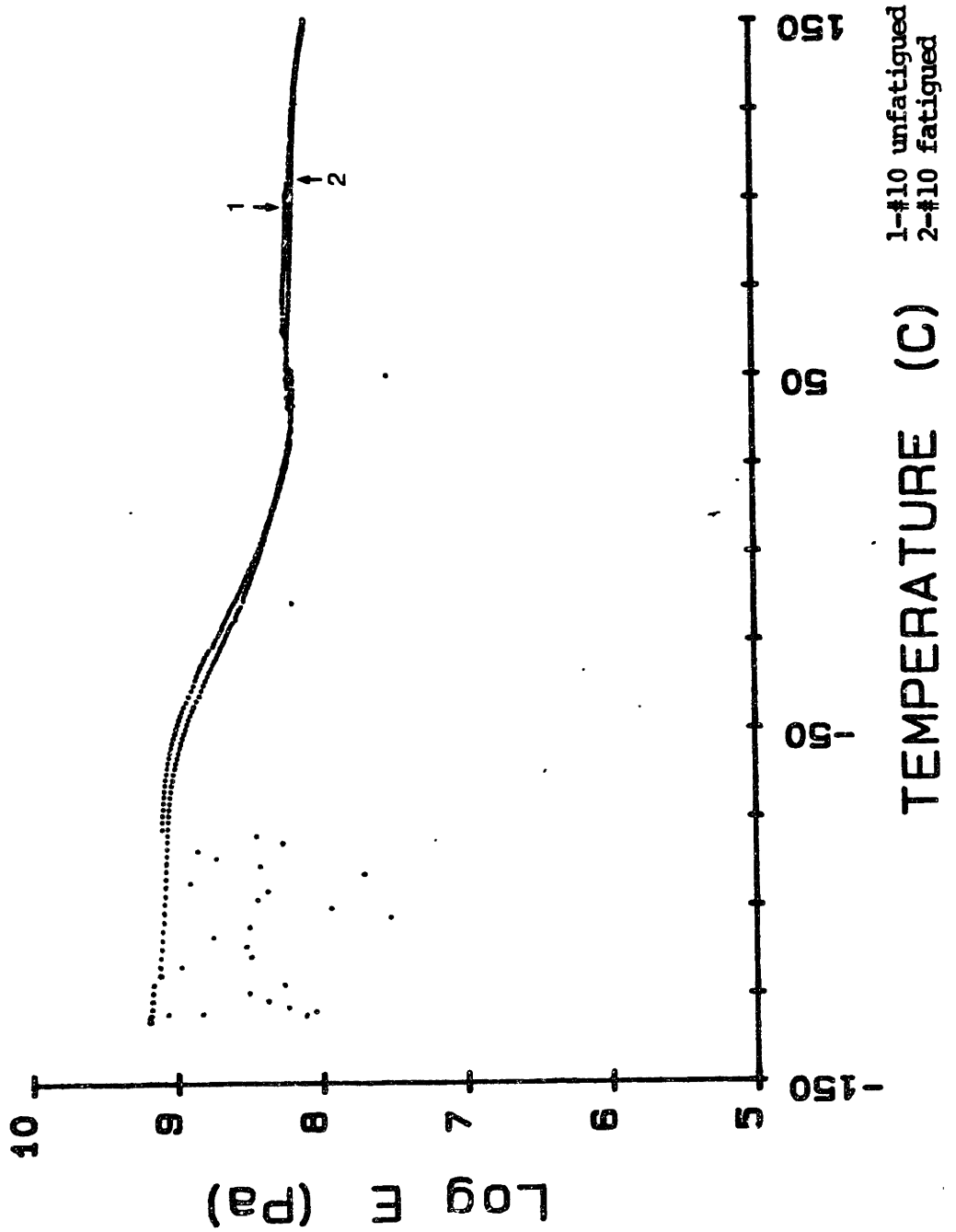

Figure 30. Comparison Plot of Storage Modulus (E') - Specimen 10

The elastic modulus in the plateau region can be used to determine the crosslink density through the theories of rubber elasticity. From elasticity theory, the stress-strain relation can be expressed as[53]:

$$f = E/3(\alpha - \alpha^{-2})$$

where f is the force per unit unstrained cross-sectional area, E is the Young's modulus, and α is the elongation. Assuming Poisson's ratio is 0.5, then[53]

$$E = 3G = 3RT(\nu_e/V)$$

We can relate the elastic modulus E' to the crosslink density by the use of this equation.

The values of E' and the crosslink density for specimens at 50, 75, and 100°C are shown below.

Table 5. Modulus - Crosslink Density At 50°C

Specimen	E' (Pa)	ν_e/V (moles/cm^3)
unfatigued 1	1.59×10^8	1.97×10^{-2}
fatigued 1	6.71×10^7	8.33×10^{-3}
fatigued 2	6.27×10^7	7.78×10^{-3}
fatigued 3	1.24×10^8	1.53×10^{-2}
unfatigued 4	1.14×10^8	1.42×10^{-2}
fatigued 4	5.47×10^7	6.79×10^{-3}
unfatigued 5	1.41×10^8	1.75×10^{-2}
fatigued 5	4.66×10^7	5.78×10^{-3}
unfatigued 6	1.26×10^8	1.56×10^{-2}
fatigued 6	7.24×10^7	8.99×10^{-3}
unfatigued 7	1.31×10^8	1.63×10^{-2}
fatigued 7	1.11×10^8	1.38×10^{-2}
unfatigued 8	1.40×10^8	1.74×10^{-2}
fatigued 8	8.90×10^7	1.10×10^{-2}
unfatigued 9	1.22×10^8	1.51×10^{-2}
fatigued 9	9.25×10^7	1.15×10^{-2}
unfatigued 10	1.49×10^8	1.85×10^{-2}
fatigued 10	1.57×10^8	1.94×10^{-2}

Table 6. Modulus - Crosslink Density At 75°C

Specimen	E' (Pa)	ν_e/V (moles/cm^3)
unfatigued 1	1.52×10^8	1.75×10^{-2}
fatigued 1	5.17×10^7	5.96×10^{-3}
fatigued 2	5.60×10^7	6.46×10^{-3}
fatigued 3	1.11×10^8	1.28×10^{-2}
unfatigued 4	1.04×10^8	1.20×10^{-2}
fatigued 4	6.21×10^7	7.15×10^{-3}
unfatigued 5	1.29×10^8	1.49×10^{-2}
fatigued 5	4.12×10^7	4.75×10^{-3}
unfatigued 6	1.21×10^8	1.39×10^{-2}
fatigued 6	6.20×10^7	7.14×10^{-3}
unfatigued 7	1.22×10^8	1.41×10^{-2}
fatigued 7	1.01×10^8	1.16×10^{-2}
unfatigued 8	1.21×10^8	1.39×10^{-2}
fatigued 8	7.40×10^7	8.53×10^{-3}
unfatigued 9	1.17×10^8	1.35×10^{-2}
fatigued 9	8.65×10^7	9.97×10^{-3}
unfatigued 10	1.71×10^8	1.97×10^{-2}
fatigued 10	1.51×10^8	1.74×10^{-2}

Table 7. Modulus - Crosslink Density At 100°C

Specimen	E' (Pa)	ν_e/V (moles/cm^3)
unfatigued 1	1.44×10^8	1.55×10^{-2}
fatigued 1	4.36×10^7	4.69×10^{-3}
fatigued 2	4.66×10^7	5.01×10^{-3}
fatigued 3	1.04×10^8	1.11×10^{-2}
unfatigued 4	9.95×10^7	1.07×10^{-2}
fatigued 4	5.68×10^7	6.11×10^{-3}
unfatigued 5	1.19×10^8	1.28×10^{-2}
fatigued 5	3.52×10^7	3.78×10^{-3}
unfatigued 6	1.13×10^8	1.21×10^{-2}
fatigued 6	5.56×10^7	5.98×10^{-3}
unfatigued 7	1.14×10^8	1.23×10^{-2}
fatigued 7	9.20×10^7	9.89×10^{-3}
unfatigued 8	1.13×10^8	1.21×10^{-2}
fatigued 8	6.59×10^7	7.08×10^{-3}
unfatigued 9	1.11×10^8	1.19×10^{-2}
fatigued 9	7.95×10^7	8.55×10^{-3}
unfatigued 10	1.60×10^8	1.72×10^{-2}
fatigued 10	1.44×10^8	1.55×10^{-2}

A calculation of the percent reduction in elastic modulus after fatigue was done for specimens number 5-10. This should allow us to compare the differences in loadings and number of cycles for each block.

Table 8. Percentage Decrease In Rubbery Modulus

Specimen	T=50°C	T=75°C	T=100°C
Block #4	52%	40%	43%
Block #5	67%	68%	70%
Block #6	42%	49%	51%
Block #7	15%	18%	20%
Block #8	37%	39%	41%
Block #9	24%	26%	28%
Block #10	-	12%	10%

All the values for crosslink density calculated by this method are higher than by swelling analysis. This is not unexpected since the modulus measurements include the reinforcing effect of the hard segment

domains. In ideal rubber elasticity only entropic effects are considered in the stress temperature equations. This causes the force at constant elongation to increase with temperature above a minimum elongation. The modulus of our specimens goes down with temperature indicating that ideal rubber elasticity is not attained[54], possibly due to internal energy contributions. This data should still give an approximate estimate of the degradation occurring.

All fatigued specimens exhibit a decreased crosslink density when taken to failure. The percentage change in modulus continues to increase with the number of cycles (temperature also increases) at the same load level.

To determine if these changes were the result of thermal annealing alone, as was the case for the hard segment transition changes, a series of thermal annealing studies was run. A brief description of the thermal annealing studies done by other workers is included.

Annealing at high temperatures may induce time dependent morphological changes in segmented polyurethanes. Wilkes and Wildnaur[55] studied the time dependent changes in the soft segment glass transition temperature and the Young's modulus of p,p'-diphenyl-methane diisocyanate (MDI) based polyurethanes after annealing for 5 minutes at 170°C. They found the Young's modulus to increase over time. Rapid changes were noted for the first two hours after annealing, with gradual increases for a period up

to seven days. Differential Scanning Calorimetry (DSC) showed an immediate increase in the soft segment transition temperature, which gradually decreased over time - the largest changes occurring in the first 80 minutes. These changes were explained by phase mixing as the hard domains soften at high temperatures, followed by time dependent phase separation at room temperature. The time dependent behavior of polyether polyurethanes was found to be less than polyester urethanes. Wilkes et al.[56] found that polyurea systems had less time dependence after annealing than urethane systems. This they attributed to higher thermal stability in the urea systems.

Lagasse offered another explanation for his own results on a study of a toluene diisocyanate (TDI) polyurethane with a polybutadiene soft segment[57]. This system was chemically crosslinked because of the multifunctionality of the polybutadiene soft segment. From Rheovibron studies he found the modulus to drop initially after annealing above the hard segment T_g, then increase over time. However, by electron microscopy no change in the degree of phase separation was found after annealing. He found no change in the soft segment transition, but the hard segment transition temperature initially dropped, then recovered with time. From DSC studies they noted the hard segment transition was comprised of an endothermic peak superimposed on a specific heat change. After annealing the endothermic peak disappeared and the specific heat step change moved to lower temperatures. With time the transition moved upwards, and the endothermic peak returned. Lagasse's explanation for

this was densification of the amorphous hard segment domains, similar to that found in amorphous glassy polymers from the reduction in free volume in sub-T_g aging.

To study this effect in our system we have annealed small strips in a vacuum oven for 10 minutes at a series of temperatures. The vacuum oven was used to minimize the exposure to oxygen. The pre-measured samples were removed from the oven and placed into the Rheovibron. It took approximately 10 minutes from removal of the sample until the first data point could be taken. The dynamic modulus of the material was measured using an Autovibron DDV-II (IMASS) at a frequency of 11 Hz and a temperature of 25°C. Data were taken every four minutes for a period of 24 to 48 hours.

The results for unannealed and annealed samples are shown in Figures 31 and 32 for specimens annealed at 195° and 220°C, respectively.

As can be seen there is no permanent change for samples annealed up to 220°C. Some time dependence is seen in the initial modulus values, but the results are the opposite of those reported in the literature. It may simply be that the sample has not had sufficient time to cool, and the rubber elasticity temperature dependence is causing this. From the results of this series of experiments it was determined that thermal annealing alone does not cause the modulus changes seen after fatigue.

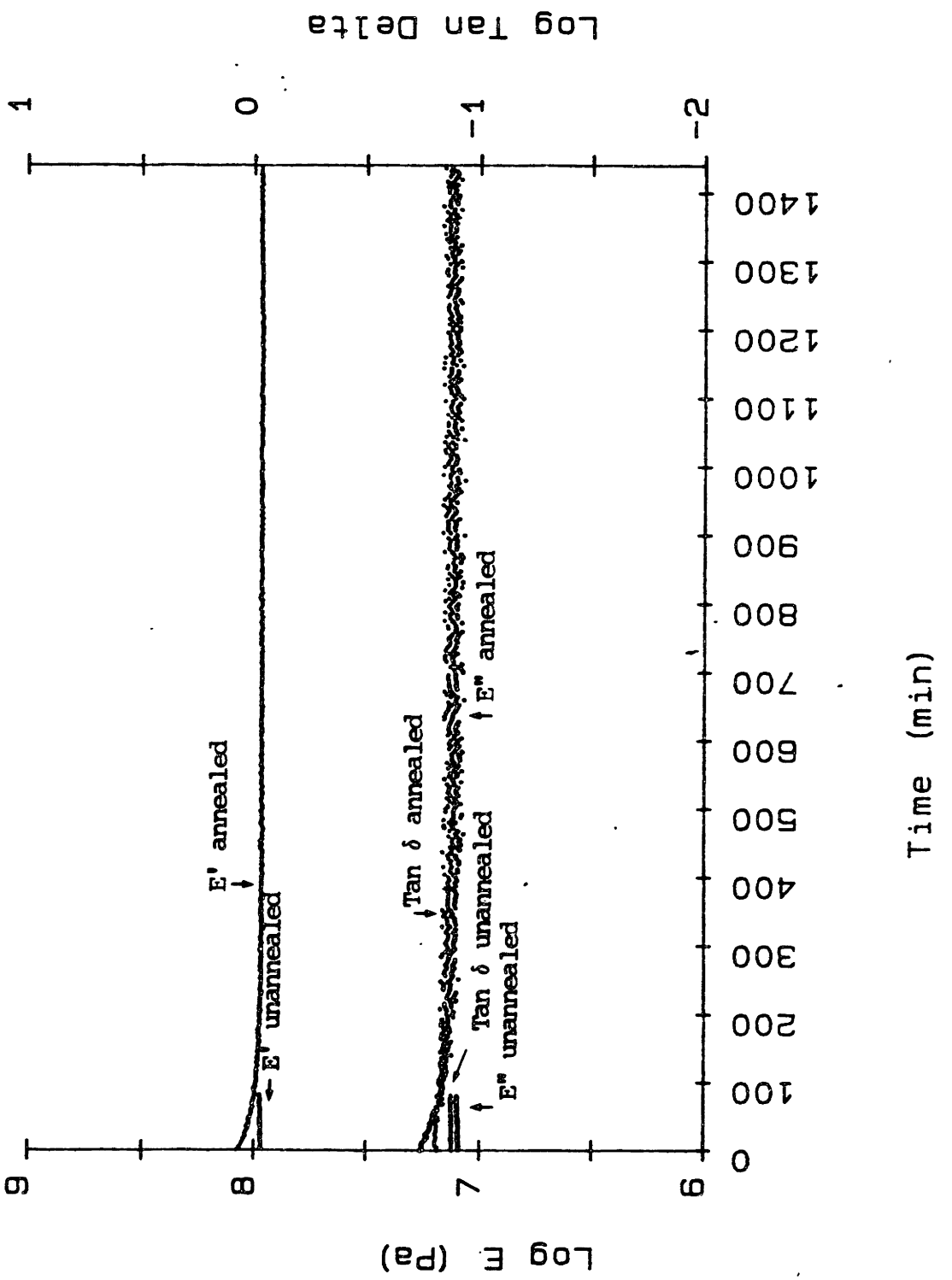

Figure 31. Rheovibron Data After Thermal Annealing-195°C

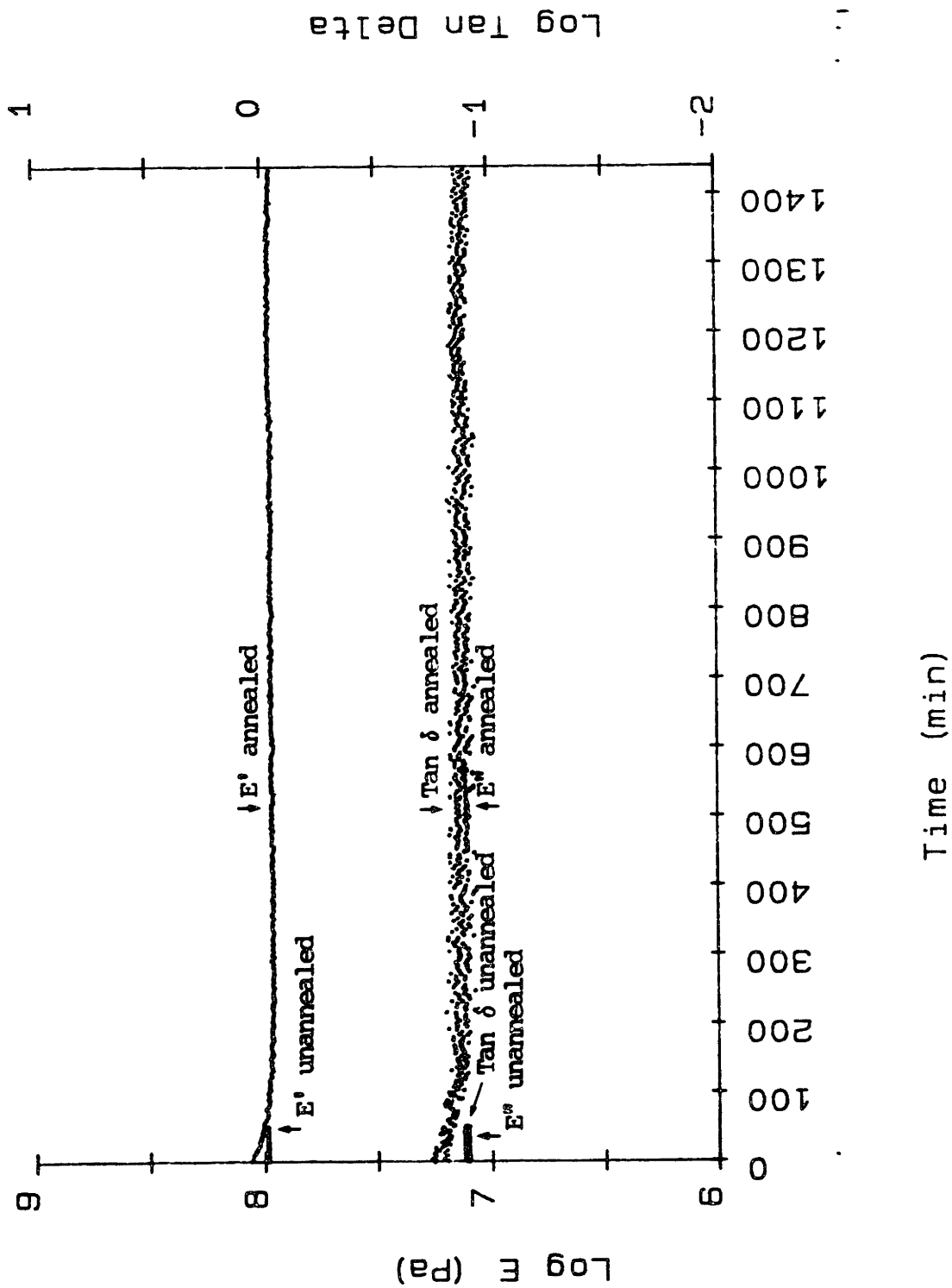

Figure 32. Rheovibron Data After Thermal Annealing-220°C

A probable explanation for this modulus reduction is the "Mullins Effect", which was originally found in filler-loaded rubbers, but has since been found in polyurethane elastomers[58]. Trick[58] found a reduction in modulus with repeated extension; almost all of the reduction occurred in the first cycle. The stress-softening phenomenon is believed to be caused by the disruption of the glassy domains under repeated stretching[59].

Crosslinking in the hard segment should lead to a reduction in the amount of stress-softening, and in fact Cooper et al.[59] found that crosslinking with triol and peroxide produced polyurethanes with a reduced "Mullins Effect". Allophanate crosslinkages did not improve the stress-softening characteristics of MDI polyurethanes. If allophanate crosslinks did not prevent the disruption of the hard domains for Cooper's system, then it is unlikely that the biuret groups present in our system would appreciably reduce the "Mullins Effect".

Kaneko et al.[60] studied the cut growth fatigue of polyurethanes prepared from PTMEG, TDI, MOCA, and hexamethylene diisocyanate (HMDI). After constant load fatigue they measured the changes in elastic modulus with the Rheovibron. For all fatigued samples a decrease in the elastic modulus was encountered, but the authors did not investigate if the amount of change was dependent on the number of fatigue cycles. Kaneko et al. suggested that the differences they noted after fatigue could be due to orientation under stress.

Either orientation or disruption of the hard domains is a possible explanation for the changes seen in compression fatigue tests. The changes seen in the modulus are clearly not caused by high temperatures alone, but require the application of stress. The continuous increase in temperature leads to softening of the material, thus increased deformation. This increased deformation amplitude will lead to continued softening[59]. Because of the heat build-up stress softening continues to occur throughout the test, rather than mainly in the first cycle. Thus, we can expect the material properties of polyurethanes to continuously change as fatigue degradation occurs. As evidenced by the results from block 10 (cycled at low load levels with little heat build-up) cyclic fatigue without heat build-up does not produce significant modulus reduction.

3.8.2. High Temperature Properties.

An understanding of the dynamic mechanical properties of our system at high temperatures, similar to those found in fatigue testing, is important for determining the failure mechanism. By insulating the Rheovibron it has been possible to study the dynamic properties of our polyurethane urea at temperatures up to 250°C. This covers the temperature range where block failure occurs (approximately 200°C).

A special gripping system was required to run the high temperature tests, because samples ruptured at the grips when the material softened.

The gripping system devised is as follows: precut specimens were glued on end to two small copper tabs with epoxy. The epoxy was allowed to cure overnight at room temperature. Two pieces of sandpaper were wrapped around the copper tabs, then the sample was placed in the Autovibron and run from room temperature to 250°C. A sample of the epoxy glue was cast onto the tabs and run in the Autovibron to distinguish any transitions for the epoxy. The absolute modulus values may be incorrect because of the tabbing system, but only the transition temperatures were of interest for this section of the work.

A high temperature test at 11 Hz is shown in Figure 33. A small transition is seen near 75°C, and a very large drop in modulus is found beginning near 175°C. A comparison of the elastic moduli (E') is seen in Figure 34. Tan delta values are compared in Figure 35.

By comparing the tan delta behavior for the epoxy with the polyurethane data, we can assign the transition at 75°C to the epoxy. Further proof for this lies in the fact that this transition was never seen in polyurethane runs without the special gripping system.

The epoxy elastic modulus remains essentially constant from 100° to 250°C. Therefore, the transition beginning at 175°C is the hard segment transition. This transition temperature correlates well with the hard segment transition temperature of 180°C found by DSC measurements.

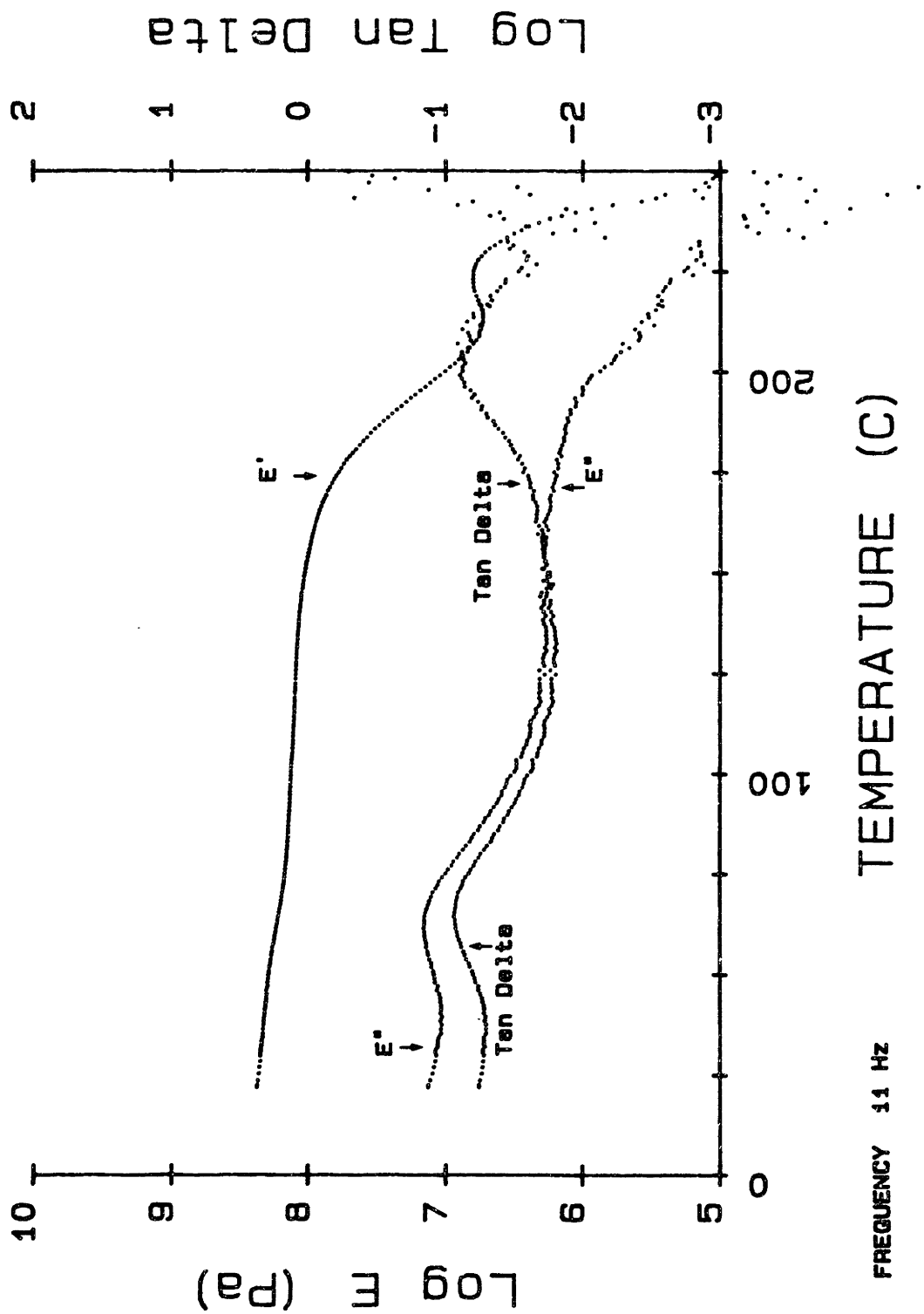

Figure 33. High Temperature Rheovibron Data

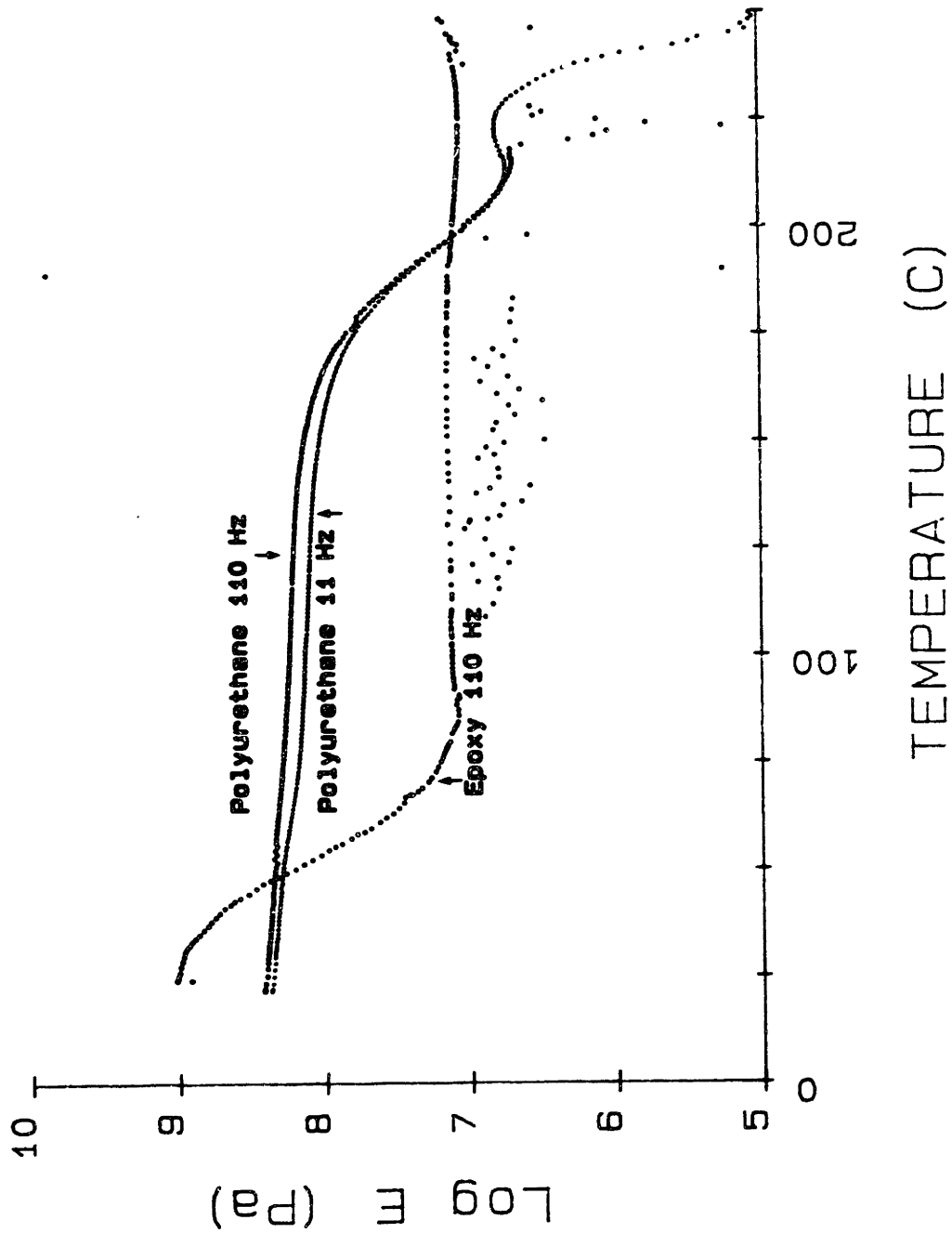

Figure 34. Comparison of Elastic Moduli (E')

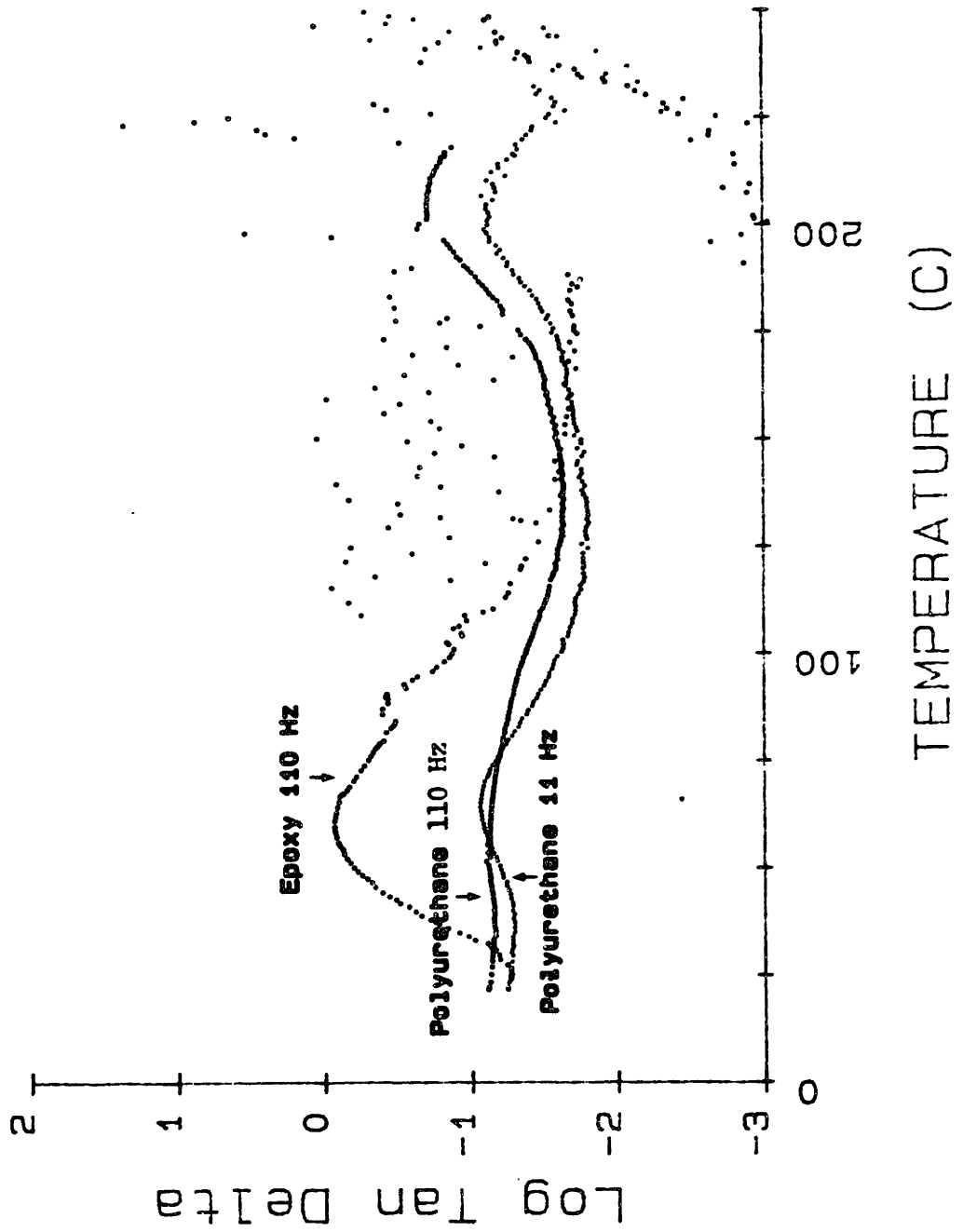

Figure 35. Comparison of Tan Delta Values

Fatigue failure occurs near 200°C, which is in the range where the elastic modulus is severely reduced. Softening of the material at these temperatures leads to rupture under the high extensions encountered during compression fatigue.

3.9. Infrared Spectroscopy.

Infrared spectroscopic analysis of the unfatigued and fatigued material was conducted in an effort to determine the types of reactions occurring during thermomechanical degradation.

Infrared radiation occurs in the range of 10,000 - 100 cm^{-1}. The absorption of infrared radiation causes a molecule to undergo bond deformation, either stretching or bending[61]. The energy for this deformation is quantized, but broad bands are usually seen because the change from one vibrational state to another also includes changes in the rotational levels[62]. The energy of this transition depends on the bond order and the masses of the atoms. For a transition to be seen in infrared spectroscopy the excitation must involve a change in the dipole moment of the bond[61].

Attenuated total reflectance (ATR) spectra were obtained using a Digilab FTS-IMX. This method was chosen because the material was insoluble and could not be cast into a film. Strip specimens, prepared as described in section 3.1, were used. The spectra for unfatigued and

fatigued specimen #1 are compared in Figures 36. Figures 37 and 38 show the FTIR spectra of unfatigued and fatigued material for specimen #6, respectively.

Inspection of the data yields information about the types of degradation reactions occurring. If oxidation were happening there should be either new peaks or an increase in the carbonyl region. There do not appear to be any real changes in this region, so it can be assumed the degradation occurs without the presence of oxygen. This is not unexpected because the concentration of oxygen present at the center of the block is likely to be small.

There also do not appear to be any peaks from isocyanate or carbodiimide groups. Based on the literature, the expected degradation reaction would be the dissociation of the urea or urethane groups, forming isocyanates, amines, and alcohols. If this is occurring the isocyanate groups must be reacting to form products other than carbodiimides.

To determine changes between unfatigued and fatigued samples, the peaks in each spectrum were ratioed to the peak at 1,600 cm^{-1} and their relative intensities compared. The band at 1,600 cm^{-1} is assigned to the phenyl group and is assumed inert to the degradation reactions.

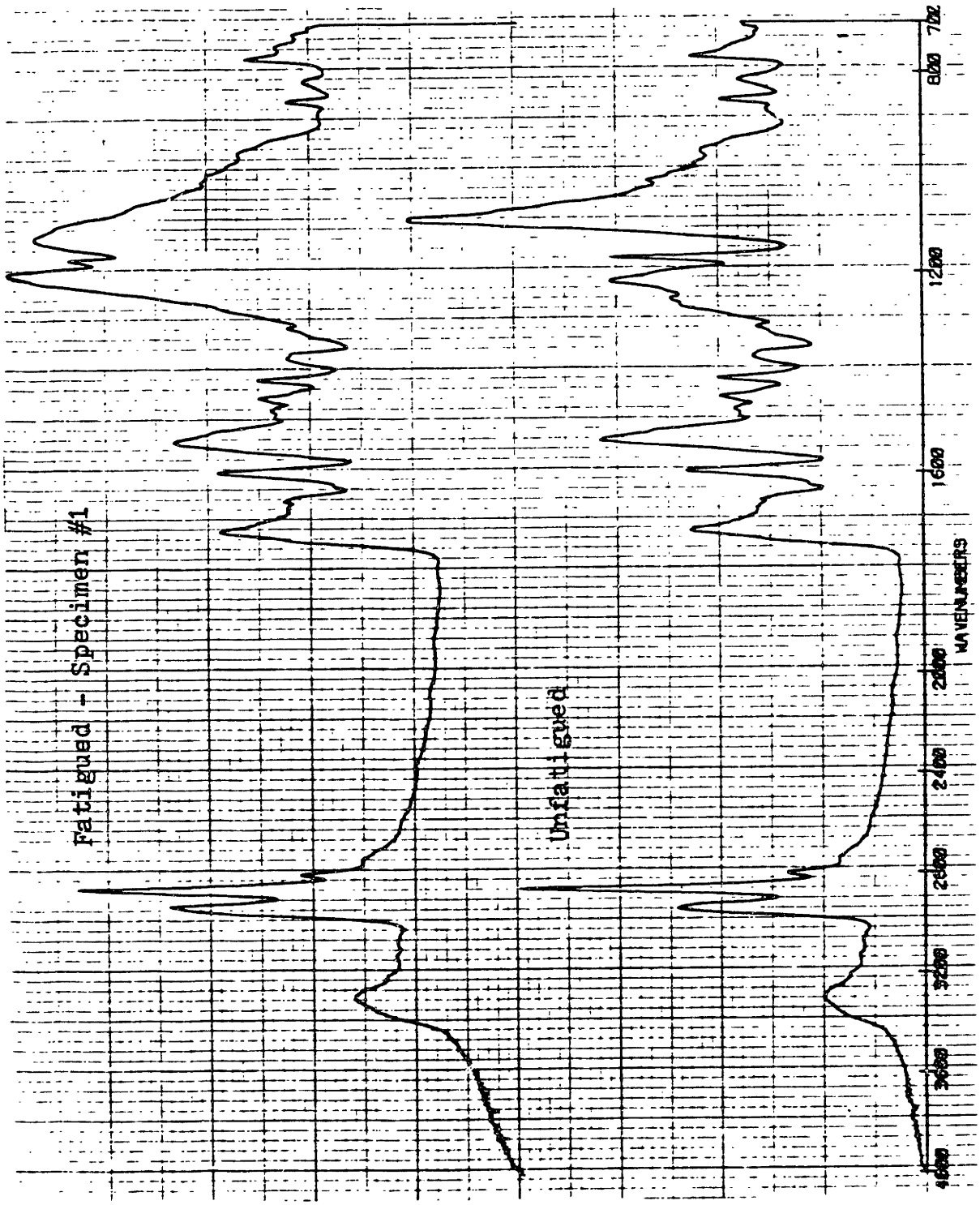

Figure 36. Comparison of FTIR Spectra - Specimen #1

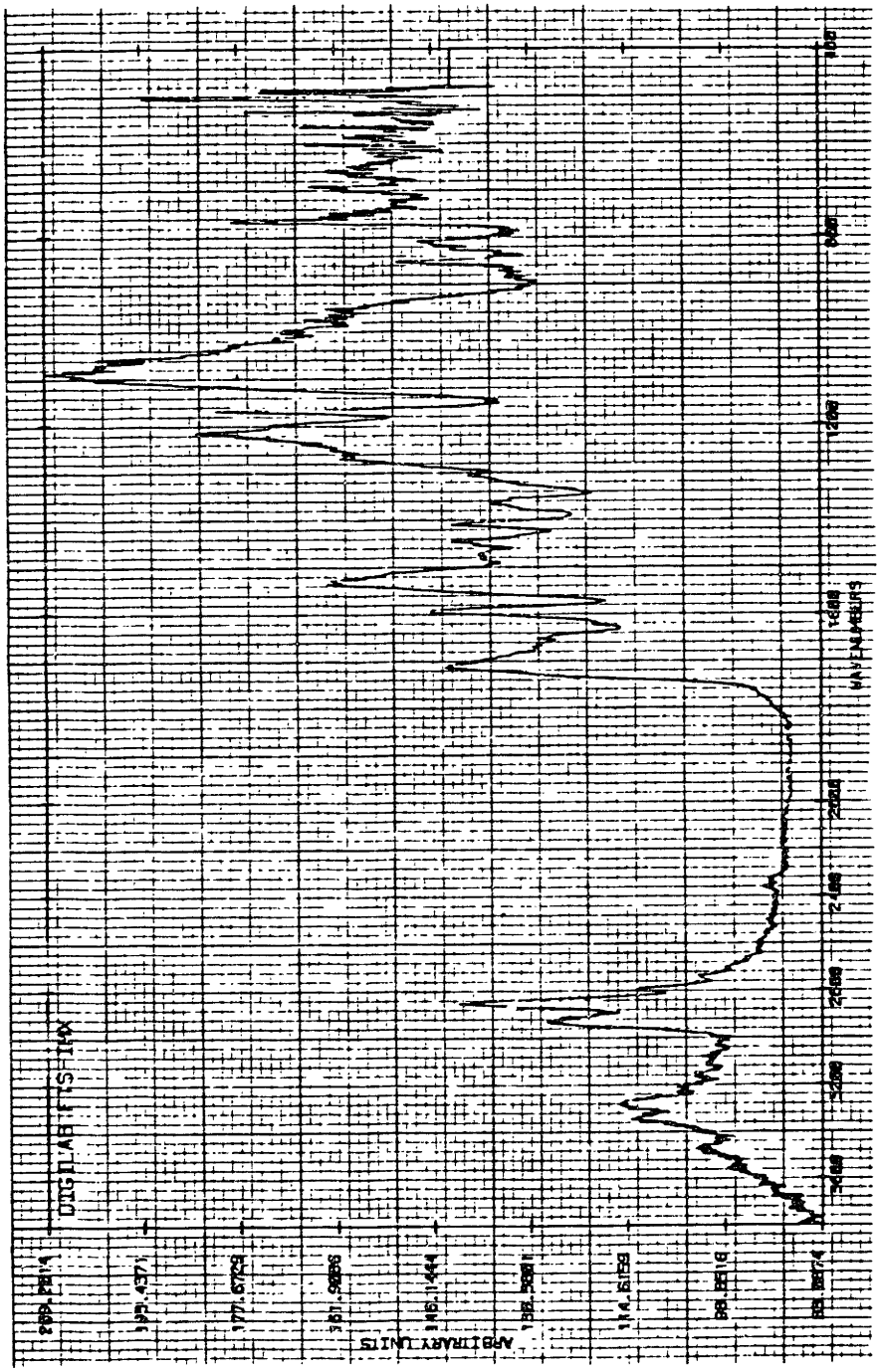

Figure 37. FTIR Spectrum of Unfatigued Specimen #6

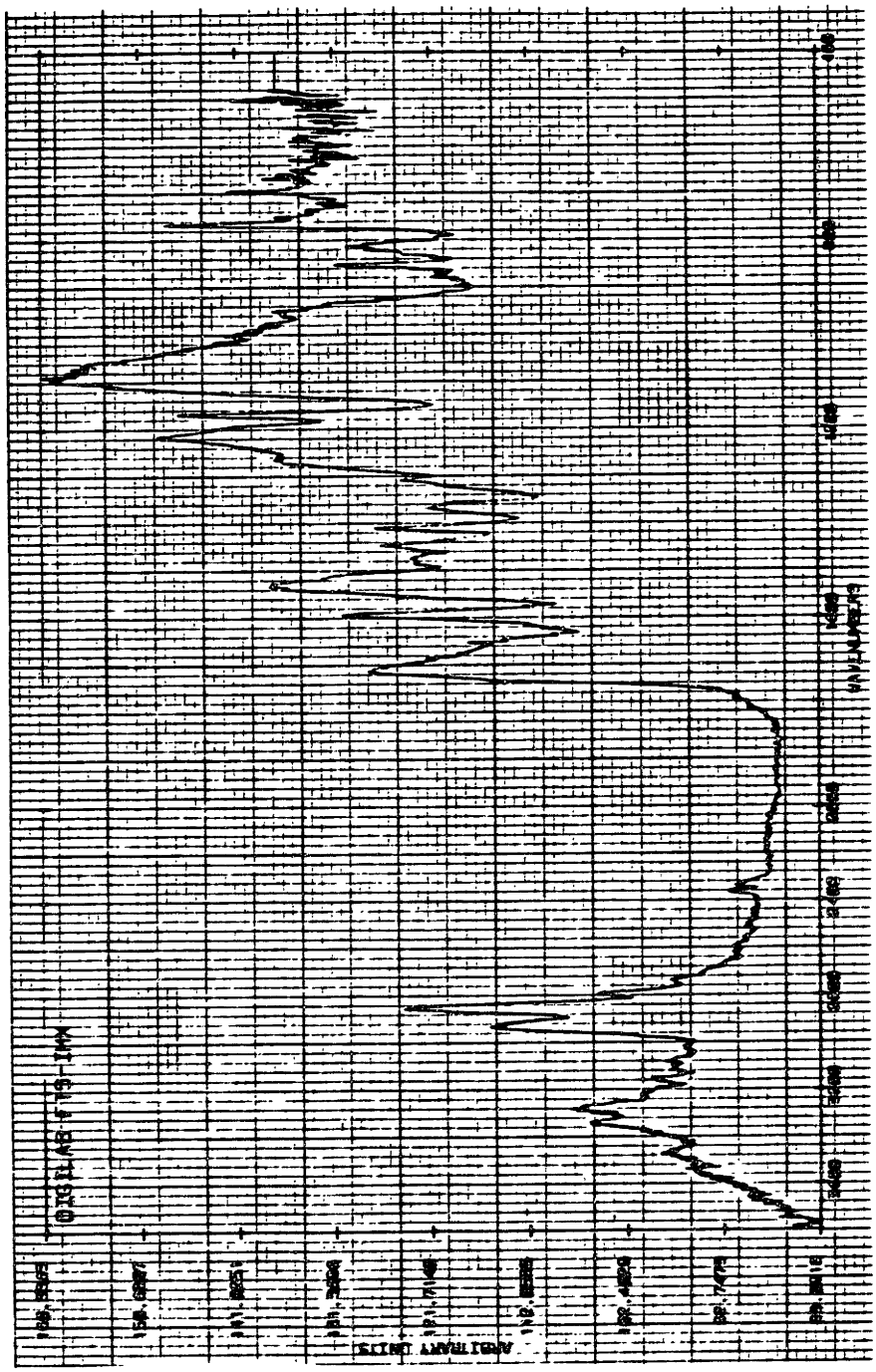

Figure 38. FTIR Spectrum of Fatigued Specimen #6

For the fatigued specimen #1 the major changes appear in the 1,200 - 1,100 cm^{-1} region, with two new peaks appearing, one at 1,190 cm^{-1} and the other at 1,140 cm^{-1}. The peak at 1,095 cm^{-1} decreases after fatigue. Peaks in this area of the infrared are generally from carbon-oxygen single bonds. The peak at 1,095 cm^{-1} is assigned to the polyether, which is undergoing some type of degradation with fatigue. At this time it is not clear what types of reactions might be occurring. One possibility would be the formation of alcohols, but there does not appear to be any significant increase in the O-H stretch region (3,700-2,500 cm^{-1})[61]. It is possible that there may be some peroxide formation, since they absorb in the 1,198 - 1,176 cm^{-1} region[62], however it seems unlikely that peroxides would be stable at the high temperatures encountered under fatigue.

Specimen #6 shows essentially no changes in the IR spectrum after fatigue. This is also true for specimen #4, although the spectra are not shown. Specimen #1 was the only specimen to show large changes in swelling behavior after fatigue. The IR spectrum of the fatigued material from specimen #1 is also the only spectrum showing any changes after fatigue. Comparing unfatigued material from specimen #1 and specimen #6 shows no major differences between the two original specimens before testing. It may be that the polyether for the prepolymer used in preparing specimen #1 was degraded in some way, either before or during sample casting, and the differences are too slight to be detected by IR.

Because no major changes were seen in the IR spectra of specimens #4 and #6, we have further support that the failure mechanism involves mechanical degradation of the specimen, without chemical reactions.

4. Conclusions

Failures are observed in urethane blocks under a variety of cyclic compressive loads; these failures were in the form of cracks generated at the center of the test specimen. From TGA experiments we found that weight loss begins at 250°C, well above the maximum temperature obtained during fatigue testing. Thus, no thermal degradation reactions (producing volatile components) appear to be involved in the failure process. However, it is possible that thermal degradation reactions not leading to volatile components could be a part of the failure mechanism.

DSC analysis showed an increased hard segment transition temperature after fatigue, which appears due to thermal annealing at the high temperatures of the fatigue test. Swelling analysis indicated that no significant breakdown in crosslink density is required for failure of specimens in compression loading. Only one block tested showed any significant changes by swelling analysis, and this anomaly may be due to some degradation of the material during processing or storage.

All samples exhibited a decreased elastic modulus after fatigue; the percentage decrease grows with increasing number of fatigue cycles. The internal temperature also increases with the number of cycles, and the continuous increase in temperature leads to softening of the material and increased deformation. Stress softening continues with increased amplitude of deformation, so the modulus decreases throughout the

duration of the test. The modulus reduction is not caused by mechanical stress or thermal annealing alone, but requires the interaction of both.

Comparison of the infrared spectra shows no major changes in fatigued specimens. This leads to the conclusion that no chemical reactions are involved in the failure mechanism, and that the failure process involves only interchain slippage of the softened urethane due to high temperatures and distortional stress components.

On a molecular scale we can calculate the maximum extension ratio of a polymer chain, from its unperturbed state. The full extension for a polymer chain, assuming an all trans configuration, can be given by the following equation[64]

$$L_{max} = n\ l \cos 35^{\circ}$$

where n is the number of main chain bonds and l is the bond length. The extension ratio α can be calculated by dividing the above equation by the unperturbed dimension, $\langle r_o^2 \rangle^{1/2}$, as shown below[64]:

$$\alpha = nl \cos 35^{\circ} / (Cnl^2)^{1/2}$$

In this equation C is the characteristic ratio for the polymer system.

For our system we have assumed that the polyether chains will reach full extension before chain slippage or disruption of the hard segment. Using the molecular weight of the polyether for our system and a value of 5.5 for C^{65}, the maximum extension ratio calculated is 2.9. A schematic of the extended polyether chains tied down by the hard segment domains is shown in Figure 39.

It is not at all unlikely that as the material softens extensions of the polymer chains at nearly this magnitude occur. Of course, there will be a distribution of chain lengths, with the shorter chains becoming fully extended first. When the hard segment transition temperature is reached the crosslinking effect of the hard segment domains is lost and the chains are free to slide by each other.

Under compression cycling heat build-up occurs due to viscous damping; the hottest portion of the specimen is the center of the block. The center portion of the block is also subjected to large extensional strain, and as the temperature at the center of the block approaches the hard segment transition temperature, the modulus of the material will decrease rapidly. This leads to higher and higher extensions, and finally, rupture of the specimen.

This weakening of the center portion of the specimen, in conjunction with the extensional strain, causes failure at the center of the specimen, rather than surface failure initiation. There is scant

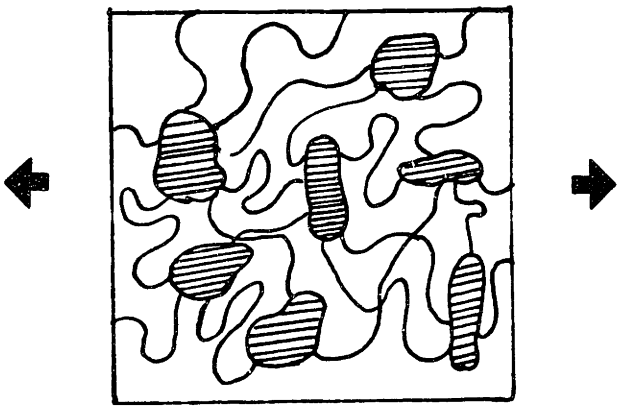

a. Before Extension

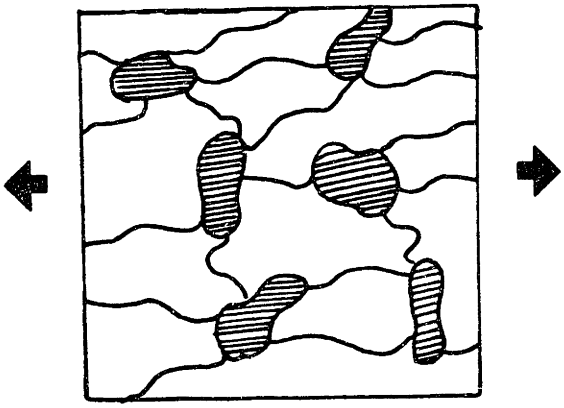

b. After Extension

Hard Segment Domains

Polyether Chains

Figure 39. Polyether Chains Under Extension

experimental evidence for chain scission; however, it is possible that the urethane and urea bonds could dissociate at high temperatures and subsequently reform as the material is cooled.

From this work it appears that the hard segment transition temperature is the primary factor governing the fatigue life of a cyclically compressed polyurethane block. For long part lifetimes the polyurethane must possess a very high temperature hard segment transition, or the heat build-up characteristics of the material must be such that the service temperature of the part is well below the hard segment transition.

Polyurethane elastomer behavior is not unlike a conventional filled rubber system. For silicon-based elastomers silica fillers are used to improve the material properties; similarly, carbon black is used in natural and synthetic rubber elastomers. The hard segment domains of the polyurethane act as a reinforcing filler, yielding a polymer with improved mechanical properties. As the high temperatures encountered during fatigue approach the hard segment transition temperature, the filler effect of the hard segment domains is reduced, giving an elastomer with reduced mechanical properties similar to an unfilled system.

Future work should be done to investigate the possibility of phase separation and orientation, perhaps by small angle x-ray scattering. This may help identify what causes the loss of modulus: disruption of the hard segment domains or orientation.

High temperature IR measurements may help determine if reversible chain scission were possible, and find the temperature at which the urethane and urea bonds dissociate for this polyurethane system.

Another area for investigation would be attempting to increase the hard segment transition temperature. One method may be through the introduction of crosslinks in the hard segment. Since the introduction of crosslinks has been known to reduce the room temperature properties, further work would be required to see if a crosslinking method could be worked out which does not reduce the room temperature properties. The crosslinking may have an additional benefit in reducing the amount of stress-softening.

LIST OF REFERENCES

[1] G. Trappe, "Relations Between Structures and Properties of Polyurethanes," in Advances in Polyurethane Technology, ed. by J.M. Buist and H. Gudgeon, chap. 3, John Wiley & Sons, Inc., New York (1968).

[2] K. A. Pigott, B. F. Frye, K. R. Allen, S. Steingiser, W. C. Darr, and J. H. Saunders, "Development of Cast Urethane Elastomers for Ultimate Properties," Journal of Chemical and Engineering Data, Vol. 5, pp. 391-395 (1960).

[3] S. L. Cooper and A. V. Tobolsky, "Anomolous Depression of Rubbery Modulus through Crosslinking," Journal of Applied Polymer Science, Vol. 11, pp. 1361-1369 (1967).

[4] C. S. Schollenberger and K. Dinbergs, "Thermoplastic Urethane Chemical Crosslinking Effects," Journal of Polymer Science: Polymer Symposium, Vol. 64, pp. 351-368 (1978).

[5] L. B. Weisfeld, J. R. Little, W. E. Wolstenholme, "Bonding in Urethane Elastomers," Journal of Polymer Science, Vol. 56, pp. 455-463 (1962).

[6] M. Rutkowska and A. Balas, "Influence of NCO:OH Relation and Chain Extender on Primary and Secondary Valence Crosslinks in Urethane Elastomers," Journal of Applied Polymer Science, Vol. 25, pp. 2531-2538 (1980).

[7] A. R. Cain, W. R. Conard, S. E. Schonfeld, and B. H. Werner, "Correlation of H-bonds via DTA, DSC, and IR to Physical Properties of Polyether Urethane-Urea Segmented Copolymers," Polymer Preprints, Vol. 17, pp. 580-584 (1976).

[8] H.N. Ng, A.E. Allegrezza, R.W. Seymour, and S.L. Cooper, "Effect of Segment Size and Polydispersity on the Properties of Polyurethane Block Polymers," Polymer, Vol. 14, pp. 255-261 (1973).

[9] N. S. Schneider, C. S. Paik Sung, R. W. Matton, J. L. Illinger, "Thermal Transition Behavior of Polyurethanes Based on Toluene Diisocyanate," Macromolecules, Vol. 8, pp.62-67 (1975).

[10] C. S. Paik Sung, "Comparison of the Structure-Properties in 2,4 TDI Based Polyether Polyurethanes and Polyurethaneureas," Polymer Science and Technology, Vol. 11, pp. 119-135 (1980).

[11] J.H. Saunders and J.K. Backus, "Thermal Degradation and Flammability of Urethan Polymers," Rubber Chemistry and Technology, Vol. 39, pp. 461-480 (1966).

[12] A. Ballisteri, S. Foti, P. Maravigna, G. Montaudo, and E. Scamporrino, "Mechanism of Thermal Degradation of Polyurethanes Investigated by Direct Pyrolysis in the Mass Spectrometer," Journal of Polymer Science: Polymer Chemistry Edition, Vol. 18, pp. 1923-1931 (1980).

[13] S. Foti, P. Maravigna, and G. Montaudo, "Effects of N-Methyl Substitution on the Thermal Stability of Polyurethanes and Polyureas," Polymer Degradation and Stability, Vol. 4, pp. 287-292 (1982).

[14] S. Foti, P. Maravigna, and G. Montaudo, "Mechanisms of Thermal Decomposition in Totally Aromatic Polyurethanes," Journal of Polymer Science: Polymer Chemistry Edition, Vol. 19, pp. 1679-1687 (1981).

[15] N. Grassie and M. Zulfiqar, "Thermal Degradation of the Polyurethane from 1,4 Butanediol and Methylene Bis(4-Phenyl Isocyanate)," Journal of Polymer Science: Polymer Chemistry Edition, Vol. 16, pp. 1563-1574 (1978).

[16] N. Grassie, M. Zulfiqar, and M.I. Guy, "Thermal Degradation of a Series of Polyester Polyurethanes," Journal of Polymer Science: Polymer Chemistry Edition Vol.18, pp. 265-274 (1980).

[17] N. Grassie and G. A. P. Mendoza, "Thermal Degradation of Polyether-Urethanes: Part 1 - Thermal Degradation of Poly(Ethylene Glycols) Used in the Preparation of Polyurethanes," Polymer Degradation and Stability, Vol. 9, pp. 155-165 (1984).

[18] A. Davis and J. H. Golden, "Thermally-Induced Degradation of Polytetramethylene Oxide," Polymer Preprints, Vol. 5, pp. 461-465 (1964).

[19] P.E. Slade, Jr. and L.T. Jenkins, "Thermal Analysis of Polyurethane Elastomers," Journal of Polymer Science, Part C, Vol. 6, pp. 27-32 (1964).

[20] J.H. Engel, S.L. Reegan, and P. Weiss, "Effect of Structure on Temperature Stability and Solubility of Polyester-Urethanes," Journal of Applied Polymer Science, Vol. 7, pp. 1679-1689 (1963).

[21] J. Ferguson and Z. Petrovic, "Thermal Stability of Segmented Polyurethanes," European Polymer Journal, Vol. 12, pp. 177-181 (1976).

[22] J.H. Flynn, W.J. Pummer, and L.E. Smith, "Initial Weight-Loss Kinetics for the Thermal degradation of Polyurethanes," American Chemical Society, Polymer Division Preprints, Polymer Preprints, Vol. 18, No.1, pp. 757-760 (1977).

[23] F. Gaboriaud and J.P. Vantelon, "Thermal Degradation of Polyurethane Based on MDI and Propoxylated Trimethylol Propane," Journal of Polymer Science: Polymer Chemistry Edition, Vol. 19, pp. 139-150 (1981).

[24] P.C. Colodny and A.V. Tobolsky, "Chemorheological Study of Polyurethane Elastomers," Journal of the American Chemical Society, Vol. 79, pp. 4320-4323 (1957).

[25] J.A. Offenbach and A.V. Tobolsky, "Chemical Relaxation of Stress in Polyurethane Elastomers," Journal of Colloid Science Vol. 11, pp. 39-47 (1956).

[26] A. Singh and L. Weissbein, "Kinetics of Urethane Cleavage in Crosslinked Polyurethanes," Journal of Polymer Science, Part A-1, Vol. 4, pp. 2551-2561 (1966).

[27] A. Singh, L. Weissbein, and J.C. Mollica, "Thermal Stability of Polyester- vs. Polyether-Based Urethanes," Rubber Age, Vol. 98, pp. 77-83 (1966).

[28] Sprey, R., "Avoiding Destructive Hysteresis in Elastomers," Machine Design, February 24, 1983.

[29] M. Jakob and G. A. Hawkins, Elements of Heat Transfer and Insulation, John Wiley and Sons, Inc., New York (1942).

[30] Lindley, P.B., "Engineering Design With Natural Rubber", NR Technical Bulletin, The Malaysian Rubber Producer's Research Association, Hertford, England.

[31] Treloar, L. R. G., The Physics of Rubber Elasticity, Clarendon Press, Oxford (1975).

[32] Buckley, D. J., "Aspects of Sample Geometry During Rapid Sinusoidal Flexing," Paper presented at Rubber Division, A.C.S., May, 1974.

[33] Gent, A. N. and Meinecke, E. A., "Compression, Bending, and Shear of Bonded Rubber Blocks," Polymer Engineering and Science, Vol. 10, pp. 48-53 (1970).

[34] Holownia, B. P., "Effect of Poisson's Ratio on Bonded Rubber Blocks," Journal of Strain Analysis, Vol. 7, pp. 236-242 (1972).

[35] Reed, A. J. and Thorpe, J., "The Use of the Digital Computer in the Design of Rubber-Bonded-To-Metal Components," in Elastomers: Criteria For Engineering Design, by C. Hepburn and R. J. W. Reynolds, Applied Science Publishers, Ltd., London, Chapter 11 (1979).

[36] Roylance, D. K., Private Communication (1985).

[37] E.S. Freeman and B. Carroll, "The Application of Thermoanalytical Techniques to Reaction Kinetics. The Thermogravimetric Evaluation of The Kinetics of Calcium Oxalate Monohydrate," Journal of Physical Chemistry, Vol. 62, pp. 394-397 (1958).

[38] L. Reich and S. Stivala, "Elements of Polymer Degradation," Chap. 2, McGraw-Hill, New York, 1971.

[39] D.A. Anderson and E.S. Freeman, "The Kinetics of The Thermal Degradation of The Synthetic Styrenated Polyester, Laminac 4116," Journal of Applied Polymer Science, Vol. 1, pp. 192-199 (1959).

[40] C.S.P. Sung and N.S. Schneider, "Infrared Studies of Hydrogen Bonding in Toluene Diisocyanate Based Polyurethanes," Macromolecules, Vol. 8, pp. 68-77 (1975).

[41] C.S.P. Sung, C.B. Hu, and C.S. Wu, "Properties of Segmented Poly(urethaneureas) Based on 2,4 Toluene Diisocyanate. 1. Thermal Transitions, X-ray Studies, and Comparison with Segmented Poly(urethanes)," Macromolecules, Vol. 13, pp. 111-116 (1980).

[42] R. Seymour and S.L. Cooper, "Thermal Analysis of Polyurethane Block Polymers," Macromolecules, Vol. 6, pp.48-53 (1973).

[43] A. R. Cain, "DTA, DSC, and Infrared Studies of Polyetherurethanes Cured With 4,4'-Methylene Bis-(Ortho-Chloroaniline)," Polymer Preprints, Vol. 17, pp. 576-579 (1976).

[44] Lawrence, H.R. Nick, "Mechanisms of Elastomer Degradation and Wear", Master's Thesis, Virginia Polytechnic and State University, 1983.

[45] E.T. Bishop and S. Davison, "Network Characteristics of the Thermoplastic Elastomers," Journal of Polymer Science - Part C, Vol. 26, pp. 59-79 (1969).

[46] B. Ellis and G.N. Welding, "Estimation, From Swelling, of the Structural Contribution of Chemical Reactions in the Vulcanisation of Natural Rubber. Part II - Estimation of Equilibrium Degree of Swelling," in Techniques of Polymer Science", Society of the Chemical Industry Monographs No. 17, Society of the Chemical Industry, London, pp. 46-53 (1964).

[47] DuPont Product Information Bulletin

[48] E.F. Cluff and E.K. Gladding, "Relation of Structure to Properties in Polyurethanes," Journal of Applied Polymer Science, Vol. 3, pp. 290-295 (1960).

[49] J.D. Ferry, Viscoelastic Properties of Polymers, John Wiley and Sons, Inc., Chap. 1, New York (1980).

[50] J. Ferguson, D.J. Hourston, R Meredith, and D. Patsavoudis, "Mechanical Relaxations in a Series of Polyurethanes With Varying Hard to Soft Segment Ratio," European Polymer Journal, Vol. 8, pp. 369-383 (1972).

[51] S. Huh and S.L. Cooper, "Dynamic Mechanical Properties of Polyurethane Block Polymers," Polymer Engineering and Science, Vol. 11, pp. 369-376. (1971).

[52] S.L. Cooper and A.V. Tobolsky, "Viscoelastic Behavior of Segmented Elastomers," Textile Research Journal, Vol. 36, pp. 800-803 (1966).

[53] G. Allen, P.L. Edgerton, and D.J. Walsh, "Model Polyurethane Networks," Polymer, Vol. 17, pp. 65-71 (1976).

[54] T.L. Smith and A.B. Magnusson, "Diisocyanate - Linked Polymers. II Mechanical and Swelling Properties of Some Polyurethane Elastomers," Journal of Polymer Science, Vol. 42, pp. 391-416 (1960).

[55] G.L. Wilkes and R. Wildnaur, "Kinetic Behavior of the Thermal and Mechanical Properties of Segmented Urethanes," Journal of Applied Physics, Vol. 46, pp. 4148-4152 (1975).

[56] G.L. Wilkes, T.S. Dziemianowicz, Z.H. Ophir, E. Artz, and R. Wildnaur, "Thermally Induced Time Dependence of Mechanical Properties in Biomedical Grade Polyurethanes," Journal of Biomedical Materials Research, Vol. 13, pp. 189-206 (1979).

[57] R.R. Lagasse, "Domain Structure and Time - Dependent Properties of a Crosslinked Urethane Elastomer," Journal of Applied Polymer Science, Vol. 21, pp. 2489-2503 (1977).

[58] G. S. Trick, "The Softening of Adiprene L Gum Stocks During Extension," Journal of Applied Polymer Science, Vol. 3, p. 252 (1960).

[59] S. L. Cooper, D. S. Huh, and W. J. Morris, "Stress-Softening in Crosslinked Block Copolymer Elastomers," Industrial Engineering and Chemistry - Product Research and Development, Vol. 7, pp. 248-251 (1968).

[60] Y. Kaneko, F. Watabe, T. Okamoto, Y. Iseda, and T. Matsunaga, "Effect of Molecular Weight Distribution of Poly(oxytetramethylene)glycol on Cut Growth Resistance of Polyurethane," Journal of Applied Polymer Science, Vol. 25, pp. 2467-2478 (1980).

[61] D.J. Pasto and C.R. Johnson, Organic Structure Determination, Chapter 4, Prentice - Hall, Inc., New Jersey (1969).

[62] R.M. Silverstein, G.C. Bassler, T.C. Morrill, Spectrometric Identification of Organic Compounds, Chapter 3, John Wiley and Sons, Inc., New York (1981).

[63] D.K. Roylance and J. Mead, "Damage Accumulation In Elastomeric Components," U.S. Army Tank-Automotive Command Technical Report, No. 13068, September (1984).

[64] Flory, P.J., Principles of Polymer Chemistry, Cornell University Press, Ithaca, New York (1953).

[65] Polymer Handbook, edited by J. Brandrup and E.H. Immergut, John Wiley and Sons, New York (1975).

[66] P.B. Kemp, S.B. Thesis, M.I.T., June (1984).